HORIZONTAL SHEAR CONNECTORS FOR PRECAST PRESTRESSED BRIDGE DECK PANELS

by

Fatmir Menkulasi

Thesis submitted to the faculty of the

Virginia Polytechnic Institute and State University

in partial fulfillment of the requirements for the degree of

MASTER OF SCIENCE

IN

CIVIL ENGINEERING

APPROVED:

_____

Carin-Roberts Wollmann, Chairperson

_____ _____

Thomas M. Murray Thomas E. Cousins

August 2002
Blacksburg, Virginia

Keywords: Precast Panels, Shear Connectors, Horizontal Shear, Grout

HORIZONTAL SHEAR CONNECTORS FOR PRECAST PRESTRESSED BRIDGE DECK PANELS

by

Fatmir Menkulasi

ABSTRACT

The full-width, full-depth precast panel system is very convenient for rehabilitation of deteriorated decks as well as for new bridge construction. The horizontal shear strength at the interface between the two interconnected elements is of primary importance in order to provide composite action. The strength of the bond between the two precast members should be high enough to prevent any progressive slip from taking place. Flexural strength, shear strength and deflection characteristics all depend on the satisfactory performance of the interface to provide composite action. However, the case when both of the interconnected elements are precast members bonded by means of grout, is not currently addressed by ACI or AASHTO. This is the main impetus for this project.

A total of 36 push-off tests were performed to develop a method for quantifying horizontal shear strength and to recommend the best practice for the system. Test parameters included different haunch heights, different grout types, different amount and different type of shear connectors. Two equations, for uncracked and cracked concrete interfaces, are proposed to be used in horizontal shear design when the precast panels are used.

Predictive equations are compared with available methods for the horizontal shear strength of the precast panel system. Conclusions and recommendations for the optimum system are made.

ACKNOWLEDGEMENTS

I would first like to thank Dr. Carin-Roberts Wollmann for her advice, guidance support, invaluable input and excellent interaction throughout the duration of this research. I would like to express sincere appreciation to Dr. Thomas E. Cousins for his earnest efforts inside and outside of the classroom on my behalf and for serving on my committee. I would also like to thank Dr. Thomas M. Murray for his academic input, thought provoking comments and help throughout the duration of my graduate studies and also for serving on my committee. Thanks also go to Bayshore Concrete Products for sponsoring this research and to Mr. Vince Campbell for his assistance throughout this project.

I would like to express tremendous gratitude to my parents, Gazmend and Kozeta Menkulasi, for their constant support throughout my entire life and for providing me with the opportunity to further my education at the institute of my choice.

Many thanks go to Brett Farmer and Dennis Huffman for their hard work and invaluable help at the structures lab. A sincere thanks goes to Mathew Harlan and Jake LaMontagne for their help at the laboratory. Thanks also go to my fellow graduate students who were so helpful along the way.

TABLE OF CONTENTS

LIST OF FIGURES

LIST OF TABLES

Page

CHAPTER 1: INTRODUCTION

1.1 Precast Bridge Deck Panels

Deck deterioration due to corrosion of reinforcing steel, caused by salts and deicing chemicals, is a process that takes place in most bridges, particularly in Northern States with a cold climate and in coastal areas. Corrosion can lead to cracking and spalling of the concrete resulting in a poor riding surface and in extreme cases structural deficiency. This phenomenon requires deck rehabilitation to maintain the bridges in good condition. Also with the increase in traffic flow in certain urban areas of cities there is a significant increase in the demand for new bridge construction or widening of existing bridges. The replacement of bridge decks and new bridge construction using conventional cast-in-place concrete interferes with traffic for prolonged periods of time. So a faster and a more economical system to cope with the problem should be developed.

One solution is the precast panel system illustrated in Figure 1.1. The utilization of full-depth, full-width precast and precast-prestressed concrete deck panels for the rehabilitation and new construction of bridges dates to 1970. The basic idea of the system is that the precast elements can be supported on steel rolled beams, plate girders, precast prestressed concrete girders or reinforced concrete girders. Precast panels are shipped from the precast yard and set in order on the supporting system. Each panel is properly aligned and adjusted in accordance with the required elevation by using leveling screws. Haunches of 1 in. minimum are provided to account for any cambering in the girders. In the transverse direction, the precast deck panels can be pretensioned at the precasting yard or post-tensioned in the field. The precast panels also contain longitudinal post-tensioning ducts. The longitudinal post-tensioning tendons run through these ducts from the live end to the dead end. The live end is the location where the tendons are tensioned and the dead end is the location where the tendons are anchored. This may be one span length or the panels may be continuous over multiple spans. At the transverse joints between adjacent precast panels, the duct is normally taped with duct tape prior to grouting. The shear keys between the precast panels are grouted, the longitudinal post-tensioning is applied and then the shear pockets and haunches are grouted to provide composite action.

One of the big advantages of this system is the reduction in construction time. Since decks are constructed more rapidly than conventional decks, the user costs related to traffic slow downs and detours are reduced. Furthermore, traffic flow can be maintained in both directions by implementing a staged construction. Half of the bridge is opened to traffic while the other half is being replaced. Also, the panels are very high quality, since concrete quality and fabrication tolerances are significantly better in a precasting yard than in the field. The decks are prestressed in both directions, which makes them stiffer under service loads and more impervious to the ingress of corrosion causing agents than mildly reinforced cast-in-place decks.

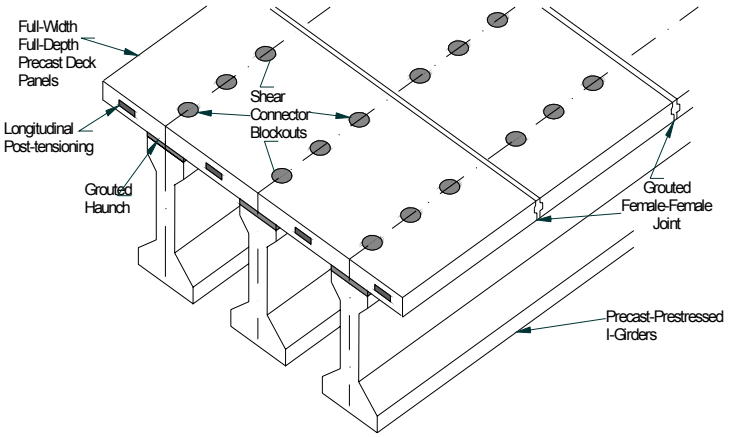

Figure 1.1 Precast deck system

This system has been used successfully in previous projects, but for the concept to become widely accepted, several aspects require additional study and improvement. The main design and construction components of this system, that need to be optimized, are as follows:

- Transverse joints between the precast prestressed concrete panels, and the type of material within the joints.

- Connections between the deck and the supporting system composed of either steel or concrete girders and the type of grout to be used.
- Post-tensioning in the longitudinal direction.
- Prestressing in the transverse direction.
- Haunches between the top flanges of the girders and the deck.
- Overlay and waterproofing membrane system

1.2 Project Objective and Scope

This type of system has been used previously in several states primarily for rapid bridge deck replacement on steel I-girders. This research project focuses on the use of the system where both the deck and the girder are precast concrete. The horizontal shear strength at the interface between the two interconnected elements is of primary importance to provide composite action. The strength of the bond between the two precast members should be high enough to prevent any progressive slip from taking place. Flexural strength, shear strength and deflection characteristics all depend on the satisfactory performance of the interface to provide composite action. None of the available codes addresses the case when both of the interconnected elements are precast members and are bonded by means of grout.

The project's objectives are to develop a better understanding of the horizontal shear strength of the connections between the deck and the precast girders, to propose a method for quantifying the horizontal shear strength at the interface between the deck and the girder, and to recommend the best practice for shear connections used with the precast decks for both new bridge construction and deck replacement. To accomplish this, 36 push-off tests were performed. Figure 1.2 illustrates the type of push-off specimens tested in this research.

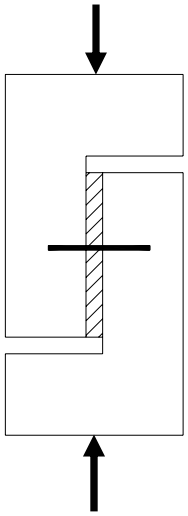

Figure 1.2 Classical push-off test specimen.

The configuration was patterned after classic push-off tests performed by Mattock (1969), except each side of the specimen was precast, and the space between grouted.

Eighteen shear connector details were tested, with two repetitions of most details. The variables studied in the first 24 tests included the area of the steel crossing the interface, the type of grout, and the height of the haunch. The last 12 tests investigated post-installed and pre-installed connectors for deck rehabilitation and inserts that might be used for future deck replacement.

1.3 Thesis Organization

The second chapter is a review of previous research and use of the precast panel system and current horizontal shear connection design methods. The third chapter is a description of the tests and the fourth chapter presents the results. Chapter five includes recommendations and conclusions.

CHAPTER 2 : LITERATURE REVIEW

2.1 Precast Bridge Deck Panel system

As the idea of the precast panel system started to gain acceptance, many studies were performed to investigate different components of the system. Issa and Yousif (1995) presented a paper on the construction procedures for rapid replacement of bridge decks. One of the most important ideas presented in this paper is that the longitudinal post-tensioning of the decks should be applied prior to grouting of the haunches and shear pockets, or in other words prior to providing composite action between the beam and the deck. The reason behind this is to prevent additional positive moments in the girder.

Yamane and Tadros (1998) performed a study on the system, which employed stemmed precast panels and welded headless studs as shear connectors. They concluded that the system has better crack control and is 10% more slender and 20% lighter in weight than solid conventional reinforced concrete decks. Also, the welded headless studs can ease panel removal.

The idea of applying longitudinal post-tensioning on the system to keep the transverse joints tight was encouraged by many researchers. However, not until 1998 was a quantitative study carried out to determine the minimum amount of prestressing force to keep the joints in compression. Issa and Yousif (1998) concluded that the minimum level of prestress is 200 psi for simply supported bridges, while a prestress level of 450 psi is needed over the interior supports for continuous bridges.

Tadros and Badie (1998) performed a study on the performance of the full-depth precast panel system and a continuous stay-in-place precast panel system with cast-in-place topping. The researchers concluded that both systems produce high quality deck slabs as they are produced under controlled conditions. Prestressed deck panels have the advantages of having no shrinkage cracks, which could result in longer life of the deck and less maintenance cost compared to the full-depth cast-in-place system.

Recently Tadros, Badie and Kamel (2002) proposed a debonded shear key system for prestressed concrete girders with cast-in-place bridge decks. Horizontal shear resistance is provided by the mechanical anchorage of concrete shear keys created on the top flange of the concrete girders, combined with the shear reinforcement crossing the interface. The system

has the advantage of facilitating future deck removal, while protecting the top flange of the girder from damage. They concluded that the equation in AASHTO LRFD Specifications (1998) is the most convenient equation to be used for determining the amount of shear reinforcement for this system with a cohesion factor c=0 due to the debonded interface and coefficient of friction μ=1.0.

Culmo (2000), investigated a design that would use full-depth precast concrete deck slabs for deck replacement. He outlines the process that the Connecticut Department of Transportation followed to research the past studies using precast bridge elements. The information from several studies in the past was compiled into a system, which was applied successfully on two different bridges using different construction approaches which were convenient for the particular bridges. The first involved a full closure of the bridge and the second involved a long viaduct that could only be closed on weekends.

Shim, Kim, Chang, and Chung (2000) performed a study on the design of shear connections with full-depth precast slab on steel beams. The researchers performed push-out tests with variations of the stud shank diameter and the compressive strength of the mortar to investigate strength, stiffness, slip capacity and fatigue endurance of the shear connections. The reserachers proposed an empirical equation for the initial shear stiffness of the connection and concluded that the static strength of the connection was similar to the tensile strength of the studs owing to the effect of the bedding layer. It was observed that deformations of the studs in a full depth precast slab were greater than those in cast-in-place slab. The friction and the bonding between the steel and the concrete slab increased the fatigue endurance of the shear connection.

Chang and Shim (2001) performed a study to build a design basis for horizontal shear connections and transverse joints in continuous bridges. The researchers proposed empirical equations for the ultimate strength and fatigue endurance of the horizontal shear connections and investigated the static and fatigue behavior of female-to-female type of transverse joints. They concluded that the basic design criterion for crack control in the transverse joints is to prevent tension under service loads.

2.2 Horizontal Shear

Ever since composite construction has been employed to create more efficient designs, horizontal shear strength at the interface has been a topic full of challenges and controversies. Figure 2.1 illustrates the horizontal shear forces required to develop composite action.

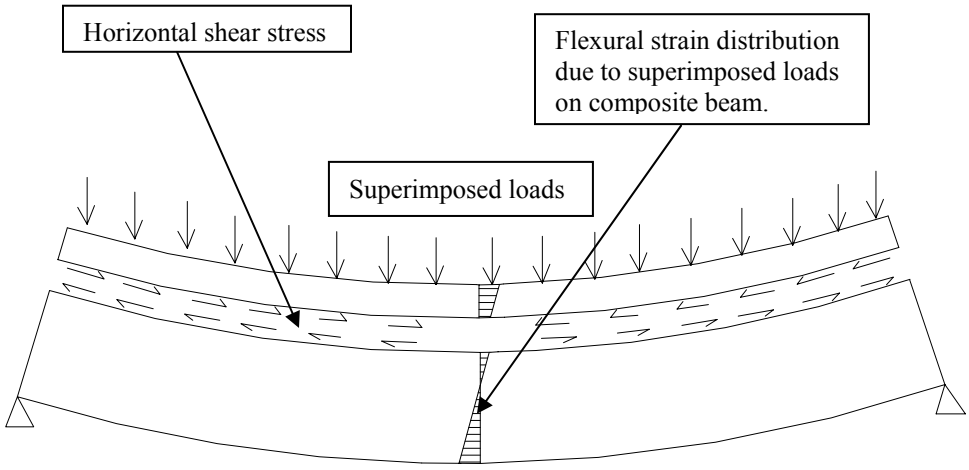

Figure 2.1 Development of shear forces during composite action.

The horizontal shear stresses, v_h, on the contact surface between an uncracked elastic precast beam and a slab can be computed from:

$$v_h = \frac{VQ}{Ib} \qquad (2.1)$$

where

v_h = horizontal shear stress

V = vertical shear force at the section considered

Q = static moment of area of the slab or flange about the neutral axis of the composite section

I = moment of inertia of the composite section

b = width of the section considered

This equation is valid as long as the section is uncracked. Loov and Patnaik (1994) determined that the above equation may yield adequate results if both the cracked section moment of inertia and area moment of the cracked composite section are used. As an alternative to this method, Kamel (1996) used equilibrium of forces to show that :

$$v_h = \frac{V}{(b_v d_v)} \qquad (2.2)$$

where

V= factored vertical shear at the section considered

d_v = distance between tension and compression resultant forces

b_v = section width at the interface between the precast beam and deck.

Another method for determining the design horizontal shear force is to compute the actual change in compressive or tensile force in any segment and transferring that force as horizontal shear to the supporting element. This method is used in the Manual of Steel Construction of the American Institute of Steel Construction (AISC 1998), and is presented as an alternative in the ACI 318/02. This method is expressed by the following equation.

$$v_h = \frac{C}{(b_v l_v)} \qquad (2.3)$$

where

C = total compression or tension in the flange

b_v = width of the interface

l_v = length of the interface

Figure 2.2 illustrates the basis of the equation.

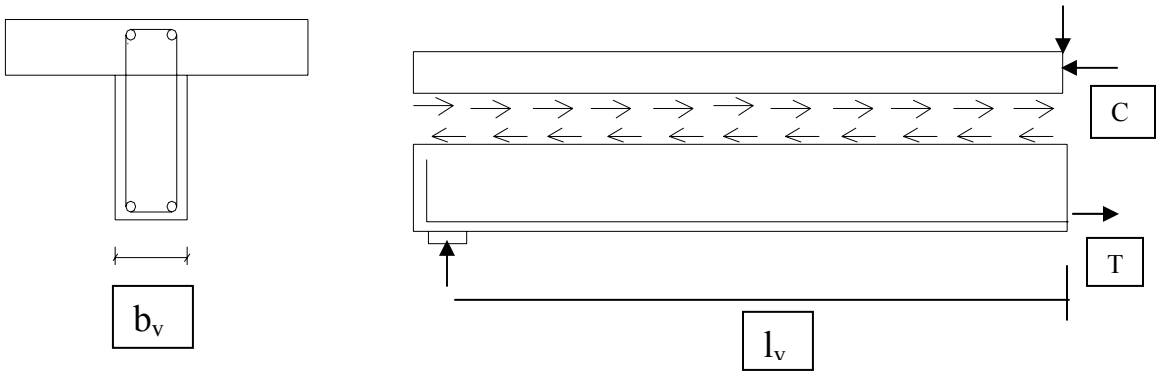

Figure 2.2 Equilibrium of forces during composite action

The above equations are used to determine the horizontal shear force or shear stresses (required strength). To ensure composite action the required horizontal shear strength must be smaller than the factored horizontal shear resistance (design strength). Research has been done to determine the horizontal shear resistance at the interface between the beam and the deck. The following sections present current code provisions for horizontal shear and conclusions of previous research. The codes that provide horizontal shear strength equations for the case when the composite members consist of a concrete beam and concrete deck are the ACI 318-02/318R-02, AASHTO Standard Specification For Highway Bridges (1996) and AASHTO LRFD Bridge Design Specifications (1998).

2.2.1 ACI 318-02/318R-02 for Horizontal Shear

The *ACI 318-02/318R-02* (2002) approach consists of four equations for horizontal shear design. The use of each of these equations depends on the magnitude of the factored shear force and on the conditions of the interface. The design for horizontal shear is based on the following fundamental equation:

$$\mathbf{V_u \leq \phi V_{nh}}$$

where

V_u = factored shear force (required strength)

V_{nh} = nominal horizontal shear resistance

$\phi = 0.75$ (strength reduction factor)

For the factored shear force *ACI 318-02/318R-02* allows the designer to choose either the factored vertical shear force or the actual change in compressive or tensile force in any segment.

The horizontal shear resistance is determined as follows:

If $V_u \geq \phi 500\, b_v d$ (lb) then

$V_{nh} = A_{vf} f_y \mu <$ min ($0.2 f_c' A_c$ or $800 A_c$) (lb)

If $V_u < \phi 500\, b_v d$ (lb) then

1) $V_{nh} = 80\, b_v d$ (lb) if the contact surface is clean free of laitance, intentionally roughened and no shear reinforcement is provided.

2) $V_{nh} = 290\, b_v d$ (lb) if minimum ties are provided ($A_v = 50 b_v s/(f_y)$) contact surfaces are clean free of laitance, and intentionally roughened.

3) $V_{nh} = (260+0.6\rho_v f_y)\lambda\, b_v d < 500\, b_v d$ (lb) if contact surfaces are clean free of laitance intentionally roughened and more than the minimum amount of shear reinforcement is provided.

In the above equations:

b_v = width of the interface (in)

d = distance from extreme compression fiber to centroid of tension reinforcement for the entire composite section (in)

A_{vf} = area of shear reinforcement crossing the interface (in^2)

f_y = yield stress of the shear reinforcement (psi)

μ = coefficient of friction and depends on surface conditions.

$\mu = 1.4\lambda$ for concrete placed monolithically

$\mu = 1.0\lambda$ for concrete placed against hardened concrete with surface intentionally roughened.

$\mu = 0.6\lambda$ for concrete placed against hardened concrete with surface not intentionally roughened.

$\mu = 0.7\lambda$ for concrete anchored to as-rolled structural steel by headed studs or by reinforcing bars

λ = 1.0 for normalweight concrete

λ = 0.85 for for sand-lightweight concrete

λ = 0.75 for all lightweight concrete

A_c = area of concrete engaged in shear transfer (in^2)

ρ_v = ratio of the area of steel to the area of concrete.

The whole procedure of the ACI Code is summarized in Figure 2.3.

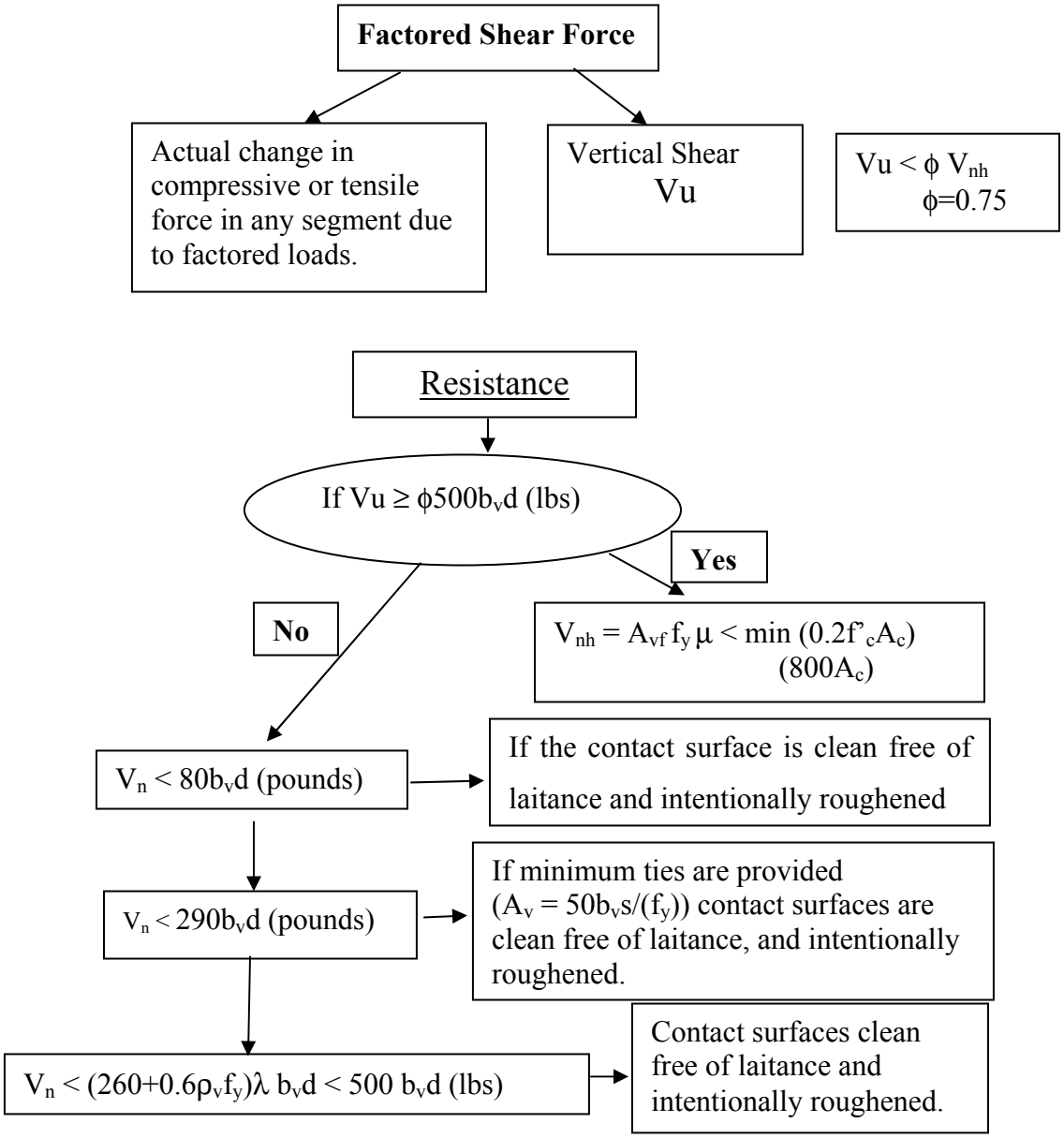

Figure 2.3 Summary of ACI 318 (02) for horizontal shear

The method provided in the ACI Code is used assuming that a crack occurs along the shear plane considered. The ACI Code allows the designer to use any other method whose results are in good agreement with comprehensive tests.

2.2.2 AASHTO Standard Specifications for Highway Bridges (Horizontal Shear)

AASHTO Standard Specifications for Highway Bridges (1998) follows a similar approach to *ACI 318/02* for horizontal shear. The design for horizontal shear is based on the fundamental equation:

$V_u < \phi V_{nh}$

where

V_u = factored vertical shear force acting at the section
V_{nh} = nominal horizontal shear strength
ϕ = strength reduction factor = 0.90

Note that the strength reduction factor is 0.9, different than 0.75, which is the strength reduction factor in the ACI 318/02.

When the contact surface is intentionally roughened, nominal shear resistance is obtained from one of the following three conditions:

a) when no reinforcement is provided:

$V_{nh} = 80 b_v d$ (lbs)

b) when minimum vertical ties are provided

$V_{nh} = 350 b_v d$ (lbs)

c) when required area of ties, $A_{vh,}$ exceeds the minimum area:

$$V_{nh} = 330\ b_v d + 0.40\ A_{vh}\ f_y d/s \qquad \text{(lbs)}$$

The minimum area of ties is:

$$A_{vh} = 50\ b_v s/f_y \qquad (in^2)$$

where, for the above equations:

b_v = width of cross-section at the contact surface being investigated for horizontal shear (in)

d = distance from extreme compression fiber to centroid of the prestressing force. As in vertical shear design, d need not be taken less than 0.80h (in)

s = maximum spacing not to exceed four times the least-web width of support element, nor 24 in. (in)

f_y = yield stress of the reinforcement (psi)

Note that the equation given in (c) above reduces to the equation in (b) when A_{vh} is set equal to $50\ b_v s/f_{y.}$

Prior to 1996 , *AASHTO Standard Specifications for Highway Bridges* required that all vertical shear reinforcement in a beam extend into cast-in-place slabs. However, that requirement has been removed from the 16th Edition, Standard Specifications, because large amounts of tie reinforcement may hinder efficient deck removal when the cast-in-place deck requires replacement. Therefore, only the minimum vertical shear reinforcement necessary to satisfy the horizontal shear requirements may extend into the deck. Also instead of extending vertical shear reinforcement, independent reinforcement may be provided. The whole procedure for horizontal shear design is summarized in Figure 2.4.

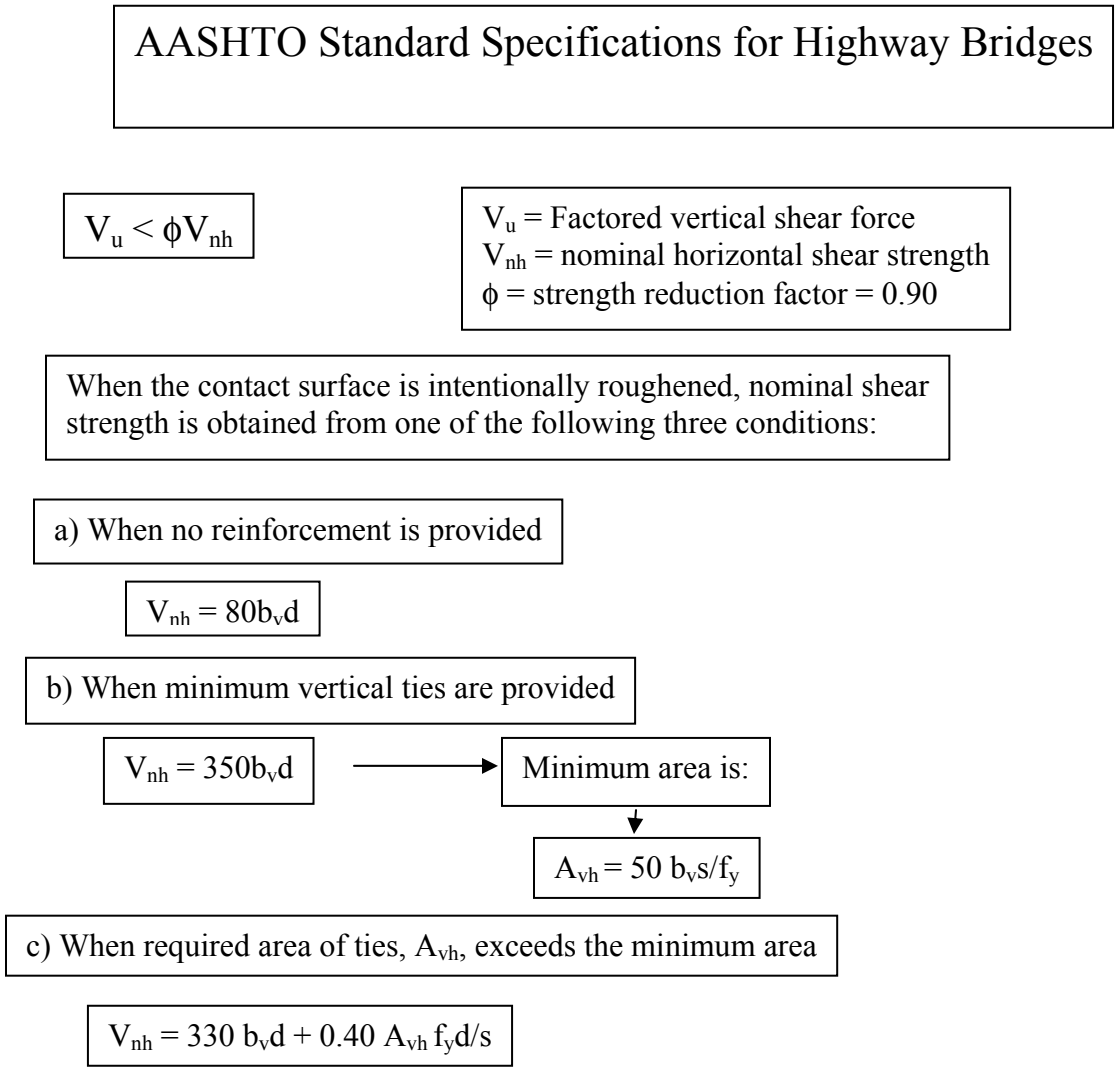

Figure 2.4 Horizontal shear approach in AASHTO Standard Specifications for Highway Bridges.

2.2.3 AASHTO LRFD Bridge Design Specifications For Horizontal Shear

Differing from the *ACI Code* and *AASHTO Standard Specifications for Highway Bridges,* the *AASHTO LRFD Bridge Design Specifications* approach for horizontal shear strength consists of a single linear equation.

To provide composite action, LRFD Specification requires that interface shear transfer be considered across a given plane at:

- An existing or potential crack
- An interface between dissimilar materials
- An interface between two concretes cast at different times.

The following formula may be used to compute the horizontal shear stress:

$$v_{uh} = \frac{V_u}{(d_v b_v)}$$

where

v_{uh} = horizontal factored shear force per unit area of interface (ksi)

V_u = factored vertical shear force at specified section due to superimposed loads (kips)

d_v = the distance between resultants of tensile and compressive forces = (d_e – a/2) (in)

b_v = interface width (in)

In design the following fundamental criteria shall be satisfied:

$$v_{uh} A_{cv} \leq \phi V_n$$

where V_n = nominal shear resistance of the interface surface (kips)

$$= c A_{cv} + \mu(A_{vf} f_y + P_c)$$

where

c = cohesion factor = 0.10 for concrete cast against concrete (ksi)

μ = friction factor = 1.0 for concrete cast against concrete

A_{cv} = interface area of concrete engaged in shear transfer (in^2)

A_{vf} = area of shear reinforcement crossing the shear plane within area A_{cv} (in^2)
P_c = permanent net compressive force normal to the shear plane (may be conservatively neglected) (kips)
f_y = yield strength of shear reinforcement (ksi)

Typically, the top surface of the beam is intentionally roughened to an amplitude of ¼ in.

Therefore, for normal weight concrete cast against hardened, roughened, normal weight concrete, the above relationships may be reduced to the following formula:

$$v_{uh} \leq \phi\ (0.1 + A_{vf}\ f_y / A_{cv}) \qquad \text{(ksi)}$$

where the minimum $A_{vf} = 0.05\ b_v s / f_y$ (in^2)
$\phi = 0.90$ (strength reduction factor).
Nominal shear resistance cannot exceed the lesser of:

$V_n < 0.2 f'_c\ A_{cv}$
$V_n < 0.8\ A_{cv}$

The whole procedure followed here is summarized in Figure 2.5.

AASHTO LRFD Bridge Design Specifications

$v_{uh} A_{cv} \leq \phi V_n$

$v_{uh} = V_u / (d_v b_v)$

v_{uh} = horizontal factored shear force per unit area of interface.
V_n = nominal horizontal shear resistance of the interface
$\phi = 0.90$

$\phi V_n = \phi(c A_{cv} + \mu(A_{vf} f_y + P_c)) < \min (0.2 f'_c A_{cv} \text{ or } 0.8 A_{cv})$

c = cohesion factor = 0.10 for concrete cast against hardened concrete (ksi)
μ = friction factor = 1.0 for concrete cast against concrete
A_{cv} = interface area of concrete engaged in shear transfer (in^2)
P_c = permanent net compressive force normal to the shear plane (may be conservatively neglected) (kips)
f_y = yield strength of shear reinforcement (ksi)
A_{vf} = area of shear reinforcement crossing the shear plane within area A_{cv} (in^2)
Min $A_{vf} = 0.05 b_v s / f_y$ (in^2)

Figure 2.5 Summary of the horizontal shear approach in AASHTO LRFD Bridge Design Specifications

AASHTO LRFD Bridge Design Specifications require that minimum reinforcement be provided regardless of the stress level at the interface, however designers may choose to limit this reinforcement to cases where v_u / ϕ is greater than 0.10 ksi. This would be consistent with the Standard Specifications, the ACI Code and other references. It might unnecessary to provide connectors in a number of common applications, such as the precast panels, if the interface stress is lower than 0.10 ksi.

2.2.4 CEB-FIP Model Code 90

CEB-FIP Model Code 90 (1990) provides an interesting approach for horizontal shear design. For rough interfaces the shear resistance due to concrete-to-concrete friction may be evaluated by means of the equation:

$$\tau_{fu,d} = 0.40 f_{cd}^{2/3} (\sigma_{cd} + \rho f_{yd})^{1/3}$$

where

f_{cd} = design value of the compressive strength of concrete (MPa)

f_{yd} = design yield stress of the reinforcement which perpendicularly intersects the interface (MPa)

ρ = reinforcement ratio

σ_{cd} = averaged normal stress acting on the interface.

The shear stress values given in this equation correspond to a shear slip value, s, approximately equal to 2.0 mm.

Where less than 2.0 mm slip occurs along the interface, the mobilized shear stress corresponding to the actual shear slip value may be calculated as follows:

For s < 0.10 mm

$$\tau_{fd} = 5\tau_{fu,d}s$$

for s > 0.10 mm

$$\left(\frac{\tau_{fd}}{\tau_{fu,d}}\right)^4 - 0.5\left(\frac{\tau_{fd}}{\tau_{fu,d}}\right)^3 = 0.3s - 0.03$$

with s in mm.

The shear slip along a rough interface is associated by a crack opening, which may be calculated as follows:

$w = 0.6s^{2/3}$

with w and s in mm.

CEB-FIP Model Code 90 addresses specifically a very important issue in horizontal shear transfer, which is dowel action. In all the other codes the term dowel action is used in horizontal shear design provisions but none of the codes specifies when the dowel action of the shear reinforcement is mobilized.

The design value of the maximum shear force, that may be transferred by a reinforcing bar crossing a concrete interface (dowel action) may be calculated by means of the following equation provided that the geometrical conditions, given in Figure 2.6 and Figure 2.7, are satisfied.

$$F_{ud} = \frac{1.30}{\gamma_{Rd}} \phi_b^{\,2} \left(\sqrt{(1+(1.3\varepsilon)^2)} - 1.3\varepsilon\right) \sqrt{(f_{cd} f_{yd} (1-\varsigma^2))} \le \frac{A_s f_{yd}}{\sqrt{3}}$$

with

$$\varepsilon = 3 \frac{e}{\phi_b} \sqrt{\left(\frac{f_{cd}}{f_{yd}}\right)}$$

where

ϕ_b = diameter of the dowel

A_s = cross-sectional area of the dowel

f_{cd} = design value of the compressive strength of concrete

f_{yd} = design value of the steel yield stress

e = load eccentricity

γ_{Rd} = supplementary partial coefficient, may be taken equal to 1.3

$\zeta = \sigma_s / f_{yd}$ (where σ_s is the simultaneous axial stress on the bar (MPa)).

The shear displacement along a concrete to concrete interface, which is needed for the mobilization of F_{ud} may be taken equal to $0.10\phi_b$.

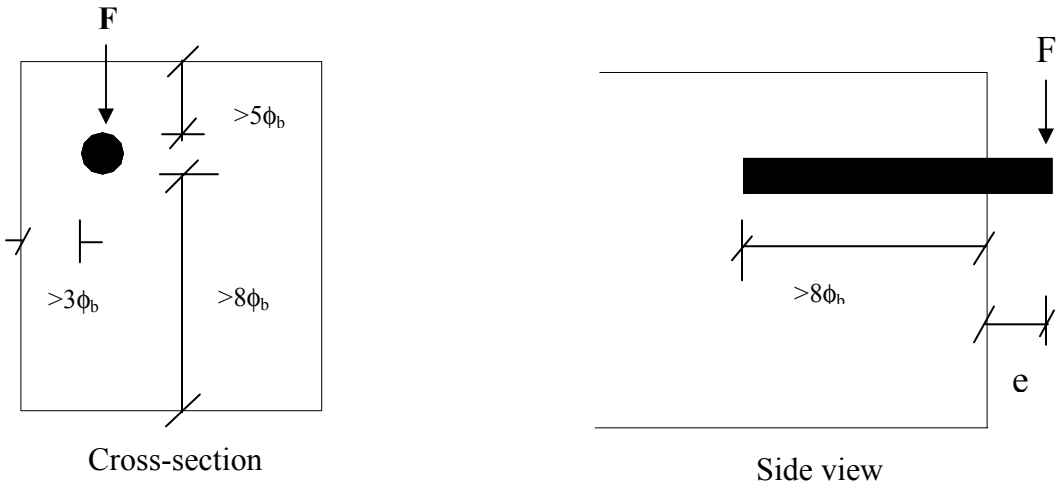

Figure 2.6. Geometrical conditions

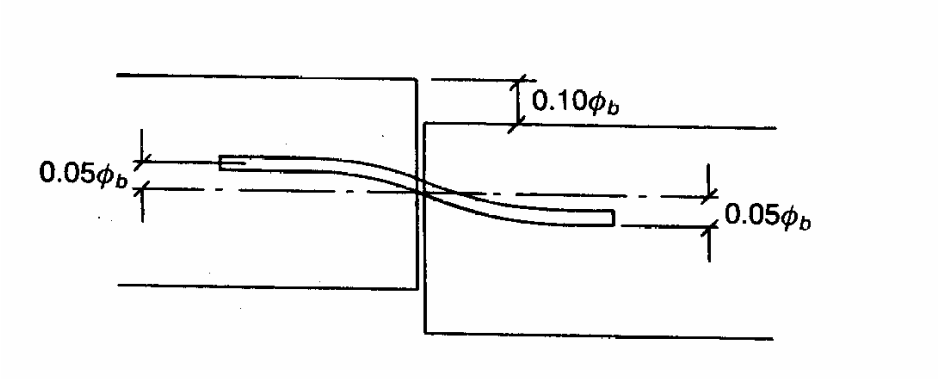

Figure 2.7 Shear displacement needed for the mobilization of F_{ud}, from *CEB-FIP Model Code 90*

2.2.5 Other Proposed Equations

Many studies have been performed to develop an equation, that provides satisfactory prediction of the interface horizontal shear strength. The following sections present different prediction equations that have been proposed by various researchers.

2.2.5.1 Mattock's Equations

Mattock (1969) proposed an equation for horizontal shear strength, which is provided in the commentary of the ACI Code. The horizontal shear strength prediction equation is:

$$V_n = 0.8*A_{vf}\, f_y + A_c K_1$$

Where A_c is the area of concrete section resisting shear transfer (in^2) and K_1 = 400 psi for normal weight concrete, 200 psi for all-lightweight concrete, and 250 psi for sand-lightweight concrete. The ACI Commentary states that the values of K_1 apply to both monolithically cast concrete and to concrete cast against hardened concrete with a rough surface to a full amplitude of ¼ in.

The ACI Commentary states that in this equation, the first term represents the contribution of friction to shear transfer resistance (0.8 representing the coefficient of friction) and the second term represents the sum of the resistance to shearing of protrusions on the crack faces and the dowel action of the reinforcement. This comment is a little ambiguous. In this equation, it would seem that the contribution of the dowel action should be considered part of the first term, which contains the area of the shear reinforcement and the yield strength of the bar. In addition, the contribution of the friction and aggregate interlock (or shearing of protrusions) are so intertwined or combined together that it is difficult to determine the effect of each separately.

Mattock authored a series of papers, which were written in the framework of providing an equation to predict horizontal shear strength. In the following equation Mattock (1972) also includes the effect of a normal force to the shear plane.

$$v_n = 0.8*(\rho f_y + \sigma_{nx}) + K_1$$

with the restrictions that v_n shall be not more than $0.3f'_c$ and $(\rho f_y + \sigma_{nx})$ shall be not less than 200 psi. σ_{nx} is the externally applied direct stress acting across the shear plane, taken as positive for a compressive stress and negative for a tensile stress.

Another conclusion made by Mattock concerning horizontal shear design is that, within their range of applicability, the shear friction provisions of ACI 318-71, which are slightly different than the provisions of ACI 318-02, yield a conservative estimate of the shear transfer strength of reinforced concrete whether or not a crack exists in the shear plane. Also for higher shear transfer strengths than the upper limit of 800 psi or $0.2f'_c$, Mattock suggests that his equation may be used to proportion shear reinforcement.

Concerning the fundamental behavior of push-off tests Mattock concludes that:

1. Changes in strength, size, and spacing of the reinforcement affect the shear strength only insofar as they change the value of the reinforcement parameter ρf_y for $f_y < 66$ ksi

2. An externally applied compressive stress acting transversely to the shear plane is additive to ρf_y in calculations of the ultimate shear transfer strength of both initially cracked and uncracked concrete.
3. The shear transfer strength of initially cracked concrete with moderate amounts of reinforcement is developed primarily by frictional resistance to sliding between the faces of the crack and by dowel action of the reinforcement crossing the crack. When large amounts of reinforcement, or sufficient externally applied compression stresses normal to the shear plane are provided, then the crack in the shear plane "locks up" and shear transfer strength is developed as in initially uncracked concrete.

Mattock (1974) added the effect of concrete strength into his previous equation and introduced it as :

$v_n = 4.5 * f'_c{}^{0.545} + 0.8 * (\rho f_y + \sigma_n)$ (psi)

$v_n < 0.3 f'_c$

2.2.5.2 Loov and Patnaik

Loov (1978) was the first to introduce a parabolic equation for horizontal shear strength and include the effect of concrete strength. The first equation that he proposed in 1978 is as follows:

$$v_n = k\sqrt{\rho f_y f'_c}$$

where *k* is a constant.

A *k* of 0.5 was suggested for initially uncracked shear interfaces.

Loov and Patnaik (1994) performed 16 beam tests to develop a strength equation for horizontal shear. The proposed equation is as follows:

$$v_n = k\lambda\sqrt{((15+\rho f_y)f'_c} \le 0.25f'_c \qquad \text{(psi)}$$

Loov suggests that for routine designs, it is desirable to use slightly lower shear strength to allow for the possibility of smoother interfaces. Therefore for composite construction, a factor of 0.5 for k is suggested. For monolithic construction, there is no joint at the shear interface. Therefore, the additional level of safety to account for the possible variation in roughness is not warranted and the value of *k* can be kept as 0.6. The factor λ varies for lightweight concrete as per ACI 318-02 stated in Section 2.2.1.

Patnaik (2001) performed a study on the behaviour of composite concrete beams with a smooth interface. He proposed the following equation for the nominal horizontal shear stress:

$v_u = 0.6 + \rho_{vf} f_{yf} \le 0.2 f'_c$ and 5.5 MPa

$v_u = 0$ for $\rho_{vf} f_{yf} \le 0.35$ MPa

2.2.5.3 Linear Shear Friction Equation

This equation was first introduced by Mast (1958) and was later developed further by Birkeland, Anderson (1960) and their co-workers:

$v_n = \rho f_y \mu$

where μ is the coefficient of friction and varies according to the conditions of the concrete surface.

The equation is simple but very conservative for low clamping stresses and unsafe for high clamping stresses.

2.2.5.4 Birkeland's Equation

Birkeland (1966) was the first to introduce a parabolic function for shear strength along an interface:

$v_n = 33.5 * \sqrt{f_y \rho}$ (psi)

2.2.5.5 Shaik's Equation

Shaikh (1978) suggested an equation which can be expressed as:

$v_u = \phi \rho f_y \mu_e$

in which

$\mu_e = 1000 \frac{\lambda^2}{v_u} \leq 2.9$ (psi)

where 1.0λ has been substituted for μ, and λ is a constant used to account for concrete density.

$\lambda = 1.0$ for normal weight concrete
$\lambda = 0.85$ for sand light-weight concrete
$\lambda = 0.75$ for all lightweight concrete

The design requirements of PCI (1999) are based on this equation for the cases when $V_u > \phi 500bvd$ and for smaller shear forces than this limit the same procedure as in the ACI Code is used.

If the equation for v_u and μ_e are combined, a parabolic equation for v_u with respect to the clamping force is obtained:

$v_u = \lambda \sqrt{1000 \phi \rho f_y} \leq 0.25 f'_c \lambda^2$

where the strength reduction factor, $\phi = 0.85$ for shear.

Loov (1994) states that this equation is similar to Rath's (1977) equation and together with Birkeland's (1966) equation it represents the test data more closely than the linear shear-friction equation, but it does not include the concrete strength as a parameter.

2.2.5.6 Walraven's Equation

Walraven (1988) performed 88 push-off tests and proposed the following equation for a precracked shear interface:

$$v_n = C_1\left(\rho f_y\right)^{C_2} \quad \text{(psi)}$$

If f'_c is assumed to be equal 0.85 of the compressive strength of 6 in cubes:

$C_1 = 16.8\ f'_c{}^{0.406}$ $\qquad$ $C_2 = 0.0371\ f'_c{}^{0.303}$

2.2.5.7 Mau and Hsu's Equation

Mau and Hsu (1976) suggested an equation similar to Loov's equation with a *k* of 0.66. They assumed that the factor 0.66 would be the same for both initially cracked and uncracked shear interfaces.

2.2.5.8 Push-off Tests

Hanson (1960) made a study to correlate push-off tests and beam tests by comparing shear slip relations of the two types of specimens. He concluded that push-off tests are representative of beam tests for "rough bonded" connections.

2.2.5.9 Limiting Slips

According to Hanson (1960) the maximum horizontal shear strength is reached at a slip of 0.005 in. However the idea to a fix a limit for slip was quite controversial. According to Grossfield and Birnstiel (1962) larger shear strengths would be recorded if

larger slips were permitted. Patnaiks (2001) says that this limit greatly restricts the full utilization of strength of composite concrete beams.

2.3 Summary of Literature Review

This chapter has presented previously performed research on the precast panel system, on horizontal shear strength and on shear friction. Also presented were current code equations for quantifying horizontal shear strength. However none of the previous studies nor any of the codes addresses the case when the interface consists of two precast elements bonded by means of grout. Hence this study was initiated and a total of 36 push-off tests were performed to investigate this case.

CHAPTER 3 : DESCRIPTION OF TESTS

3.1 Specimen Description

To develop a better understanding of the horizontal shear strength at the interface between the slab and girder in the precast deck panel system, 36 push-off tests were performed. Figure 3.1 illustrates a typical push-off test specimen.

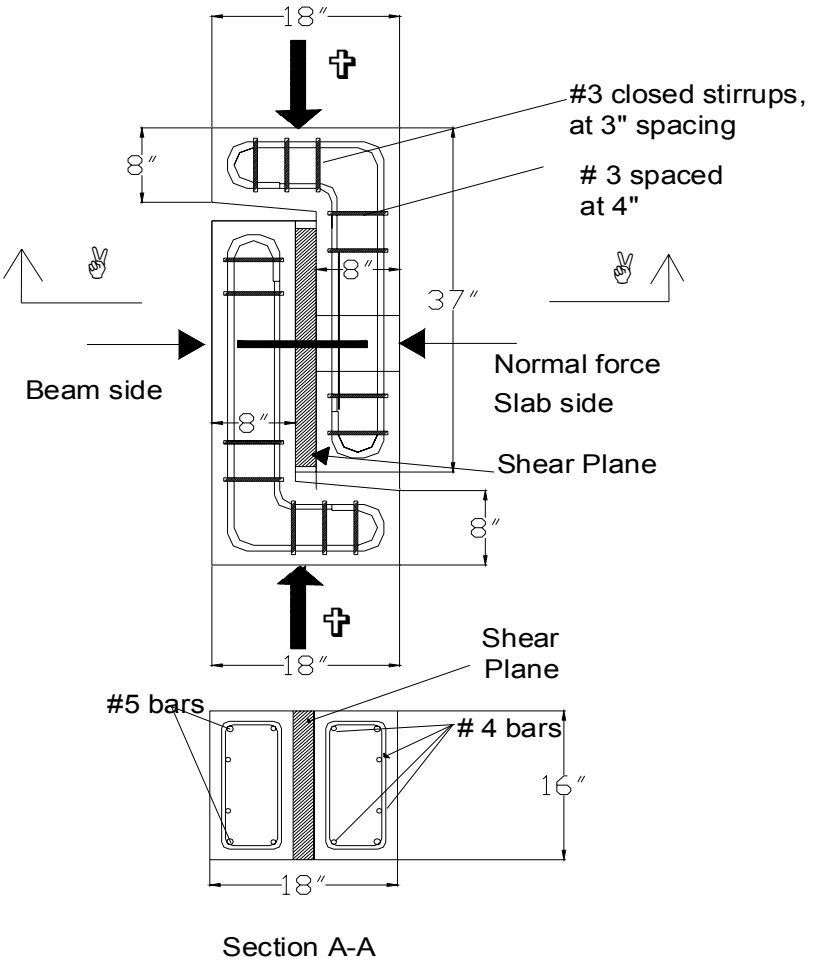

Figure 3.1 Typical push-off test specimen.

This type of push-off test was performed by Mattock (1969) with the exception that his specimens were cast monolithically. The objective of having two L-shaped specimens positioned and loaded as shown in Figure 3.1 is to apply a direct shear force, without any eccentricity at the interface. In this way the interface is tested only for its shear resistance. The gap between the beam and the slab element is filled with grout in order to provide bond.

3.2 Specimen Fabrication

In this testing program one-half of the specimen represents the precast beam and the other half the precast slab. Figure 3.2 illustrates the casting position of each element. This orientation was selected to mimic the interface conditions of the beam and the slab

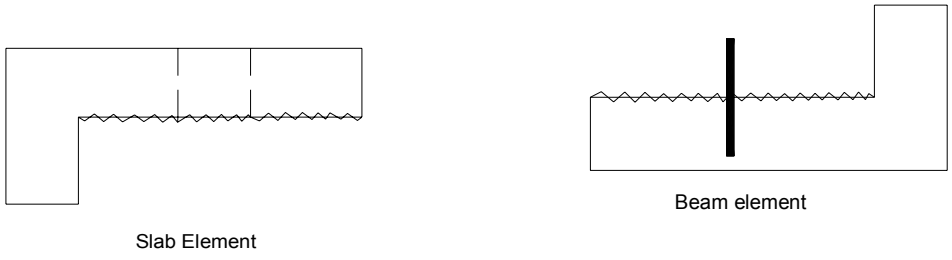

Figure 3.2 Casting orientation of beam and slab elements.

in the precasting yard. The top surface of the beam is exposed to the air and the bottom surface of the slab is supported on the formworks.

The top surface of each precast beam element was raked at the time the concrete was placed so it would provide a better bond with the grout. On the slab element, before pouring the concrete into the formwork a piece of cloth soaked in a retarder mix was placed on the formwork. The day after placing the concrete, the slab formwork was stripped, the piece of cloth was taken off and the bottom part of the slab element was hosed with water to remove the outer sand and unhydrated mortar, and expose the aggregates. The role of the retarder as its name implies is to retard the hydration of the cement so the sand and mortar can be easily removed when it is hosed with water.

With these procedures, the surfaces of the beam and the slab at the interface were rough to create a better bond with the grout. Figure 3.3 show the exposed aggregates on the bottom of the slab element and Figure 3.4 shows the raked surface of the beam element.

Figure 3.3 Formation of the rough surface on the slab element

Figure 3.4 The raked surface of the beam element.

The concrete mix consisted of ¾ in. angular, crushed limestone aggregates and the desired strength for both the beam and the slab element was 5000 psi. The grout pockets on the slab side were formed by placing 6 in. by 12 in. cylinder molds on the formwork before the concrete was poured and by removing them the following day.

3.3 Grouting the Interface

To provide a bond between the slab and the beam element the interface was grouted. The beam elements had various types of shear connectors and the slab elements had shear pockets. When the elements were put together, the shear connector from the beam side was positioned in the shear pocket on the slab side. This is illustrated in Figure 3.5.

Figure 3.5 Shear connector on the beam element and shear pocket on the slab element.

A space between the two elements was provided to represent the haunch between the beam and the slab in practice. Later this haunch and the shear pocket were grouted. Figure 3.6 shows the haunch and formwork before and after grouting. The formwork for grout was placed in the gap that was provided for the relative slip of the elements.

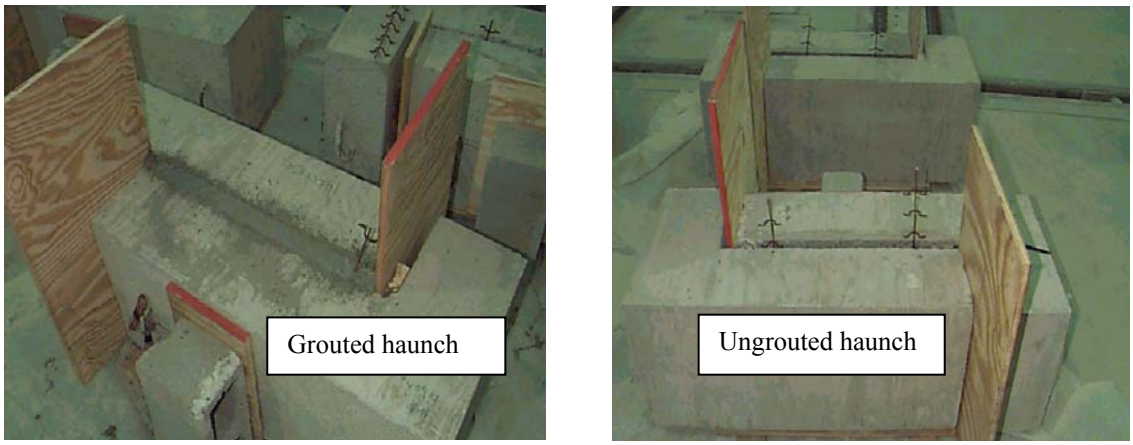

Figure 3.6 The haunch and formwork before and after grouting

3.4 Test Set-Up

After the interface grout had achieved the required strength, the specimens were prepared for testing.

3.4.1 Description

The two bonded elements; the precast beam and the precast slab were supported as shown in Figure 3.7 on four steel pipes, which served as rollers to allow the elements to slip relative to each other as the direct shear force was applied. The shear force was applied by a hydraulic ram and was monitored by a 150 kip load cell. A normal force was applied to represent the self-weight of the deck on the top of the girder. A force of approximately 2.5 kips was calculated using a 10 ft spacing of girders a 8.5 in. thick deck with a concrete of unit weight 150 pcf. In practice the spacing of the beams, the thickness of the deck, the wearing surface and the type of concrete varies, however the normal force was kept in the range of 2.5-3.5 kips.

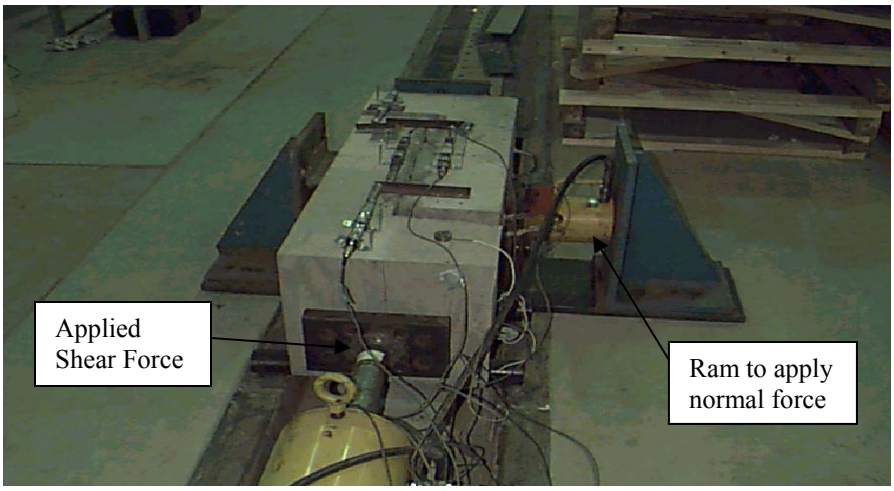

Figure 3.7 Test set-up

3.4.2 Instrumentation

The instrumentation that was used includes a 150 kip load cell which was used to monitor the applied shear force, a 10 kip load cell to monitor the normal force, potentiometers to measure the slip at the interface and bonded electrical resistance (ER) strain gages to measure the strain in the shear connectors. Each potentiometer was fixed to one of the elements, either the beam or the slab, and a piece of angle was fixed at the other element. In this way as the beam and the slab elements moved relative to each other the plunger in the potentiometer was compressed and the slip was measured. This is illustrated in Figure 3.8. Strain gages were bonded to both legs of the shear connectors. Strain gages were waterproofed to protect them from the moisture of the grout as the grouting process was performed.

3.4.3 Procedure

The first operation in the testing procedure was to apply the normal force on the slab element with a hydraulic ram. The force was monitored with a 10 kip load cell. The beam element was supported by a steel plate on the side opposite the ram, as shown in Figure 3.8 . The steel plate was supported on rollers so that it could slide as the shear

force was applied. When the normal force was approximately 2.5 kip, the shear force was applied by the 150 kip ram, which was controlled by a hand pump. Load was increased until the bond at the interface was broken. At the point when a crack formed at interface, the specimen had a tendency to expand increasing the normal force. But since the normal force was applied to represent the self-weight of the slab in the field and since this weight is constant the normal force was dropped back to the range 2.5 – 3.5 kips. Loading continued until the specimens had slipped approximately 1 in. or the gap between the sides of the specimen closed.

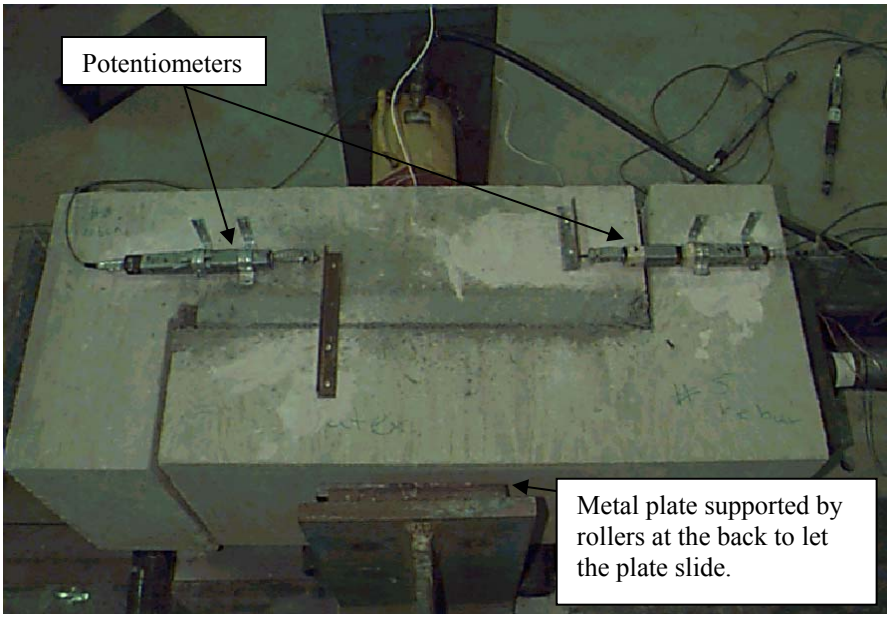

Figure 3.8 Test set-up details

3.5 Test Parameters and Series Details

A total of three series of tests were performed. Each series consisted of 12 tests. The test parameters included grout type, haunch height, and the alternative shear connectors. Tables 3.1, 3.2 and 3.3 present the test parameters for the three series.

Table 3.1 Test Parameters in Series 1

Test designation	Number of tests	Type of Grout	Haunch height	Type of shear connectors
Test 1- series 1- latex- 1”haunch- no connectors Test 2- series 1- latex- 1”haunch- no connectors	2	Latex	1”	No connectors
Test 3- series 1- latex- 1”haunch- 1#4 stirrup Test 4 - series 1- latex- 1”haunch- 1#4 stirrup	2	Latex	1”	1 # 4 stirrup
Test 5 -series 1- latex - 1”haunch -1#5 stirrup Test 6- series 1- latex- 1”haunch- 1#5 stirrup	2	Latex	1”	1 # 5 stirrup
Test 7- series 1- set 45- 1”haunch- no connectors Test 8- series 1- set 45- 1”haunch- no connectors	2	Set 45	1”	No connectors
Test 9- series 1- set 45- 1”haunch- 1#4 stirrup Test 10- series 1- set 45 1”haunch- 1#4 stirrup	2	Set 45	1”	1 # 4 stirrup
Test 11 -series 1- set 45- 1”haunch- 1#5 stirrup Test 12- series 1- set 45- 1”haunch -1#5 stirrup	2	Set 45	1”	1 # 5 stirrup

Table 3.2 Test Parameters in Series 2.

Test designation	Number of tests	Type of Grout	Haunch height	Type of shear connectors
Test 1- series 2- set 45- 3”haunch- no connectors Test 2- series 2- set 45- 3”haunch- no connectors	2	Set 45	3”	No connectors
Test 3 -series 2- set 45- 3”haunch- 1#4 stirrup Test 4- series 2 -set 45- 3”haunch -1#4 stirrup	2	Set 45	3”	1 # 4 stirrup
Test 5- series 2- set 45- 3”haunch -1#5 stirrup Test 6- series 2- set 45- 3”haunch- 1#5 stirrup	2	Set 45	3”	1 # 5 stirrup
Test 7- series 2- set 45- 1”haunch- 2#4 stirrup Test 8- series 2- set 45 1”haunch- 2#4 stirrup Test 12- series 2- set 45- 1”haunch- 2#4 stirrup	3	Set 45	1”	2 # 4 stirrup
Test 9- series 2- set 45- 2”haunch- 1#5 stirrup Test 10- series 2- set 45- 2”haunch- 1#5 stirrup	2	Set 45	2”	1 # 5 stirrup
Test 11- series 2- set 45- 3”haunch- 2#4 stirrup	1	Set 45	3”	2 # 4 stirrup

Table 3.3 Test Parameters in Series 3.

Test Designation	Number of tests	Type of Grout	Haunch height	Installed as	Interface state	Type of shear connectors
Test 1- series 3- set 45- 3"haunch 1#5 stirrup Test 2- series 3- set 45- 3"haunch- 1#5 stirrup	2	Set 45	3"	Pre-installed	Intentionally roughened	1#5 stirrup
Test 3- series 3- set 45- 1"haunch -2 hooked#5 Test 4 - series 3 - set 45- 1"haunch- 2 hooked#5	2	Set 45	1"	Post-installed with epoxy	Intentionally roughened	2 hooked #5 bar
Test 5- series 3- set 45- 1"haunch -2 hooked#6	1	Set 45	1"	Post-installed with epoxy	Intentionally roughened	2 hooked #6 bar
Test 6- series 3- set 45- 1"haunch -1 hooked#6	1	Set 45	1"	Post-installed with epoxy	Intentionally roughened	1 hooked #6 bar
Test 7- series 3- set 45- 1"haunch - 4 hooked #5 Test 8- series 3- set 45- 1"haunch -4 hooked #5	2	Set 45	1"	Post-installed with epoxy	Intentionally roughened	4 hooked #5 bar
Test 9- series 3- set 45- 1"haunch- ¾ coil bolt Test 10- series 3- set 45- 1"haunch- ¾ coil bolt.	2	Set 45	1"	Post-installed bolt with pre-installed insert	Intentionally roughened	¾ coil bolt
Test 11- series 3- set 45- 1"haunch- ¾ coil bolt shear keys Test 12- series 3- set 45- 1"haunch- ¾ coil bolt shear keys	2	Set 45	1"	Post-installed bolt with pre-installed insert	Not-intentionally roughened with shear keys.	¾ coil bolt

3.5.1 Series 1

The goal of the first series was to investigate the performance of two different types of grouts, which were a latex modified mix and Set 45 Hot Weather grout.

The latex modified mix was prepared in the laboratory. The mix design and the compressive strength are given in Table 3.4:

Table 3.4 Mix design and tested compressive strength of Latex Modified Grout.

Mixture designs for 1 cubic yard (27 ft^3) of latex modified mix.	
Cement Type I/II	658 lb
Sand	1503.53 lb
Aggregate	1250.2 lb
Water	145.78 lb
Latex	204 lb
W/C	0.38 lb

Time (days)	Compressive strength (ksi)
1	1.75
28	6.75
48	6.96

Set 45 hot weather mix, which is also known as Magnesium Amonium Phosphate ($MgNH_4PO_4$), is produced by Master Builders. The hot weather formula was extended by adding 25 lb of angular ¼ in. aggregate to each 50 lb bag of Set 45. The recommended water content is 3.75 lb per 50 lb bag. But since the hot weather mix was extended with aggregates an additional of 1.09 lb of water per bag was added. The typical tested compressive strength of Set 45 Hot Weather mix is provided in Table 3.5.

Table 3.5 Tested compressive strength of Set 45.

Time (days)	Compressive strength (ksi)
7	4.38
12	6.58
28	6.94

For each type of grout, three horizontal shear connector details were tested: no connectors, 1 No. 4 stirrup, and 1 No. 5 stirrup.

3.5.2 Series 2

The second test series was performed to investigate the influence of varying the haunch height. The haunch height will vary because of the camber in the precast prestressed beam. The prestressing force, which is usually applied at an eccentricity below the centroid of the beam, causes the beam to camber up. This phenomenon is illustrated in Figure 3.9.

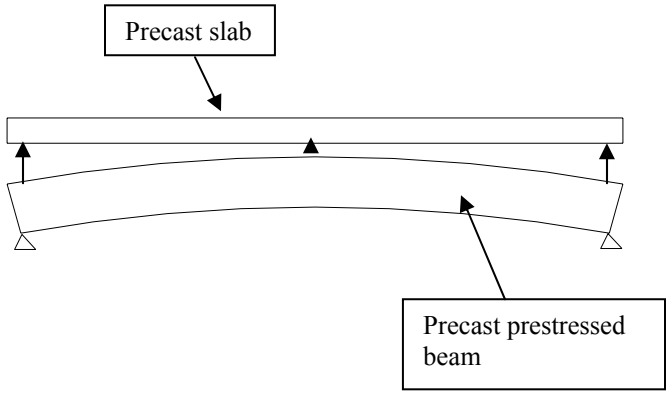

Figure 3.9 Camber in the precast prestressed beam

After the completion of the second Series there were four connector details (no connetors, 1 No. 4, 1 No. 5, and 2 No. 4 stirrups), each tested with a 1in. and 3 in.

haunch. And there was one detail (1 No. 5 stirrup) tested with a 1 in., 2 in., and 3 in. haunch.

In the first two series six tests had no shear connectors at all. This was done to quantify the contribution of the cohesion between the grout and the concrete to the horizontal shear strength. For the other specimens in the first two series, the shear connectors were extended double leg stirrups as shown in Figure 3.10.

Figure 3.10 Extended double leg stirrups used as shear connectors.

3.5.3 Series 3

The goal of the last series of tests was to investigate the performance of different types of shear connectors other than conventional extended stirrups. These shear connectors included post-installed hooked rebars and Dayton Richmond anchors. Both of these shear connectors are illustrated in Figures 3.11 and 3.12. The hooked rebars were very convenient and practical to install. After the casting of concrete, a hole is drilled on the beam element. The hole is cleaned of the dust with compressed air. Epoxy is then poured in the hole to provide the bond and the hooked rebar is put in the hole.

As can be seen from Figure 3.12 the Dayton Richmond anchors consist of two parts, the coil insert and the bolt. The coil insert is installed before the pouring of concrete on the beam element and the bolt is threaded in once the beam and the slab element are placed together. A big advantage of this type of shear connection is that during the rehabilitation process or slab removal the bolts can be unscrewed, making the slab removal process easier.

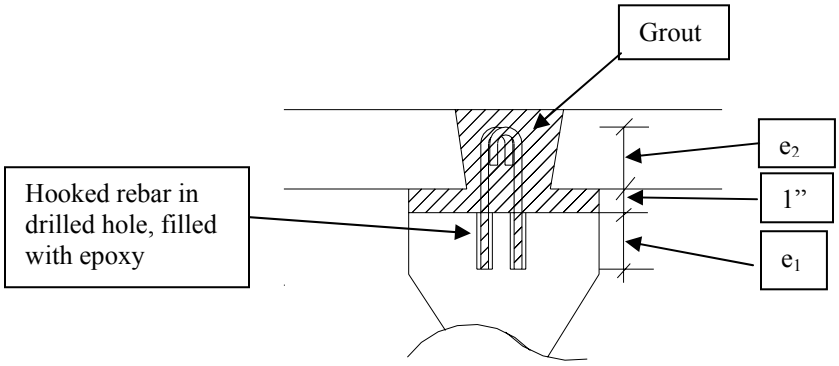

embedment depth e_1 = 5 “ for # 5 bars
embedment depth e_2 = 5.5 “ for # 5 bars
embedment depth e_1 = 6.5 “ for # 6 bars
embedment depth e_2 = 5.25 “ for # 6 bars

Figure 3.11 Post-installed hooked rebars

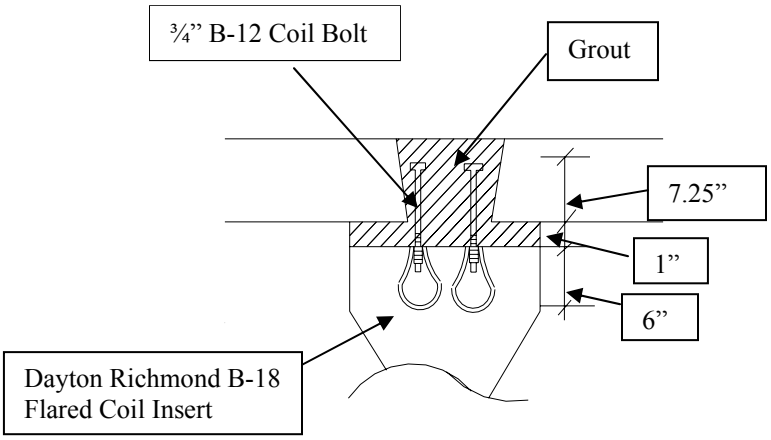

Figure 3.12 Dayton Richmond anchors

Two of the tests in Series 3 investigated the use of shear keys on the beam side. These shear keys are illustrated in Figure 3.13. In these two tests the top surface of the beam element was not roughened. Prior to placing the concrete two pieces of 2 x 4 lumber were fixed at the top of the beam formwork. After the concrete was hardened these two pieces of 2 x 4 were removed providing the shear keys.

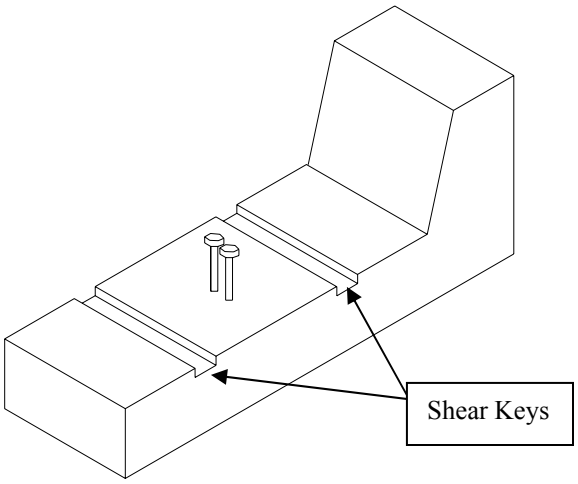

Figure 3.13 Shear keys at the top of the beam element.

This type of system was investigated by Tadros (2002) for cast-in-place decks, to create a more easily replaceable deck. The system uses the mechanical anchorage of shear keys on the top flange of the girder. To make the deck removal process easier a debonding agent is applied on the shear keys. In this project the debonding agent was not applied.

CHAPTER 4: PRESENTATION OF RESULTS AND ANALYSIS

This chapter presents results of the testing program. Typical load slip plots are presented and failure modes discussed. All results are then compared to current code strength prediction equations. The load-slip and load-strain plots of all the tests are presented in Appendix A and Appendix B, respectively.

4.1 Typical Push-off Test Behavior

In almost all of the tests the specimen reached its maximum load immediately before the bond was broken. After the crack occurred, for the specimens that had no connectors, some small shear capacity was maintained. For the specimens that had shear connectors, once the bond was broken the load was reduced and maintained for large slips at a value equal to the yield capacity of the connectors times some factor. Figure 4.1 presents a load slip curve for a typical specimen with no shear connectors. At the peak load the strain level at the rebars was different for different tests. In some of the tests the strain prior to cracking of the interface was close to the yield strain and in some others much smaller than the yield. Figure 4.2 shows load versus strain diagram prior to the crack and Figure 4.3 shows load versus strain diagram after the crack. In figure 4.2 the strain level at the rebar for that particular test was about 650 microstrain which is about 30 % of the yield strain. Figure 4.3 shows the strain level in the rebar during the whole duration of the test. Once the specimen reached its maximum load and the bond was broken the strain in the rebar passed its yield point.

4.1.1 Tests with No Shear Connectors

As can be seen from Figure 4.1, for the specimens with no connectors, the post-crack load maintained is about 8 kips. The load divided by the area of the interface, which is 16 in. x 26 in. = 416 in.^{2}, results in an average shear stress of approximately 19 psi. The maximum load divided by the area of the interface results in a maximum shear stress of 125 psi for this specific test.

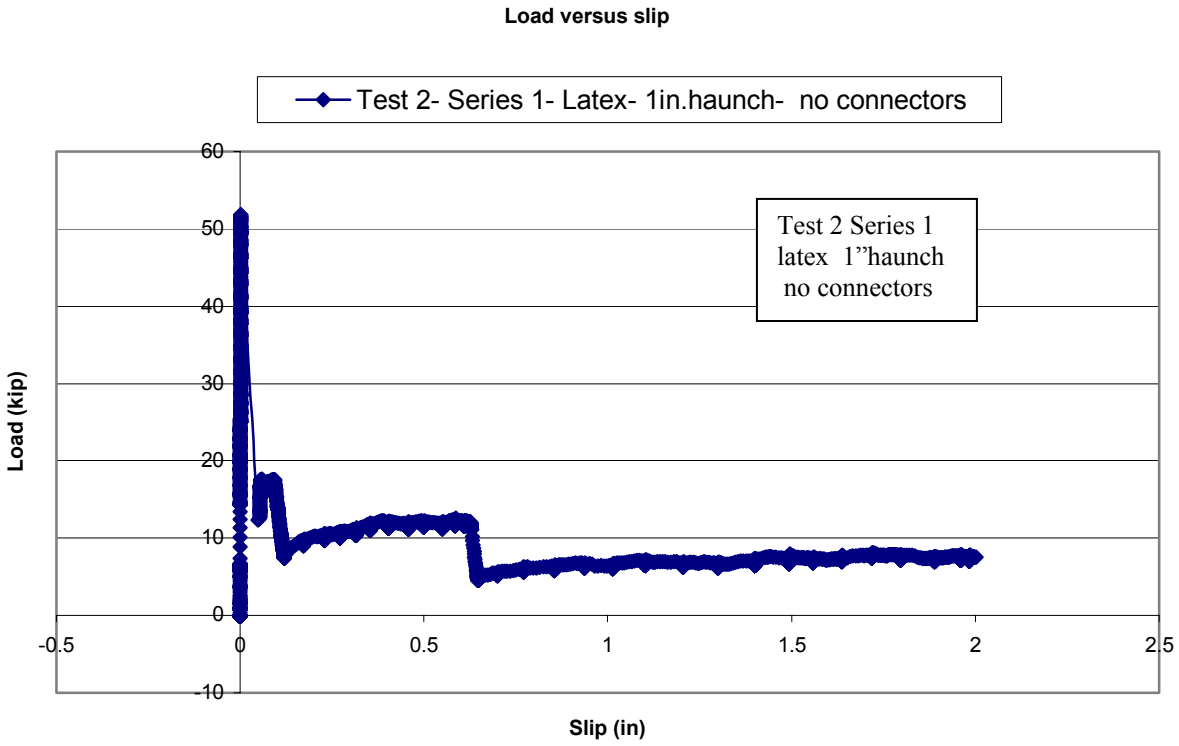

Figure 4.1 Typical load slip behavior of a specimen with no shear connectors.

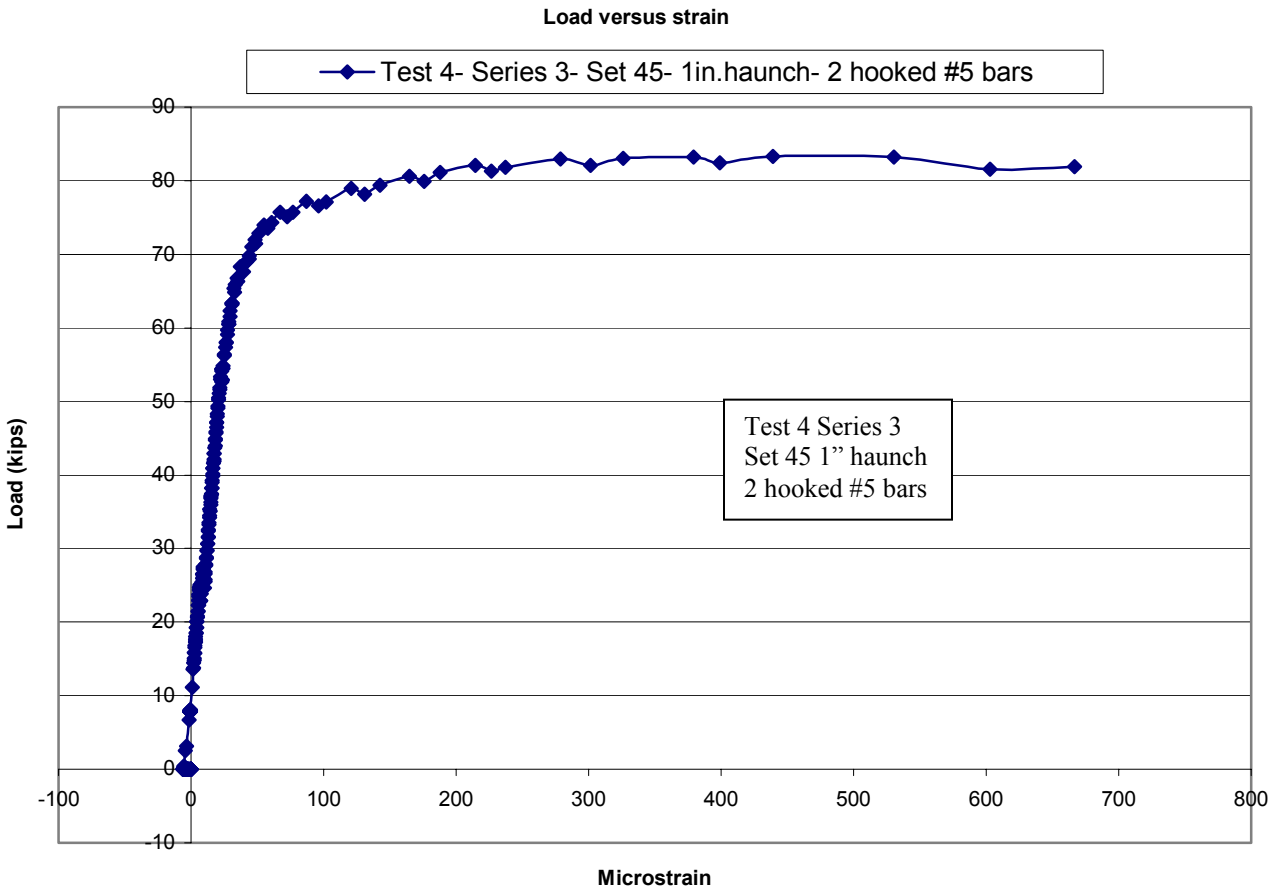

Figure 4.2 Load versus strain diagram for Test 4 Series 3.

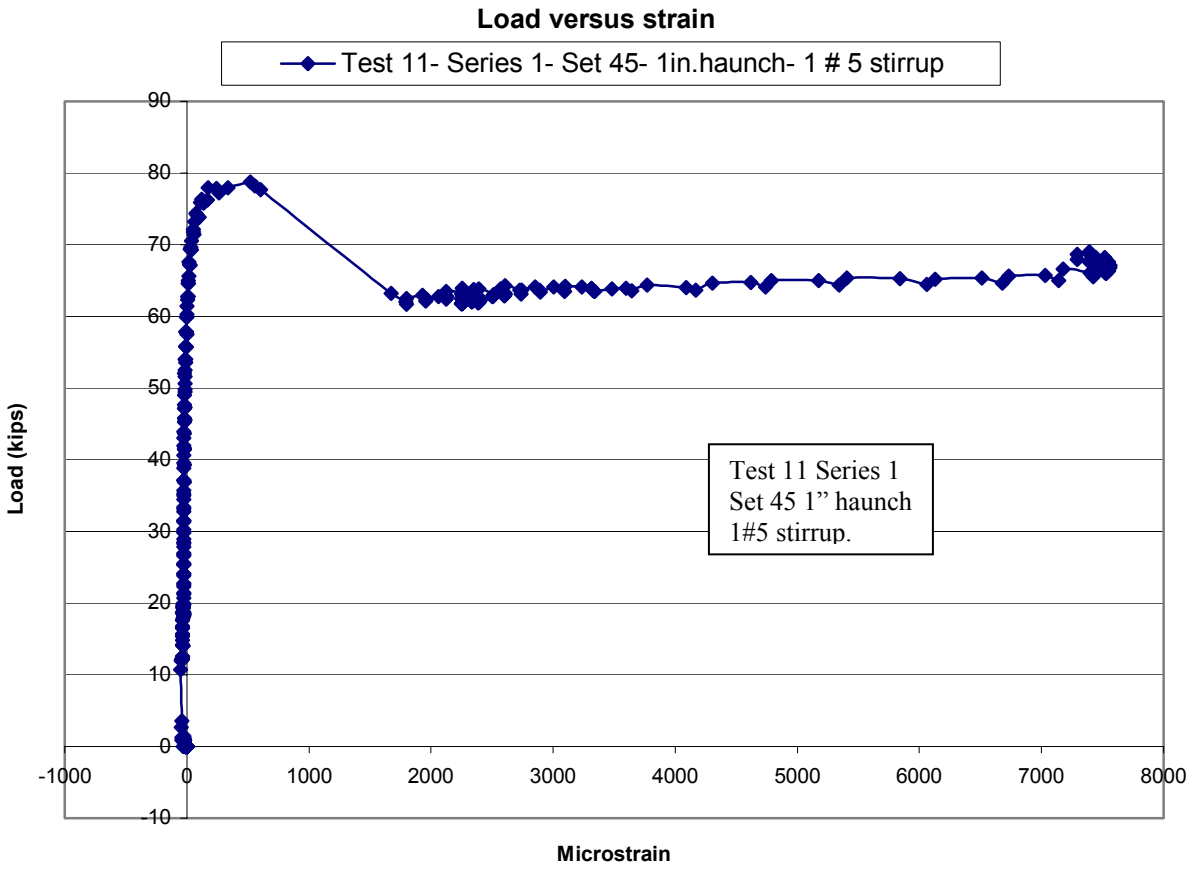

Figure 4.3 Load versus strain diagram including after crack stage for Test 11 Series 1.

4.1.2 1 in. Haunch and Stirrups

Figure 4.4 presents the load-slip behavior of a typical specimen with a No. 4 double leg stirrup. The area of the connector crossing the interface is 0.2 x 2 = 0.4 in^2. The area, multiplied by the yield stress of the stirrups, which was tested at the laboratory as 65 ksi, results in a maximum normal force of 26 kips. As can be seen in Figure 4.4 the shear capacity of the specimen after the crack has occurred stays around 26 kips, although the shear force fluctuates within certain limits as the sides of the specimen travel relative to one another.

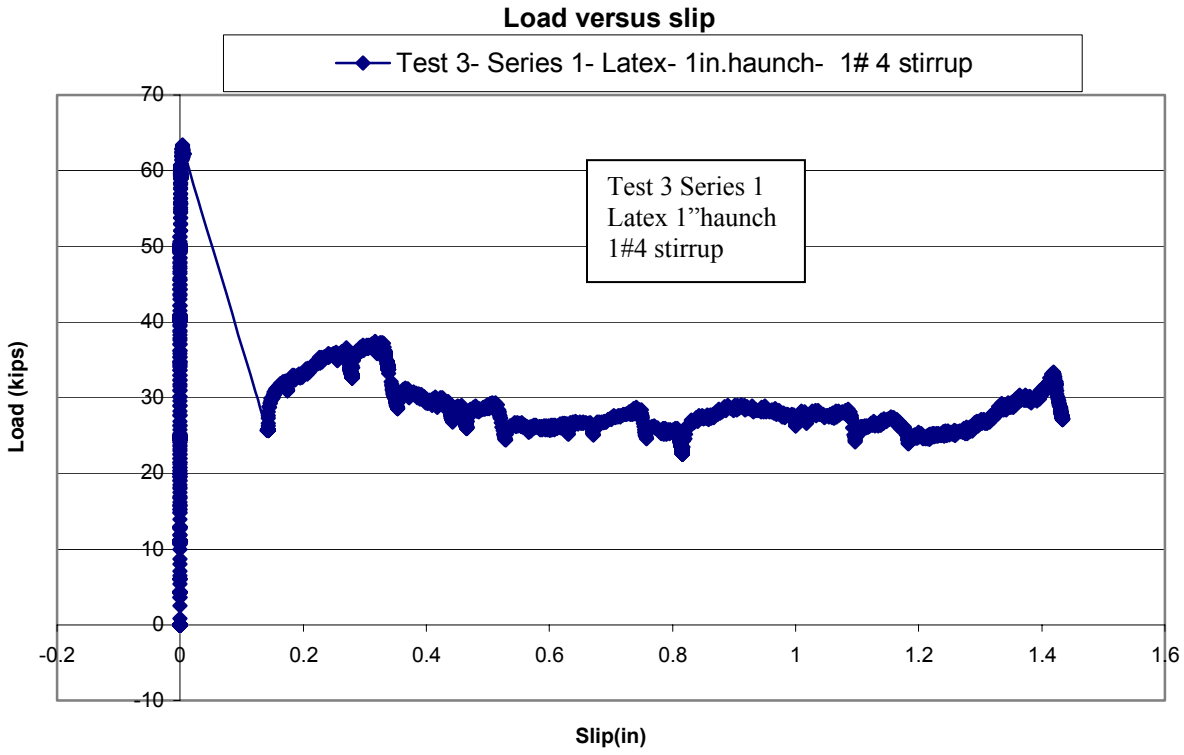

Figure 4.4 Typical load slip behavior of a specimen with extended stirrups as shear connectors.

In Test 4 in Series 1, only one leg of the double leg No. 4 stirrup was used in the shear transfer due to improper bonding of the other leg with the grout. As a result, the

post-crack shear force to cause continued slip was about half that of test 3 (26/2 = 13 kip) (see Figure 4.5).

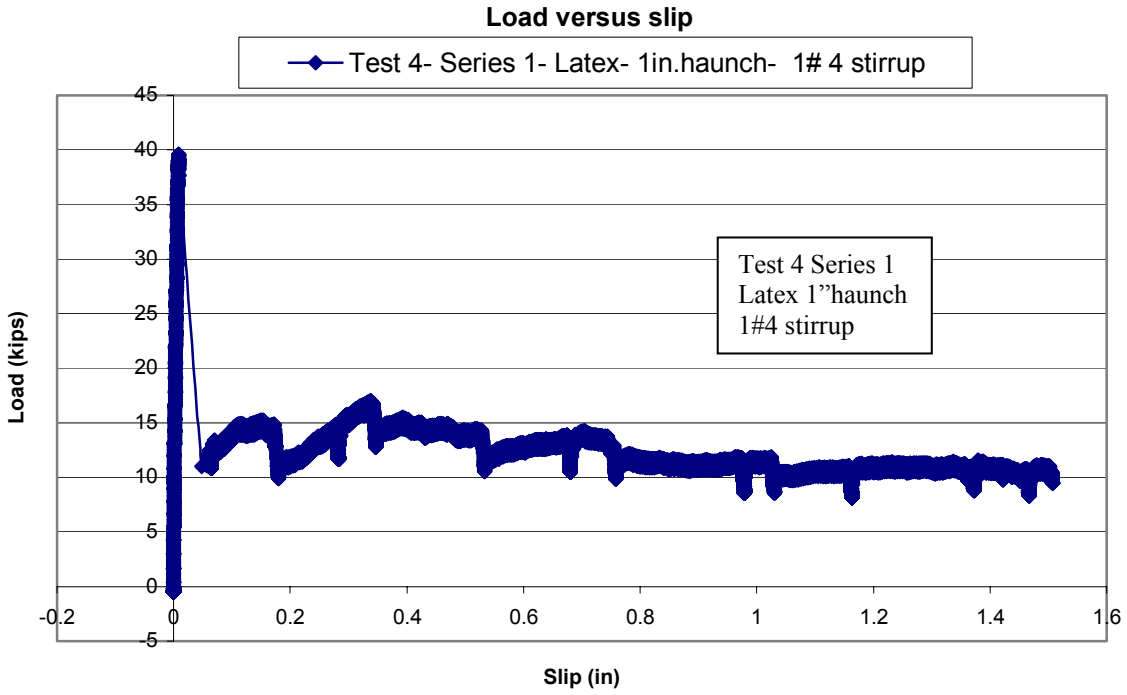

Figure 4.5 Load slip behavior of the specimen in Test 4 Series 1.

4.1.3 3 in. Haunch and Stirrups

In most of the tests in Series 2 the haunch height was 3 in. These high haunch heights caused the failure mode in most of the specimens in Series 2 to be a pry-out failure due to insufficient embedment length of the shear connectors on the slab side. Figure 4.6 illustrates the cone of concrete pried out on the slab side. The embedment lengths for these specimens were about 3 to 4 in. Two of the tests in Series 3 with double leg extended stirrups as shear connectors had 5 in. embedment length on the slab side and no pry-out failure occurred. So based on this observation, to prevent pry-out failures, the embedment length of the shear connectors should be at least 5 in. In bridges, this issue is critical at the areas near the support where both the haunch is tall and the shear is large and the connectors must have sufficient embedment length to provide composite action. The average shear strength of the specimens with 1 in. haunch in Series 1 and 2 was 208

psi as compared to 222 psi, which was the average strength of the specimens with 3 in. haunch in these two series. Also the average strength of the specimens with 1 No. 5 double leg stirrups and 1 in. haunch in all the series of tests is 228 psi as compared to 225 psi and 225 psi whi were the average strengths for the specimens with 2 in. and 3 in. haunches respectively. Based on this observation it can be said that the pre-crack strength of the specimens is not influenced by haunch height.

Figure 4.6 Concrete pry-out failure.

4.1.4 Insert Anchors

Four of the tests in Series 3 included Dayton-Richmond anchors as shear connectors. Out of these four tests, in two of them the contact surface of the beam element was intentionally roughened. In the other two tests, shear keys were provided at the top surface of the beam element and the surface was not roughened. The specimens in which the Dayton-Richmond shear connectors were used exhibited brittle behavior. Figure 4.7 presents a typical load-slip plot. In this test, both the connectors were broken at a slip of about 0.5 in. However, the Dayton-Richmond anchors are a very convenient and practical type of shear connector, especially for the rehabilitation or slab removal process, because the bolts can be unscrewed, making it easier for the slab to be removed.

The presence of the shear keys at the top surface of the beam increased the interface shear capacity tremendously. One of the specimens with shear keys had a maximum capacity of 149 kips and the other specimen had a capacity of 136 kips, compared to the maximum capacity with a roughened interface of 130 kips. The failure mode was the shearing of the shear keys. Based on this observation, a debonding agent may be applied to facilitate the slab removal process as it is recommended by Tadros (2002). More research including shear keys should be performed in order to develop a method for quantifying the interface strength.

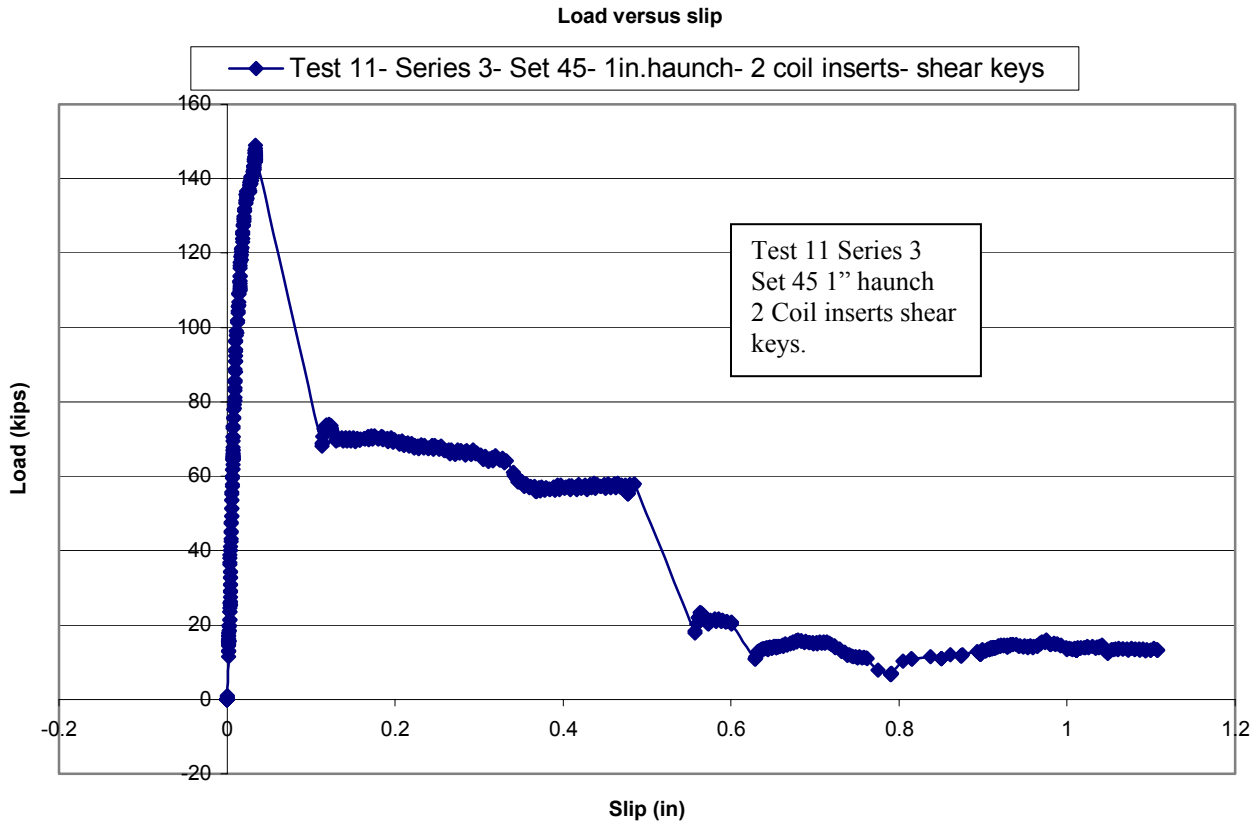

Figure 4.7 Typical behavior of insert anchors

4.2 Grout Types

The first series of tests was performed to investigate the performance of two different types of grout, Set 45 Hot weather mix and Latex modified mix. Set 45 Hot weather mix performed better than the Latex modified mix as can be seen in Table 4.1.

As indicated earlier, the first six tests in Series 1 had Latex modified mix grout and the other six had Set 45 Hot weather mix. The average stress at first crack for Set 45 Hot Weather mix was 181 psi and the average stress at first crack for Latex modified mix was 147 psi. Therefore, Set 45 Hot Weather mix was used in the remainder of tests.

The failure mode of all the tests was a bond failure at the interface between the grout and the beam element or slab element. In all the tests in Series 1 the failure mode was along the beam side. In Series 2 and in Series 3 failure mode was alternating between the beam side and the slab side depending on where the weakest bond was formed. Since the failure never took place in the body of the grout the strength of the interface appears to be a function of the strength of the bond between the grout and concrete rather than the strength of the grout itself.

4.3 Strength Prediction

The results from all 36 push-off tests are presented Tables 4.1-4.3. For the specimens that failed in pry-out failure or due to improper grouting of the shear pockets, no post-crack shear capacity was determined and they were not used in deriving the equation for post-crack shear capacity of the specimens. The test results were used to derive two strength prediction equations. One of the equations presents the pre-crack interface strength and the other one the strength of the interface after cracking has occurred (post-crack interface strength). The two derived equations were then compared to the current code and specification equations for horizontal shear strength. These codes are *ACI 318/02*, *AASHTO Standard Specifications for Highway Bridges* and *AASHTO LRFD Bridge Design Specifications.*

4.3.1 Shear Friction, Dowel Action and Cohesion

In accordance with the results of the tests that were performed, the following equations were determined to quantify the horizontal shear resistance when precast panels are supported on precast girders with a 1 in. to 3 in. grouted haunch. Two equations for the uncracked and cracked interfaces are presented in Figure 4.8. One of the equations is a best fit of the test data and the other one a lower bound of the test data. The

best-fit equations were derived using the least square method. Tests 11 and 12 in Series 3 were not included in the derivation of equations since the contact surface of the beam element consisted of shear keys and was not intentionally roughened. The lower bound equation for the uncracked interfaces was derived by substracting a value 1.82*standard deviation from the y-axis intercept of the best fit equation and by applying the same slope. The proposed best fit equations for both cracked and uncracked interfaces, knowing the fact that they are a best fit, predict conservatively 50 % of the test data. The lower bound equation for uncracked interfaces should predict conservatively 96 % of any similar test data. The lower bound equation for the cracked interfaces was derived by moving the y-axis intercept of the best fit equation to the origin and by applying the same slope. The distance between the y-axis intercept of the best fit equation for post-crack test data and the origin is 0.02*standard deviation. The lower bound equation for cracked interfaces predicts conservatively 82 % of the test data. To determine the post crack strength, only the tests in which the post-crack load was maintained constant within certain limits for increasing amounts of slip, were considered. The tests where Dayton-Richmond anchors were used as shear connectors were not included in post-crack equation derivation because they exhibited brittle behaviour. All the derived equations are presented below and are also shown in Figure 4.8.

For uncracked interfaces the nominal horizontal shear resistance in terms of stress is:

$v_{nh}= 0.16 + 0.51 (A_{vh}*f_y + P_n)/(b_v s)$ (best fit equation) (ksi) (4.1)

$v_{nh}= 0.06 + 0.51 (A_{vh}*f_y + P_n)/(b_v s)$ (lower bound equation) (ksi) (4.2)

For cracked interfaces the nominal horizontal shear resistance in terms of stress is:

$v_{nh} = 0.02 + 0.86 (A_{vh}*f_y + P_n) /(b_v s)$ (best fit equation) (ksi) (4.3)

$v_{nh} = 0.86 (A_{vh}*f_y + P_n)/(b_v s)$ (lower bound equation) (ksi) (4.4)

where:

v_{nh} = the nominal horizontal shear resistance in terms of stress (ksi)

A_{vh} = area of reinforcement that crosses the interface ($in.^2$)

f_y = yield stress of the reinforcement (ksi)

b_v = width of the interface (in.)

s = length of the interface (in.)

The above equations are valid when both the surface of the beam and the slab are intentionally roughened. The first term of these equations represents the resistance provided by the cohesion between the interfaces, and the second term represents the resistance provided by the reinforcement. However, this is not a very definite explanation of the mechanics of the interface shear, because the proposed equations are empirical ones. The contribution of aggregate interlock and concrete-to-concrete friction, which are so intertwined and combined together, are present in both of the terms. It would be wrong to make a very definite separation for the contribution of these terms.

The theory of shear friction says that the interface shear resistance is provided as the two interfaces try to separate from each other as a result of aggregate interlock. In turn the reinforcing bars do not allow these interfaces to separate from each other applying an opposite force according to Newton's Third Law. This force is considered to be high enough to yield the reinforcements and is taken equal to $A_{vh}f_y$ and it is multiplied by a friction coefficient (sometimes referred to as angle of internal friction), which translates the normal force to horizontal shear resistance.

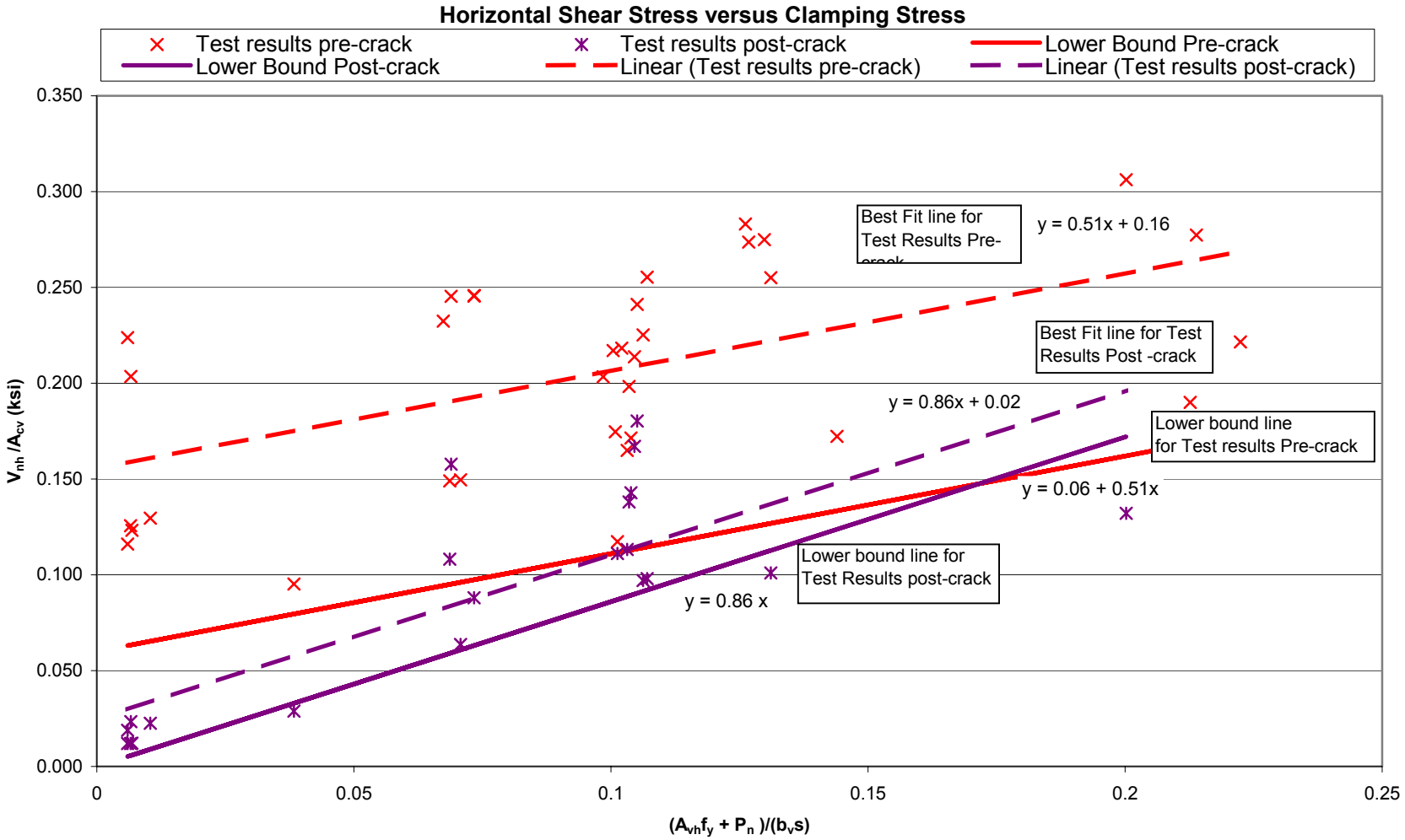

Figure 4.8 Proposed equations to be used in horizontal shear design of precast panels

On the other hand, in almost all the codes the term dowel action is used to refer to the contribution of the rebars to horizontal shear. From this standpoint, shear friction theory contradicts the dowel action of reinforcement for it considers the force in the bars only as a normal force. Before crack or at small amounts of slip, the shear friction theory might be a good explanation of the mechanics of horizontal shear because according to CEB-FIP Model Code 90 (1990) the dowel action is not mobilized until a slip of $0.1*\phi_b$ (the diameter of the bar) has taken place. However at greater amounts of slip the contribution of the rebar crossing the interface reshapes itself more as a dowel action than a normal force. So the overall behavior could be explained by both shear friction theory and dowel action plus cohesion. Another interesting fact about dowel action is presented in CEB-FIP Model Code 90. The Code gives an equation, for the design value of the maximum shear force, which may be transferred by a reinforcing bar crossing a concrete interface. This force cannot be greater than:

$$\frac{A_s f_{yd}}{\sqrt{3}} = 0.57\ A_s f_{yd}$$

4.3.2 Strut-and-Tie Modeling

An alternative method from shear friction for determining the interface shear strength of the specimens is by using strut-and-tie modeling. Strut-and-tie modeling is used in areas of high stress concentrations or the so-called “disturbed regions”. The objective of strut and tie modeling is to establish a truss, which consists of compression and tension elements, and which represents the flow of forces in the considered region. A strut represents a compression elements and a tie a tension element. Figure 4.9 shows two possible strut-and-tie models for push-off specimens. The dashed lines represent the compression struts and the continuous lines the tension ties. The failure of the compression of the struts at the interface might represent the shear capacity of the interface. By using statics a relationship between the tension tie that represents the shear connectors and the compression struts in concrete may be established. The angle between the compression struts in concrete and the tension tie representing the shear

connector would be of primary importance. Mattock refers to this angle as the angle of internal friction. On the other hand this angle depends on the dimensions of the specimens.

Examining the model (a) in Figure 4.9, it can be seen that if the maximum tie force, T, is $A_s f_y$, then the corresponding shear force P is T tanθ. In the specimens of this test program, depending on the location of the nodes A and B in the model, the angle θ will be between 40 and 45°. This would result in a prediction of the shear strength between 1.0 and 0.85 $A_s f_y$. This compares reasonably well to the best fit, post-crack equation 4.3 :

$$P = 0.86 (A_s f_y + P_n) + 0.02 b_v s \qquad \text{(ksi)}$$

Model (b) is shown only as a possible strut-and-tie model for future research. More research should be performed on this issue and after an acceptable strut-and-tie model has been established, then it should be compared to the test results from previous research.

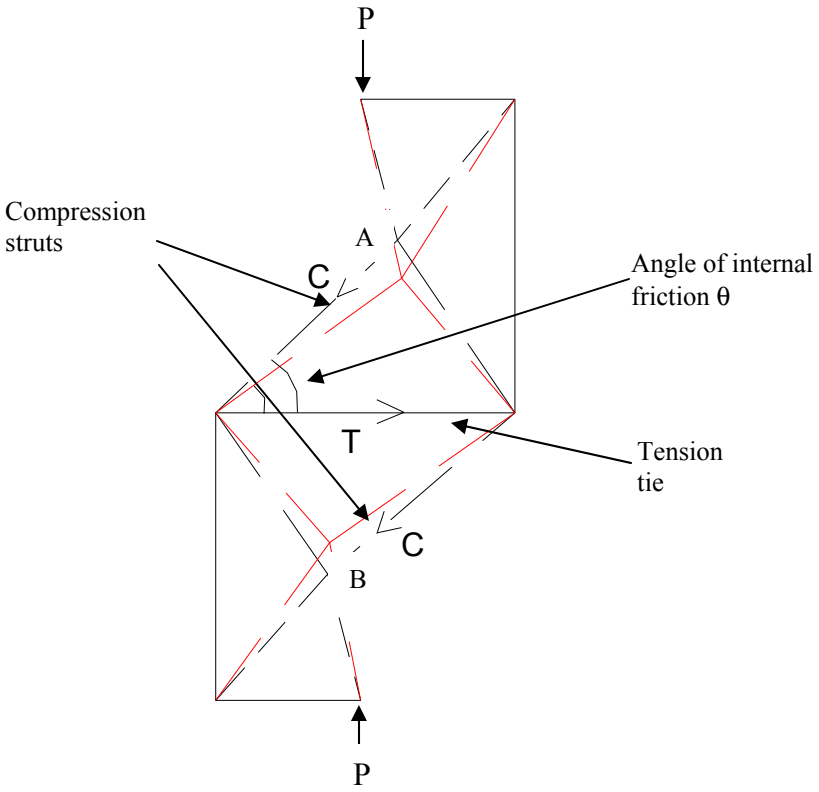

(a)

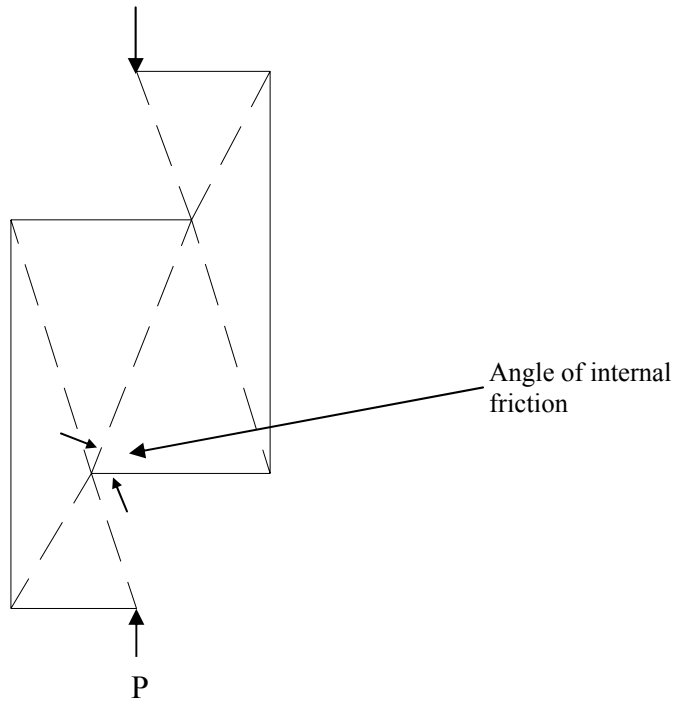

(b)

Figure 4.9 Possible Strut-and-Tie Modeling of push-off specimens

4.4 Results Compared to Existing Equations

The test results were compared to equations for calculating horizontal shear resistance in *ACI 318/02*, *AASHTO Standard Specifications for Highway Bridges* and *AASHTO LRFD Bridge Design Specifications.* This comparison is presented in Figures 4.10 and 4.11 for pre-crack and post-crack strength respectively. Also shown on each figure are two lines, associated with two equations, derived from test results. One of the lines represents the best fit of the test results and the other line is a lower bound. Normal Distribution Probability Function was used to determine the percentage of specimens whose strengths were conservatively predicted by each equation.

The equation available in LRFD Specifications does the best job in predicting tests loads from this research as shown in Figure 4.10 and Table 4.4. It is very close to the best fit line of the test results for the pre-crack strength. It predicts 61 % of the test specimens conservatively. The equations available in ACI Code or Standard Specifications are unconservative for the precast panel system. They predict conservatively only 41 % and 22 % of the test specimens respectively. It should be kept in mind that the difference between the test results and the code equations may always be attributed to the fact that in this project both beam and the slab elements were precast members and were bonded by means of grouting. None of the codes includes the case when both of the elements composing the interface are precast and this was the impetus for this research. The Proposed Best Fit equation, knowing the fact that it is the best fit of the test results predicts conservatively 50 % of the tests specimens. The Proposed Lower Bound equation should predict conservatively 96 % of any similar test specimens, and is proposed to be used in design.

Figure 4.11 shows the test results for the post-crack (sustained load) strength. Two equations derived from the best fit line and lower bound line of the test results are shown. The equation derived from the lower bound line is proposed to be used for the transfer of shear force in interfaces where a crack exists.

Table 4.1 Test Results and Code Prediction Strengths for Series 1.

Series 1		test1	test 2	test3	test4	test5	test6	test7	test8	test9	test10	test11	test12
	b_v (in)	16	16	16	16	16	16	16	16	16	16	16	16
	s (in)	26.5	25	26.5	26	26.5	27	26	25.74	26	25.75	26	26.18
	f_y (ksi)			64.8	64.8	66.1	66.1			64.8	64.8	6.61	6.61
	f'_c grout (Test day) (ksi)	6.75	6.75	6.75	6.75	6.75	6.75	3.6	3.6	3.6	3.6	3.6	3.6
	f'_c concrete (ksi)	4.2	4.2	4.2	4.2	4.2	4.2	4.2	4.2	4.2	4.2	4.2	4.2
	A_{cv} (in^2)	424	400	424	416	424	432	416	411.84	416	412	416	418.88
	A_{vh} (in^2)	0	0	0.4	0.2	0.62	0.62	0	0	0.4	0.4	0.62	0.62
Standard Spec	V_{nh}/A_{cv} (ksi)	0.08	0.08	0.354	0.342	0.369	0.368	0.330	0.330	0.355	0.355	0.334	0.334
AASHTO LRFD	V_{nh}/A_{cv} (ksi)	0.106	0.11	0.171	0.138	0.203	0.201	0.106	0.107	0.169	0.169	0.116	0.116
Test results pre-crack	V_{nh} (kip)	94.89	51.81	63.4	39.62	69.93	50.68	48.26	50.77	62	101.07	100.32	89.55
Test results post-crack	V_{nh} (kip)	8	9	27	12	48	48	5	5	45	65	75	70
stress pre-crack	V_{nh}/A_{cv} (ksi)	0.224	0.13	0.150	0.095	0.165	0.117	0.116	0.123	0.149	0.245	0.241	0.214
stress post-crack	V_{nh}/A_{cv} (ksi)	0.019	0.023	0.064	0.029	0.113	0.111	0.012	0.012	0.108	0.158	0.180	0.167
	$(A_{vh}f_y+P_n)/(b_vs)$ (ksi)	0.006	0.01	0.071	0.038	0.103	0.101	0.006	0.007	0.069	0.069	0.016	0.016
ACI Code	V_{nh}/A_{cv} (ksi)	0.08	0.08	0.297	0.279	0.318	0.317	0.08	0.08	0.297	0.298	0.266	0.266
Normal force	P_n (kip)	2.54	4.17	4.07	3	2.75	2.76	2.5	2.82	2.64	2.48	2.74	2.81

Table 4.2 Test results and code prediction strengths for Series 2.

Series 2		test1	test 2	test3	test4	test5	test6	test7	test8	test9	test10	test11	test12
	b_v (in)	16	16	16	16	16	16	16	16	16	16	16	16
	s (in)	26.7	27	27	26	27.2	26.3	27.72	25.24	26.75	27.13	27	26
	f_y (ksi)		66.1	64.8		66.1	64.8	66.1	64.8	64.8	66.1	64.8	64.8
	f'_c grout (Test day) (ksi)	4.38	4.38	4.38	4.38	4.38	4.38	4.38	4.38	4.38	4.38	4.38	4.38
	f'_c concrete (ksi)	5.38	5.38	5.38	5.38	5.38	5.38	5.38	5.38	5.38	5.38	5.38	5.38
	A_{cv} (in^2)	427.2	432	432	416	435.2	420.8	443.52	403.84	428	434.08	432	416
	A_{vh} (in^2)	0	0.62	0.8	0	0.62	0.8	0.62	0.4	0.4	0.62	0.8	0.8
Standard Spec	V_{nh}/A_{cv} (ksi)	0.330	0.368	0.378	0.330	0.368	0.379	0.367	0.356	0.354	0.368	0.378	0.380
AASHTO LRFD	V_{nh}/A_{cv} (ksi)	0.107	0.202	0.227	0.107	0.201	0.230	0.198	0.173	0.167	0.200	0.226	0.231
Test results pre-crack	V_{nh} (kip)	86.96	94.31	118.23	52.27	76.02	115.68	90.18	99.23	99.49	94.225	122.32	106.12
Test results post-crack	V_{nh} (kip)	10			5								42
stress pre-crack	V_{nh}/A_{cv} (ksi)	0.204	0.218	0.274	0.126	0.175	0.275	0.203	0.246	0.232	0.217	0.283	0.255
stress post-crack	V_{nh}/A_{cv} (ksi)	0.023			0.012								0.101
	$(A_{vh}f_y+P_n)/(b_vs)$ (ksi)	0.007	0.102	0.127	0.007	0.101	0.130	0.098	0.073	0.067	0.100	0.126	0.131
ACI Code	V_{nh}/A_{cv} (ksi)	0.08	0.317	0.332	0.08	0.317	0.334	0.315	0.299	0.296	0.317	0.332	0.335
Normal Force	P_n (kip)	2.83	3.13	2.93	2.73	2.91	2.8	2.69	3.7	2.92	2.6	2.67	2.7

Table 4.3 Test Results and Code Prediction Strengths for Series 3.

Series 3		test1	test 2	test3	test4	test5	test6	test7	test8	test9	test10	test11	test12
	b_v (in)	16	16	16	16	16	16	16	16	16	16	16	16
	s (in)	25.75	25.5	25	26.25	26.5	26.25	26.5	27	26.5	25.5	26.75	25.75
	f_y (ksi)	66.1	66.1	66.1	66.1	66.1	66.1	66.1	66.1	100	100	100	100
	f'_c grout (Test day) (ksi)	3.67	3.67	3.67	3.67	3.67	3.67	3.67	3.67	3.67	3.67	3.67	3.67
	f'_c concrete (ksi)	4.8	4.8	4.8	4.8	4.8	4.8	4.8	4.8	4.8	4.8	4.8	4.8
	A_{cv} (in^2)	412	408	400	420	424	420	424	432	424	408	428	412
	A_{vh} (in^2)	0.62	0.62	1.24	0.62	1.24	0.62	0.88	0.44	0.88	0.88	0.88	0.88
Standard Spec	V_{nh}/A_{cv} (ksi)	0.370	0.370	0.412	0.369	0.407	0.369	0.385	0.357	0.413	0.416	0.412	0.415
AASHTO LRFD	V_{nh}/A_{cv} (ksi)	0.206	0.207	0.313	0.204	0.300	0.204	0.244	0.173	0.314	0.322	0.312	0.320
Test results pre-crack	V_{nh} (kip)	92.81	104.2	75.98	83.29	129.84	71.97	73.02	106.08	117.604	90.384	148.99	136.64
Test results post-crack	V_{nh} (kip)	40	40		58	56	60		38				
stress pre-crack	V_{nh}/A_{cv} (ksi)	0.225	0.255	0.190	0.198	0.306	0.171	0.172	0.246	0.277	0.222	0.348	0.332
stress post-crack	V_{nh}/A_{cv} (ksi)	0.097	0.098		0.138	0.132	0.143		0.088				
	$(A_{vh}f_y+P_n)/(b_v s)$ (ksi)	0.106	0.107	0.213	0.104	0.200	0.104	0.144	0.073	0.214	0.222	0.212	0.220
ACI Code	V_{nh}/A_{cv} (ksi)	0.320	0.320	0.383	0.319	0.376	0.319	0.342	0.300	0.385	0.389	0.383	0.388
Normal Force	P_n (kip)	2.79	2.7	3.1	2.49	2.92	2.65	2.88	2.62	2.68	2.74	2.71	2.62

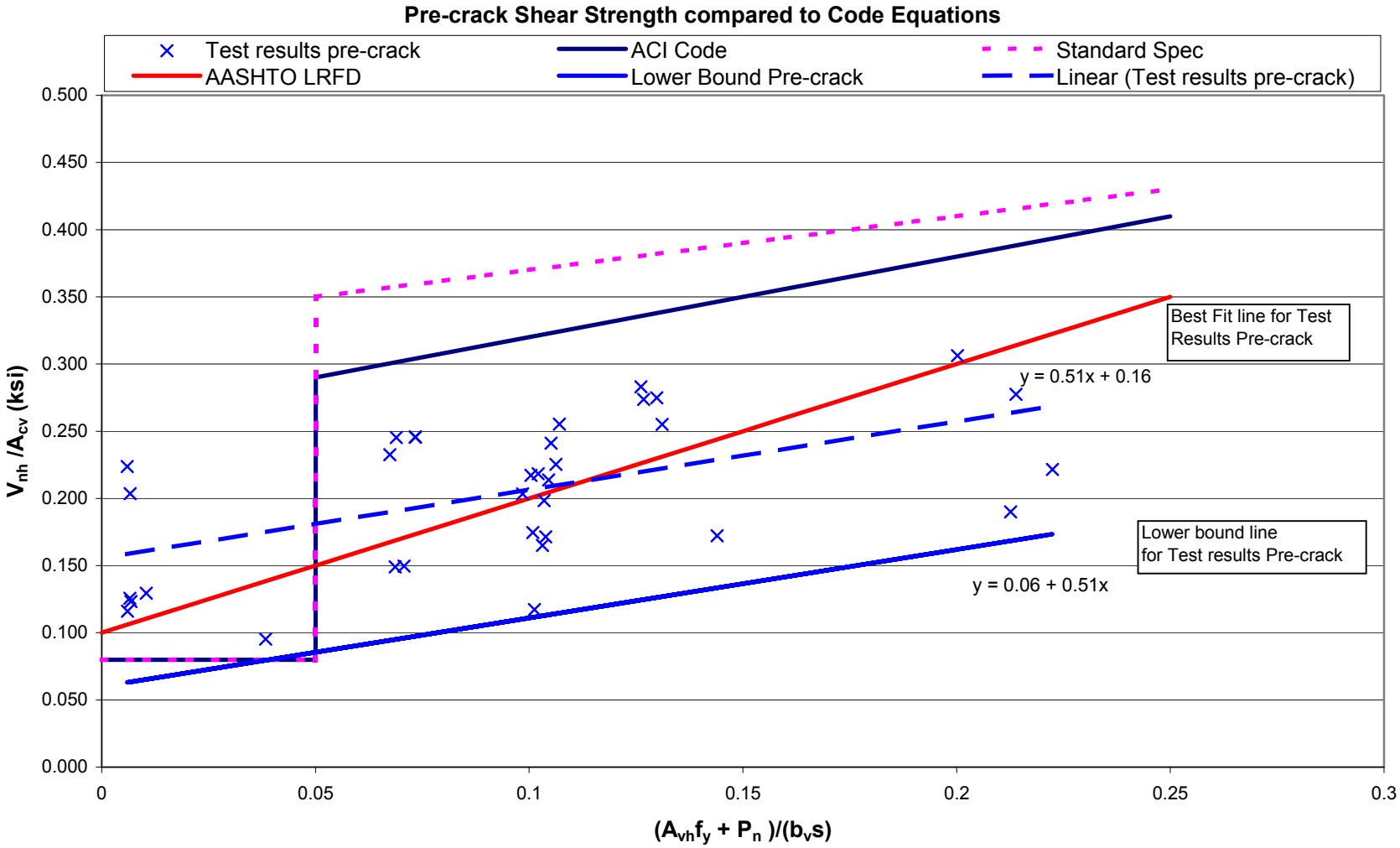

Figure 4.10 Test results pre-crack compared to code equations.

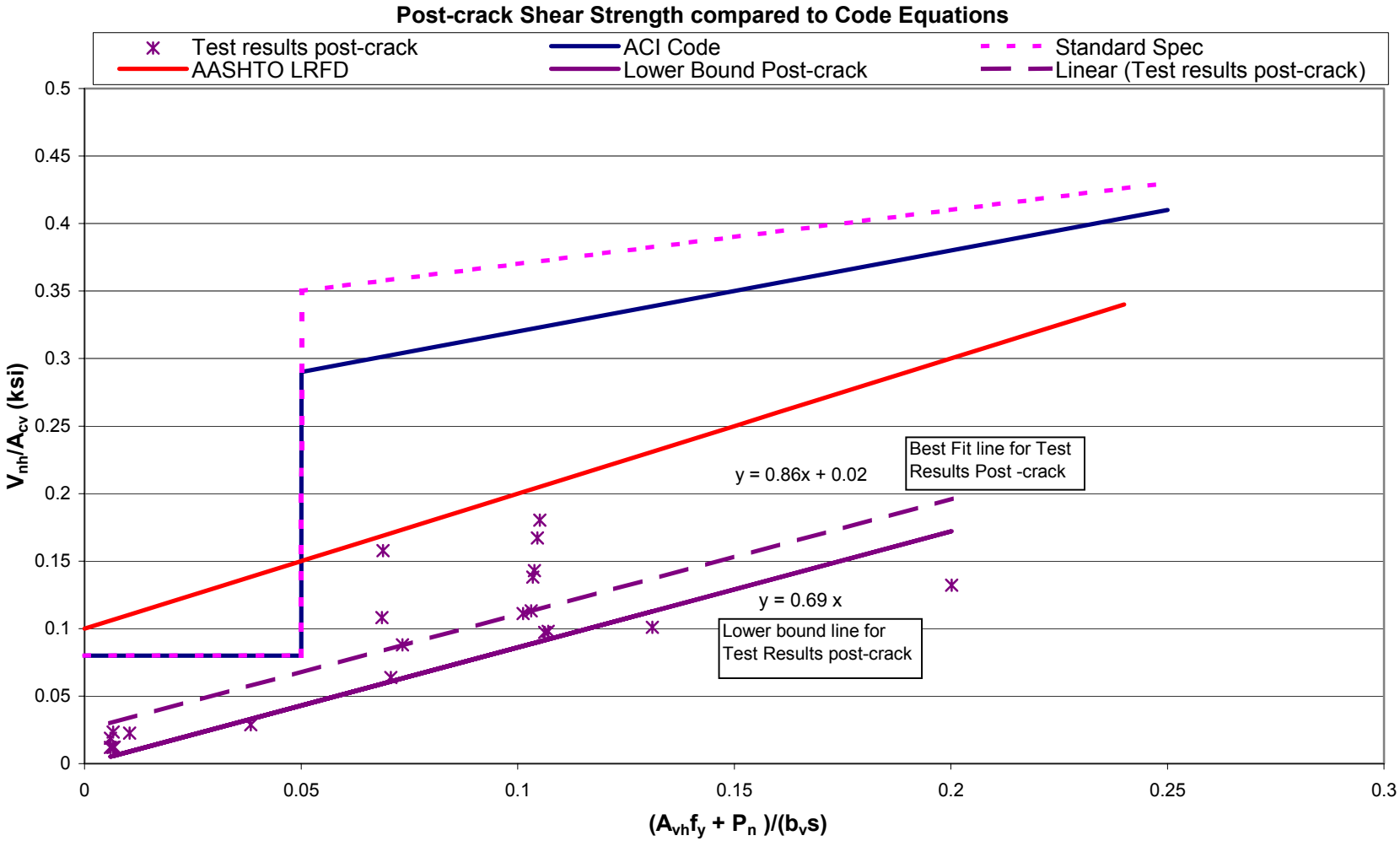

Figure 4.11 Test results post-crack compared to code equations.

Table 4.4 Comparison of Test Results with Design Equations

Test	Peak						Test Results / Prediction Equations				
		ACI	Standard	LRFD	Proposed	Proposed	ACI	Standard	LRFD	Proposed	Proposed
			Spec	Spec	Best Fit	Lower Bound		Spec		Best Fit	Lower Bound
	(ksi)	(ksi)	(ksi)	(ksi)	(ksi)	(ksi)					
Test 1 Series 1	0.224	0.080	0.080	0.106	0.158	0.063	2.80	2.80	2.11	1.41	3.55
Test 2 Series 1	0.130	0.080	0.080	0.110	0.161	0.065	1.62	1.62	1.17	0.81	1.98
Test 3 Series 1	0.150	0.297	0.354	0.171	0.191	0.096	0.50	0.42	0.88	0.78	1.56
Test 4 Series 1	0.095	0.279	0.342	0.138	0.175	0.080	0.34	0.28	0.69	0.54	1.20
Test 5 Series 1	0.165	0.318	0.369	0.203	0.208	0.113	0.52	0.45	0.81	0.79	1.46
Test 6 Series 1	0.117	0.317	0.368	0.201	0.207	0.112	0.37	0.32	0.58	0.57	1.05
Test 7 Series 1	0.116	0.080	0.330	0.106	0.158	0.063	1.45	0.35	1.09	0.73	1.84
Test 8 Series 1	0.123	0.080	0.330	0.107	0.159	0.063	1.54	0.37	1.15	0.78	1.94
Test 9 Series 1	0.149	0.297	0.355	0.169	0.190	0.095	0.50	0.42	0.88	0.78	1.57
Test 10 Series 1	0.245	0.298	0.355	0.169	0.191	0.095	0.82	0.69	1.45	1.29	2.58
Test 11 Series 1	0.241	0.319	0.369	0.205	0.209	0.114	0.76	0.65	1.18	1.15	2.12
Test 12 Series 1	0.214	0.319	0.369	0.205	0.209	0.113	0.67	0.58	1.05	1.02	1.89
Test 1 Series 2	0.204	0.080	0.330	0.107	0.159	0.063	2.54	0.62	1.91	1.28	3.21
Test 2 Series 2	0.218	0.317	0.368	0.202	0.208	0.112	0.69	0.59	1.08	1.05	1.95
Test 3 Series 2	0.274	0.332	0.378	0.227	0.220	0.125	0.82	0.72	1.21	1.24	2.20
Test 4 Series 2	0.126	0.080	0.330	0.107	0.159	0.063	1.57	0.38	1.18	0.79	1.98
Test 5 Series 2	0.175	0.317	0.368	0.201	0.207	0.111	0.55	0.48	0.87	0.84	1.57
Test 6 Series 2	0.275	0.334	0.379	0.230	0.222	0.126	0.82	0.72	1.20	1.24	2.18
Test 7 Series 2	0.203	0.315	0.367	0.198	0.206	0.110	0.64	0.55	1.02	0.99	1.84
Test 8 Series 2	0.246	0.299	0.356	0.173	0.193	0.097	0.82	0.69	1.42	1.27	2.52
Test 9 Series 2	0.232	0.296	0.354	0.167	0.190	0.094	0.78	0.66	1.39	1.22	2.46
Test 10 Series 2	0.217	0.317	0.368	0.200	0.207	0.111	0.69	0.59	1.08	1.05	1.95
Test 11 Series 2	0.283	0.332	0.378	0.226	0.220	0.124	0.85	0.75	1.25	1.29	2.28
Test 12 Series 2	0.255	0.335	0.380	0.231	0.222	0.127	0.76	0.67	1.10	1.15	2.01
Test 1 Series 3	0.225	0.320	0.370	0.206	0.210	0.114	0.70	0.61	1.09	1.07	1.97
Test 2 Series 3	0.255	0.320	0.370	0.207	0.210	0.115	0.80	0.69	1.23	1.22	2.23
Test 3 Series 3	0.190	0.383	0.412	0.313	0.264	0.168	0.50	0.46	0.61	0.72	1.13
Test 4 Series 3	0.198	0.319	0.369	0.204	0.208	0.113	0.62	0.54	0.97	0.95	1.76
Test 5 Series 3	0.306	0.376	0.407	0.300	0.258	0.162	0.81	0.75	1.02	1.19	1.89
Test 6 Series 3	0.171	0.319	0.369	0.204	0.208	0.113	0.54	0.46	0.84	0.82	1.52
Test 7 Series 3	0.172	0.342	0.385	0.244	0.229	0.133	0.50	0.45	0.71	0.75	1.29
Test 8 Series 3	0.246	0.300	0.357	0.173	0.193	0.097	0.82	0.69	1.42	1.27	2.52
Test 9 Series 3	0.277	0.385	0.413	0.314	0.265	0.169	0.72	0.67	0.88	1.05	1.64
Test 10 Series 3	0.222	0.389	0.416	0.322	0.269	0.173	0.57	0.53	0.69	0.82	1.28
						Average	**0.88**	**0.65**	**1.09**	**1.00**	**1.94**
					Standard	**Deviation**	**0.555**	**0.441**	**0.328**	**0.236**	**0.544**
					Predicted	**conservatively**	**41%**	**22%**	**61%**	**50%**	**96%**

CHAPTER 5: SUMMARY, CONCLUSIONS AND RECOMMENDATIONS

5.1 Summary

The precast panel system is very convenient for rehabilitation of deteriorated decks as well as for new bridge construction. It reduces the construction time avoiding traffic delays and detours. Traffic flow can be maintained in both directions by implementing a staged construction. The decks are prestressed in both directions, which makes them stiffer and slows down the ingress of corrosion causing agents. The decks are high quality as they are produced under controlled conditions. They have the advantages of having no shrinkage cracks, which can result in longer life of the deck and less maintenance cost compared to the full depth cast-in-place system.

The horizontal shear strength at the interface between the two interconnected elements is of primary importance in order to provide composite action. The strength of the bond between the two precast members should be high enough to prevent any progressive slip from taking place. Flexural strength, shear strength and deflection characteristics all depend on the satisfactory performance of the interface to provide composite action. None of the codes addresses the case when both of the interconnected elements are precast members bonded by means of grout, which was the main impetus for this project.

Test parameters included different grout types, different haunch heights, and different amounts and types of shear connectors. A total of 36 push-off tests were performed to develop a method for quantifying horizontal shear strength and to recommend the best practice for the system. Two equations for an uncracked and cracked concrete interfaces are proposed to be used in horizontal shear design when the precast panels are used. Recommendations about the most convenient type of shear connectors are presented

5.2 Conclusions

In the light of this research the following conclusions are made:

- The Set 45 Grout performed better than the latex modified mix, so it is recommended to be used in practice.
- As haunch heights vary along the span, it may also be necessary to vary the extension of shear connectors above the top of the beams. The shear connectors should be developed at least 5 in. into the slab in order to prevent pry-out failures. The pre-crack strength of the interface is not influenced by haunch height.
- The single-leg post-installed hooked rebars are a very convenient type of shear connector because they eliminate the problems faced in the pre-installed connectors due to mismatching of the position of the connectors with the shear pockets. Epoxy is a very convenient type of adhesive to provide the bond between the hooked rebars and the concrete.
- The Dayton-Richmond anchors are a very convenient type of shear connectors from the stand point of slab removal, because during that process the bolts can be unscrewed, making it easier for the deteriorated slab to be removed. However they are unable to undergo excessive slips and exhibit a very brittle behavior.
- The presence of shear keys on the beam side made the shear capacity of the specimens increase significantly. The failure mode was the shearing of the shear keys.
- The following equations can be used in design of the precast panel system for horizontal shear for uncracked and cracked interfaces. The equation proposed for the uncracked interfaces predicts conservatively 96 % of the pre-crack test data and the equation proposed for cracked interfaces predicts conservatively 82 % of the post-crack test data. The surfaces of the beam and the slab at the interface should be intentionally roughened and bonded by means of grouting.

$v_{nh} = 0.05 + 0.65\ (A_{vh} * f_y + P_n)/(b_v s)$ (lower bound equation) (ksi) (uncracked)

$v_{nh} = 0.69\ (A_{vh} * f_y + P_n)/(b_v s)$ (lower bound equation) (ksi) (cracked)

- Of the three code equations considered (ACI, AASHTO Standard, AASHTO LRFD) all result in unconservative predictions of the strength of the grouted haunch. Of the three, AASHTO LRFD resulted in the best prediction of shear strength of the 36 test specimens. This difference may be attributed to the fact that the code equations address the case of concrete cast against hardened concrete, whereas in our project both the elements at the interface were precast members bonded by means of grouting.

5.3 Recommendations for Future Research

- More tests should be performed to test the influence of different parameters associated with the system and to further develop the method for quantifying the interface shear strength.
- Various types of grout should be tested to investigate their bonding performance with concrete.
- Various types of shear connectors, which would facilitate the slab removal process, be easy to install and have a ductile failure mode should be investigated.
- The shear key system should be investigated further, for it increases the interface shear strength tremendously. An optimization of the shear key dimensions is required to yield a desired failure. An investigation of debonding agents to ease deck removal is recommended.
- Strut-and-Tie modeling of the interface should be investigated to develop a method that will satisfactorily represent the flow of forces in the region and match well with tests results.

REFERENCES

AASHTO LRFD Bridge Design Specification, Second Edition (1998). American Association of State Highway and Transportation Officials, Washington D.C.

Anderson, A.R. (1960). "Composite Designs in Precast and Cast-in-Place Concrete," *Progressive Architechture*, V.41, No. 9, September 1960, 172-179.

Birkeland, P.W. (1966). "Connections in Precast Concrete Construction," *ACI Journal*, V. 63, No. 3, March 1966, 345-367.

Buliding Code Requirements for Structural Concrete (2002). American Concrete Institute, Farmington Hills, Michigan.

Chang, P.S., Chang, S.S. (2001). "Continuous Composite Bridges with Precast Decks", *Steel Structures 1* (2001), 123-132.

Comite Euro-International du Beton (CEB)-Federation Internationale de la Precontrainte (FIP) (1990). Model Code for Concrete Structures, (MC-90), CEB, Thomas Telford, London.

Culmo, P.M. (2000). " Rapid Bridge Deck Replacement Using Full Depth Precast Concrete Slabs", Paper No. TRB 00-1220.

Hanson, N. W., (1960). "Precast Prestressed Concrete Bridges-2. Horizontal Shear Connections," *Journal PCA Research and Development Laboratories*, V. 2, No. 2, 1960, 38-58.

Grossfield, B., and Birnstiel, C. (1962). " Tests os T-Beams with Precast Webs and Cast-in-Place Flanges" ACI Journal, V. 59, No. 6, June 1962, 843-851.

Hsu, T. T.C. (1976). " Horizontal Shear Tests of PSI Prestressed Composite Beams," Report To Prestressed Systems Inc., August 1976.

Hwang, S., Yu, H., Lee, H. (2000). "Theory of interface shear capacity of reinforced concrete", *Journal of Structural Engineering*, June 2000, 700-707.

Issa, M.A., Yousif, A.A, Issa, M.A. (1995). " Construction Procedures for Rapid Replacement of Bridge Decks", *PCI JOURNAL*, February 1995, 49-52.

Issa, M.A., Yousif, A.A., Issa, M.A., Kaspar, I., Khayyat, S.Y. (1998). " Analysis of Full Depth Precast Concrete Bridge Deck Panels", *PCI Journal*, January-February 1998, 74-85.

Loov , R. E. (1994). "Horizontal Shear Strength of Composite Concrete Beams with a rough interface", *PCI JOURNAL*, January-February 1994, 48-65.

Mast,R.F, (1968). ”Auxiliary Reinforcement in Concrete Connections,” *ASCE Journal*, V.94, No.ST6, June 1968, 1485-1504.

Mattock, A. H. (1969). “ Shear Transfer in Reinforced Concrete,” *ACI Journal*, February 1969 17-42.

Mattock, A. H, Hawkins, M.N. (1972). “Shear transfer in Reinforced Concrete-Recent Research” *PCI JOURNAL*, V. 17, No.2, March-April 1972, 55-75.

Mattock, A. H. (1974). “ Shear Transfer in Concrete having Reinforcement at an Angle to the Shear Plane,” Shear in Reinforced Concrete, ACI Special Publication SP-42, V.1, 17-42 American Concrete Institute, Detroit, Michigan.

Mattock, A. H. , Li,W. K., and Wang, T. C. (1976). “Shear Transfer in Lightweight Reinforced Concrete,” *PCI JOURNAL*, V. 21, No.1, January-February 1976, 20-39.

Patnaik, K.A. (2001). “ Behavior of composite Concrete Beams with Smooth Interface”, *Journal of Structural Engineering*, April 2001, 359-366.

PCI Design Handbook - Precast and Prestressed Concrete, Fifth Edition (1999). *Precast/Prestressed Concrete Institute*, Chicago, Illinois.

STANDARD SPECIFICATION for HIGHWAY BRIDGES, Sixteenth Edition (1996). American Association of State Highway and Transportation Officials, Washington D.C.

Shaikh, A.F. (1978). “Proposed Revisions to Shear-Friction Provisions,” *PCI JOURNAL*, V. 23, No. 2, March-April 1978, 12-21.

Shim, C.S., Kim, J.H., Chang, S.P., Chung, C.H. (2000). “The behavior of shear connections in a composite beam with a full depth precast slab” *Proceedings of the Institution of Civil Engineers*, Structures and Buildings, February 2000, 101-110.

Tadros, K.M., Badie, S.S, Baishya, C.M., Yamane, T.(1998). “Innovative Prestressed Concrete Bridge Deck Panel Systems”, *National Cooperative Highway Research Program* (NCHRP) Project No. 12-41.

Tadros, K.M., Badie, S.S., Kamel, R.M (2002). “Girder Deck Connection for Rapid Removal of Bridge Decks”, *PCI JOURNAL*, May-June 2002, 58-69.

Yamane, T., Tadros, M.K., Badie, S.S., Baishya, M.C. (1998). “ Full Depth Precast, Prestressed Concrete Bridge Deck System”, *PCI JOURNAL*, May-June 1998, 50-66.

Walraven, J., Frenay, J., and Pruijssers, A. (1987). “Influence of concrete Strength and Load History on the Shear Friction Capacity of Concrete Members,” *PCI JOURNAL*, V. 32, No. 1, January-February 1987, 66-84.

APPENDIX A

Load versus Slip Diagrams

Series 1

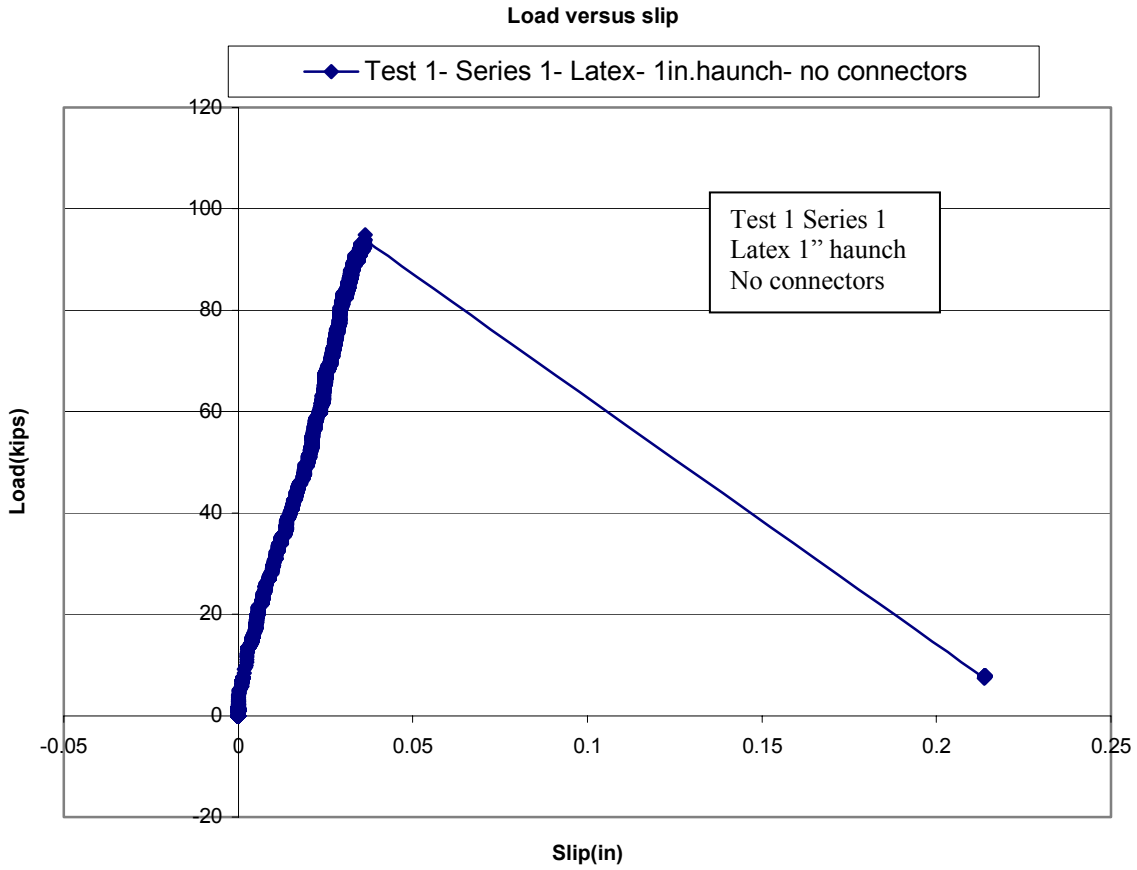

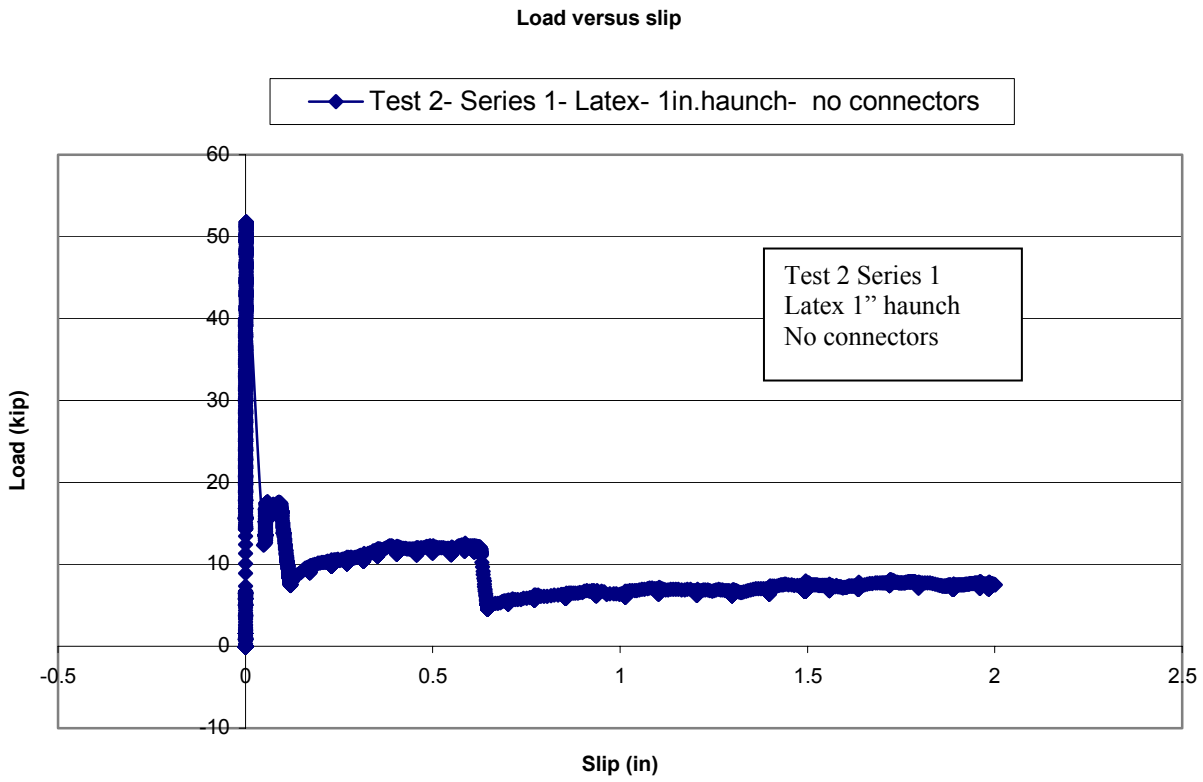
Load versus slip
Test 2- Series 1- Latex- 1in.haunch- no connectors
Test 2 Series 1
Latex 1" haunch
No connectors
Load (kip)
60
50
40
30
20
10
0
-10
-0.5
0
0.5
1
1.5
2
2.5
Slip (in)

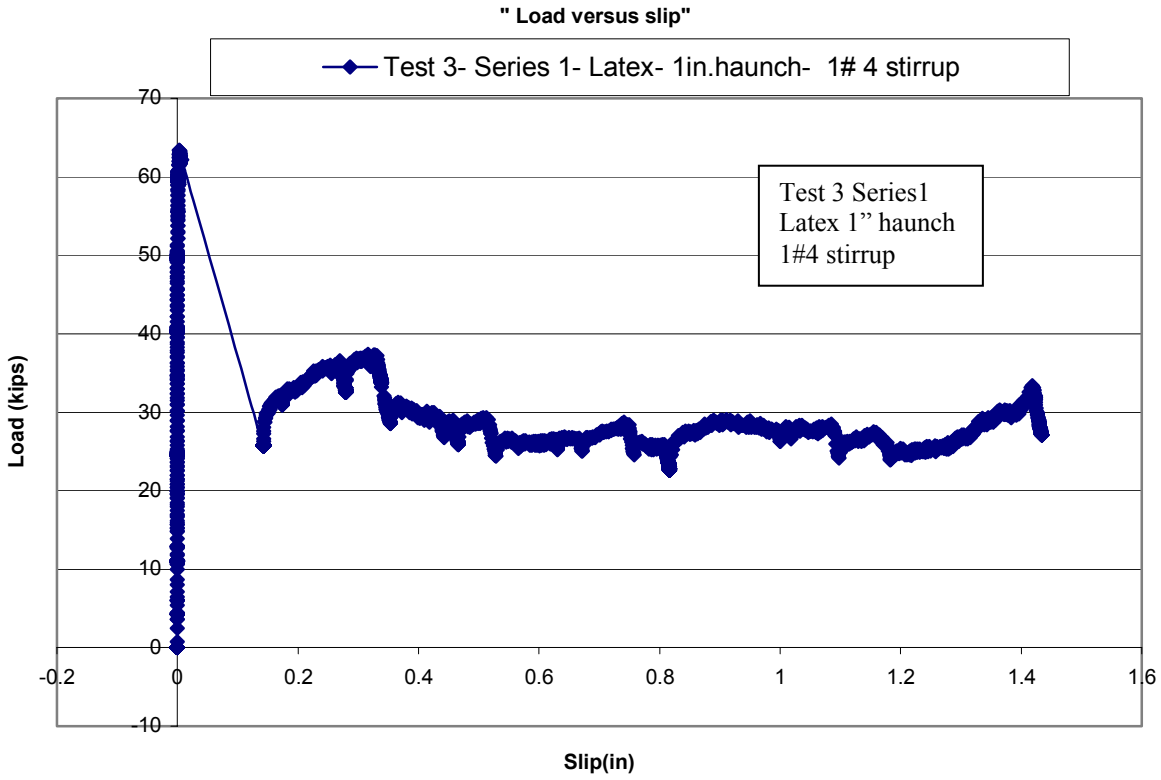
" Load versus slip"
Test 3- Series 1- Latex- 1in.haunch- 1# 4 stirrup
Test 3 Series1
Latex 1" haunch
1#4 stirrup
Load (kips)
70
60
50
40
30
20
10
0
-10
-0.2
0
0.2
0.4
0.6
0.8
1
1.2
1.4
1.6
Slip(in)

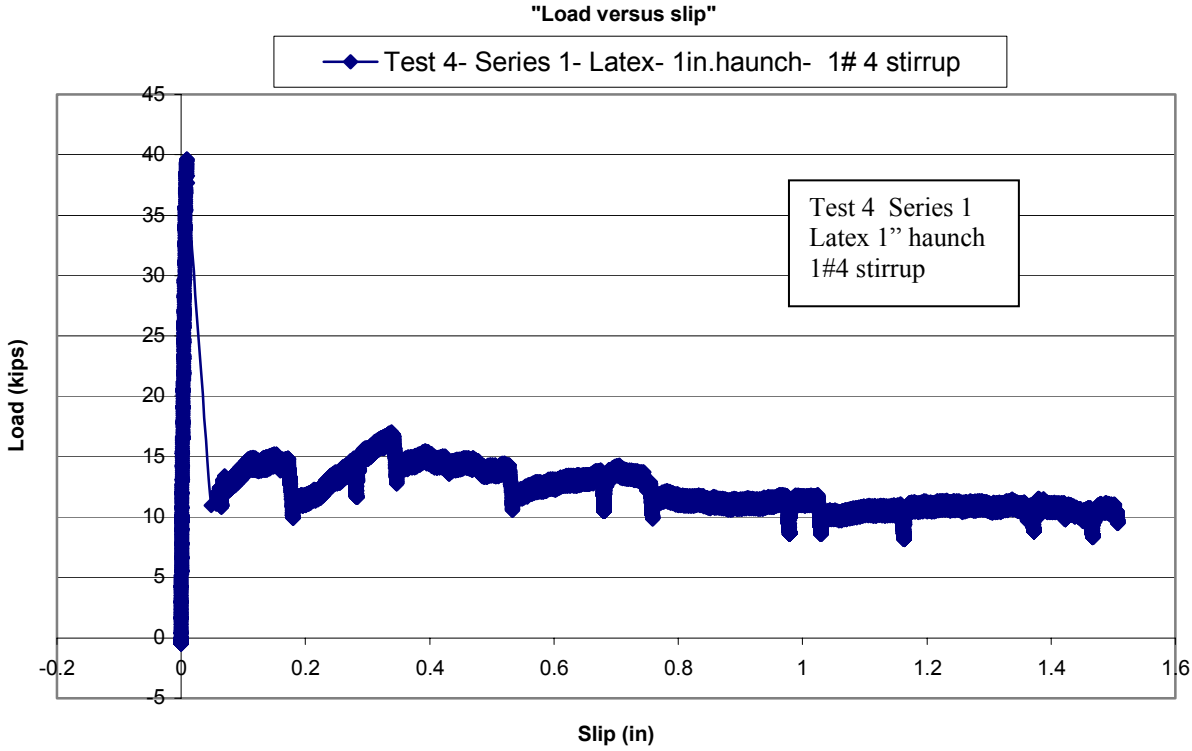
"Load versus slip"
Test 4- Series 1- Latex- 1in.haunch- 1# 4 stirrup
Test 4 Series 1
Latex 1" haunch
1#4 stirrup
Load (kips)
Slip (in)
45
40
35
30
25
20
15
10
5
0
-5
-0.2
0
0.2
0.4
0.6
0.8
1
1.2
1.4
1.6

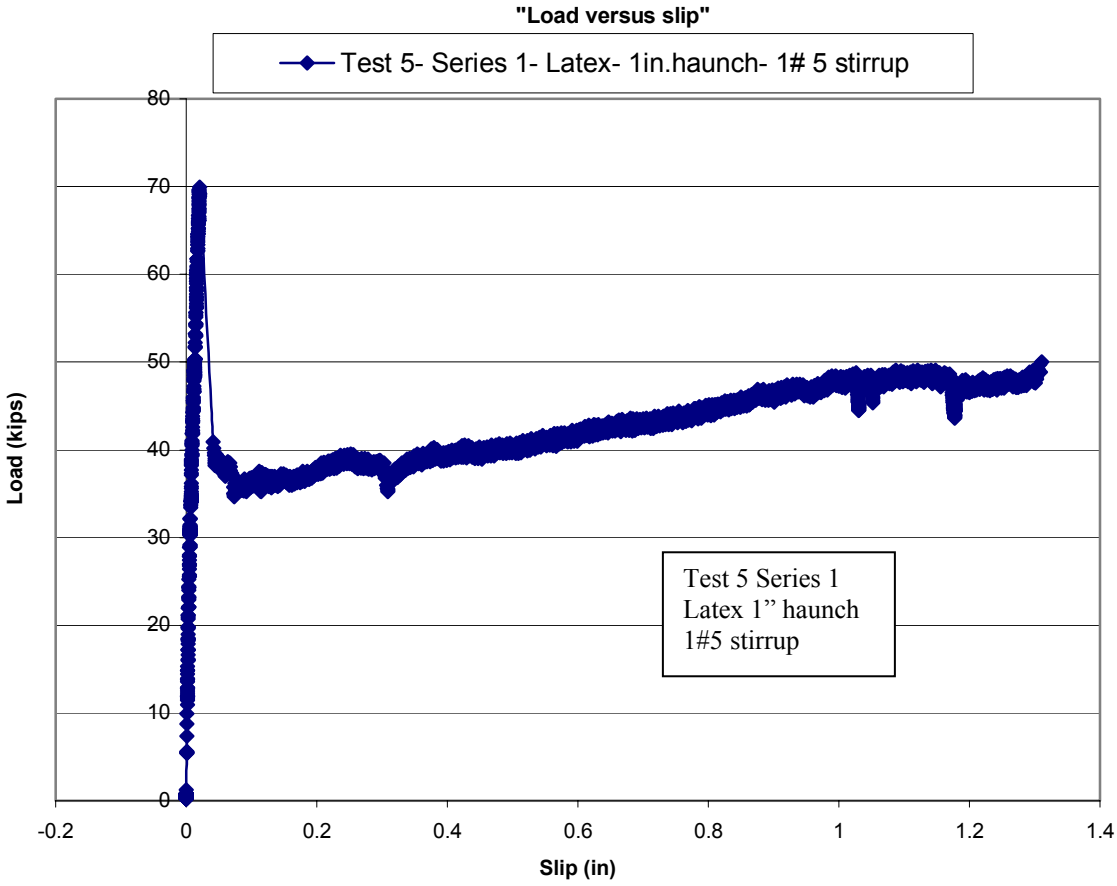
"Load versus slip"
Test 5- Series 1- Latex- 1in.haunch- 1# 5 stirrup
Load (kips)
80
70
60
50
40
30
20
10
0
-0.2
0
0.2
0.4
0.6
0.8
1
1.2
1.4
Slip (in)
Test 5 Series 1
Latex 1" haunch
1#5 stirrup

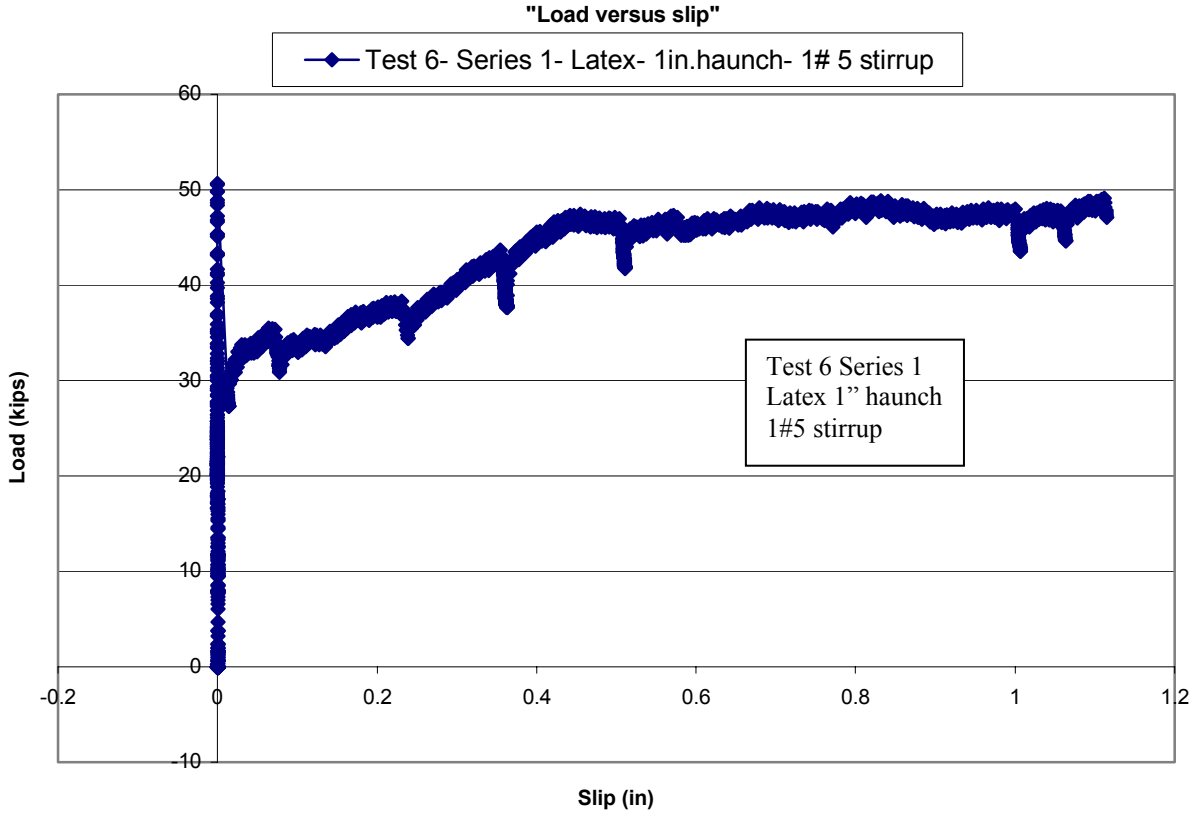
"Load versus slip"
Test 6- Series 1- Latex- 1in.haunch- 1# 5 stirrup
Load (kips)
60
50
40
30
20
10
0
-10
-0.2
0
0.2
0.4
0.6
0.8
1
1.2
Slip (in)
Test 6 Series 1
Latex 1" haunch
1#5 stirrup

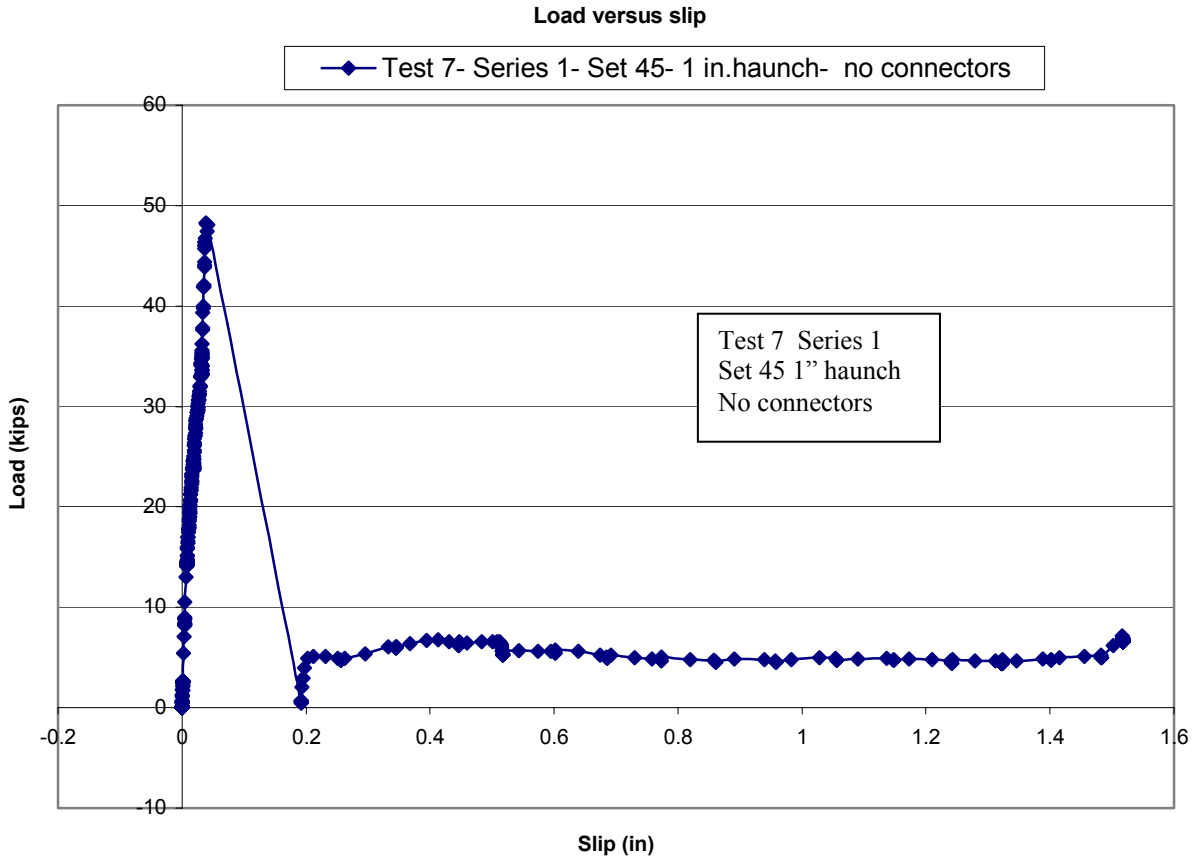
Load versus slip
Test 7- Series 1- Set 45- 1 in.haunch- no connectors
Test 7 Series 1
Set 45 1" haunch
No connectors
Load (kips)
Slip (in)
60
50
40
30
20
10
0
-10
-0.2
0
0.2
0.4
0.6
0.8
1
1.2
1.4
1.6

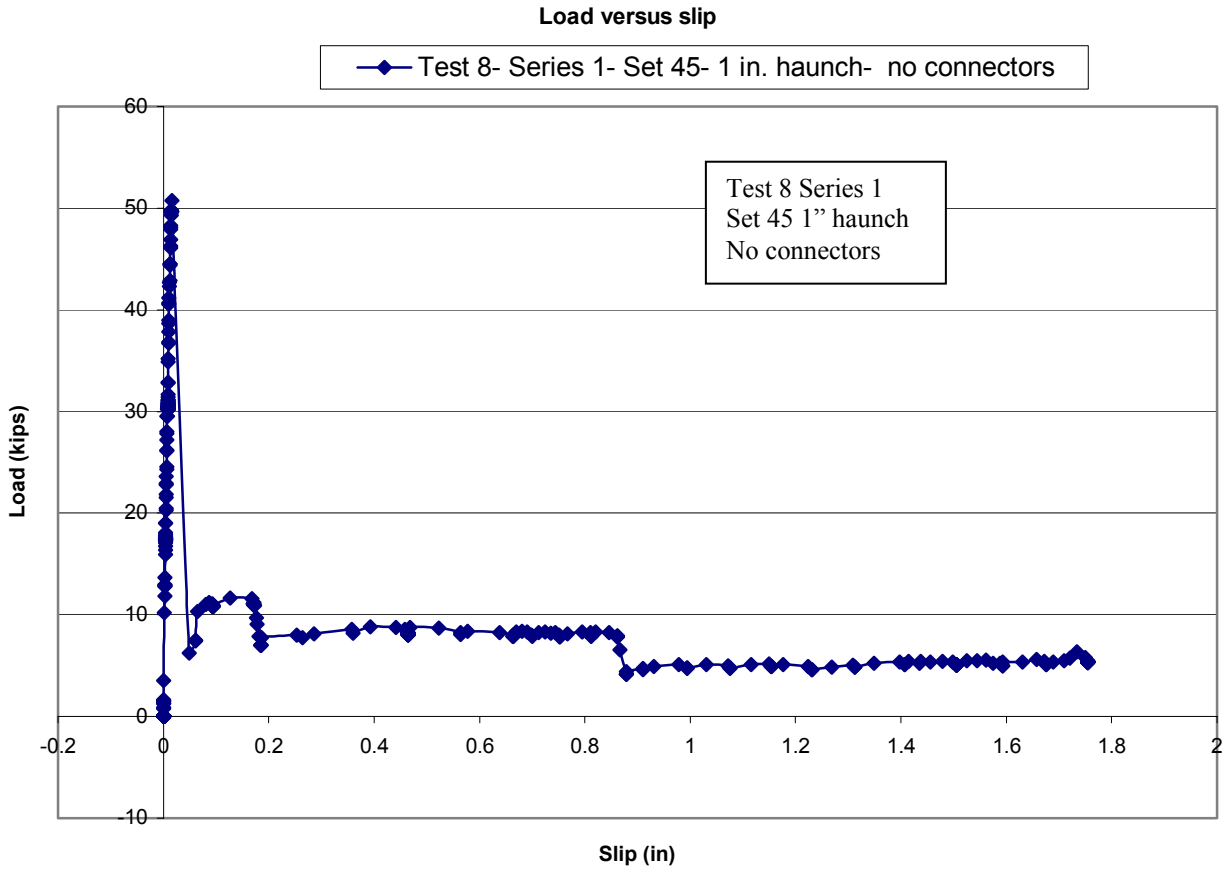
Load versus slip
Test 8- Series 1- Set 45- 1 in. haunch- no connectors
Test 8 Series 1
Set 45 1" haunch
No connectors
Load (kips)
60
50
40
30
20
10
0
-10
-0.2
0
0.2
0.4
0.6
0.8
1
1.2
1.4
1.6
1.8
2
Slip (in)

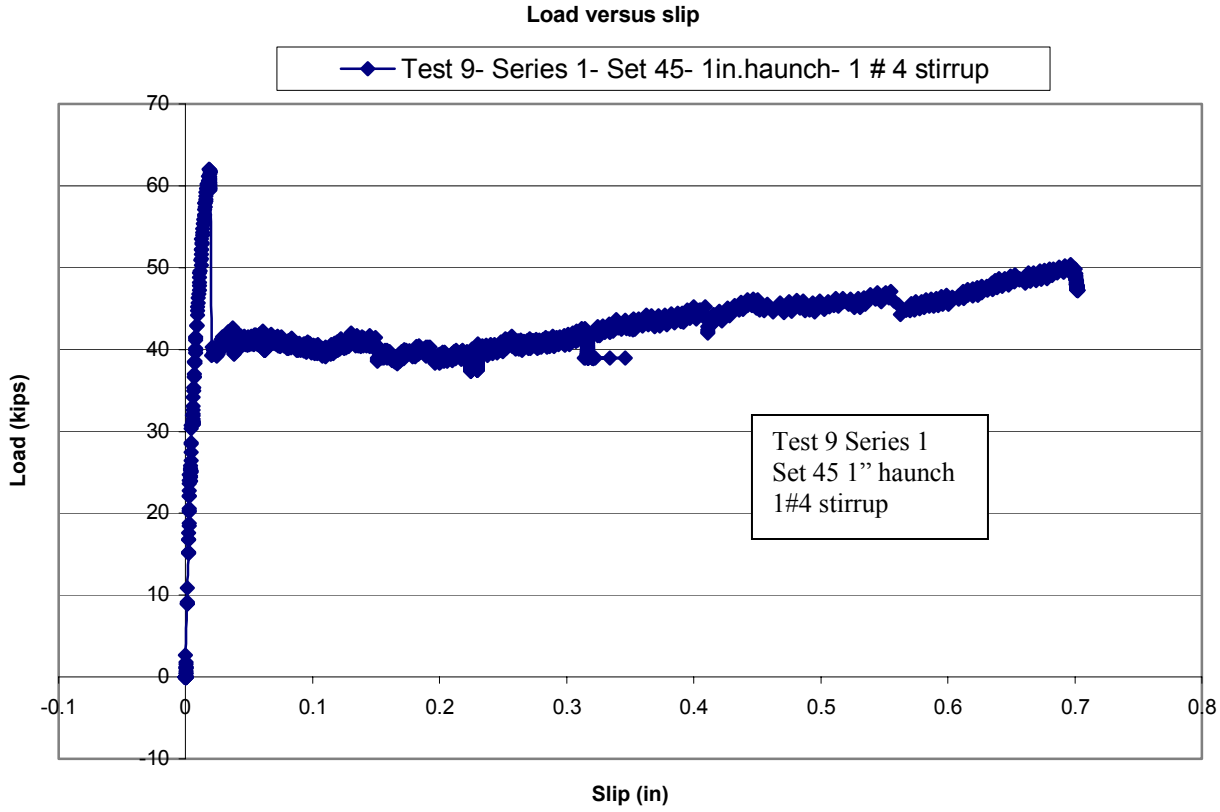
Load versus slip
Test 9- Series 1- Set 45- 1in.haunch- 1 # 4 stirrup
Load (kips)
70
60
50
40
30
20
10
0
-10
-0.1
0
0.1
0.2
0.3
0.4
0.5
0.6
0.7
0.8
Slip (in)
Test 9 Series 1
Set 45 1" haunch
1#4 stirrup

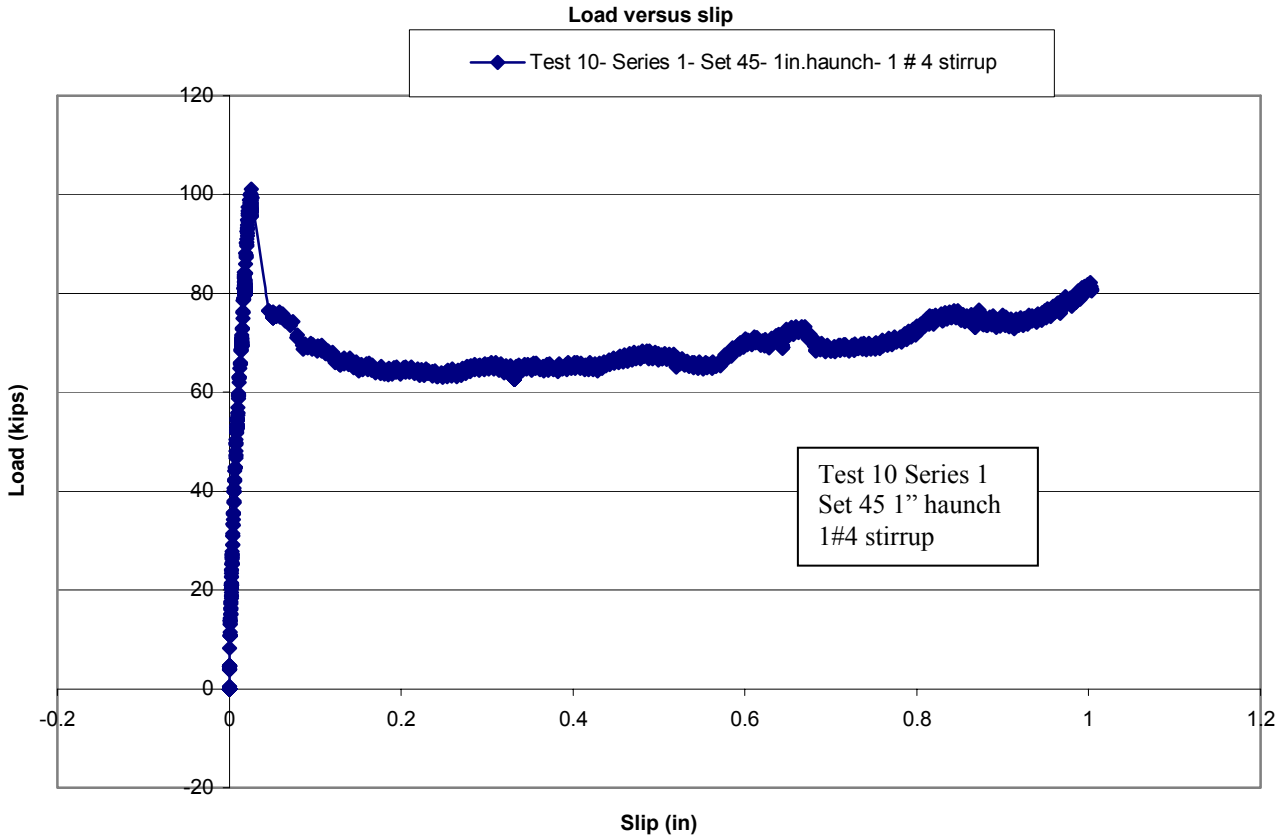
Load versus slip
Test 10- Series 1- Set 45- 1in.haunch- 1 # 4 stirrup
Load (kips)
120
100
80
60
40
20
0
-20
-0.2
0
0.2
0.4
0.6
0.8
1
1.2
Slip (in)
Test 10 Series 1
Set 45 1” haunch
1#4 stirrup

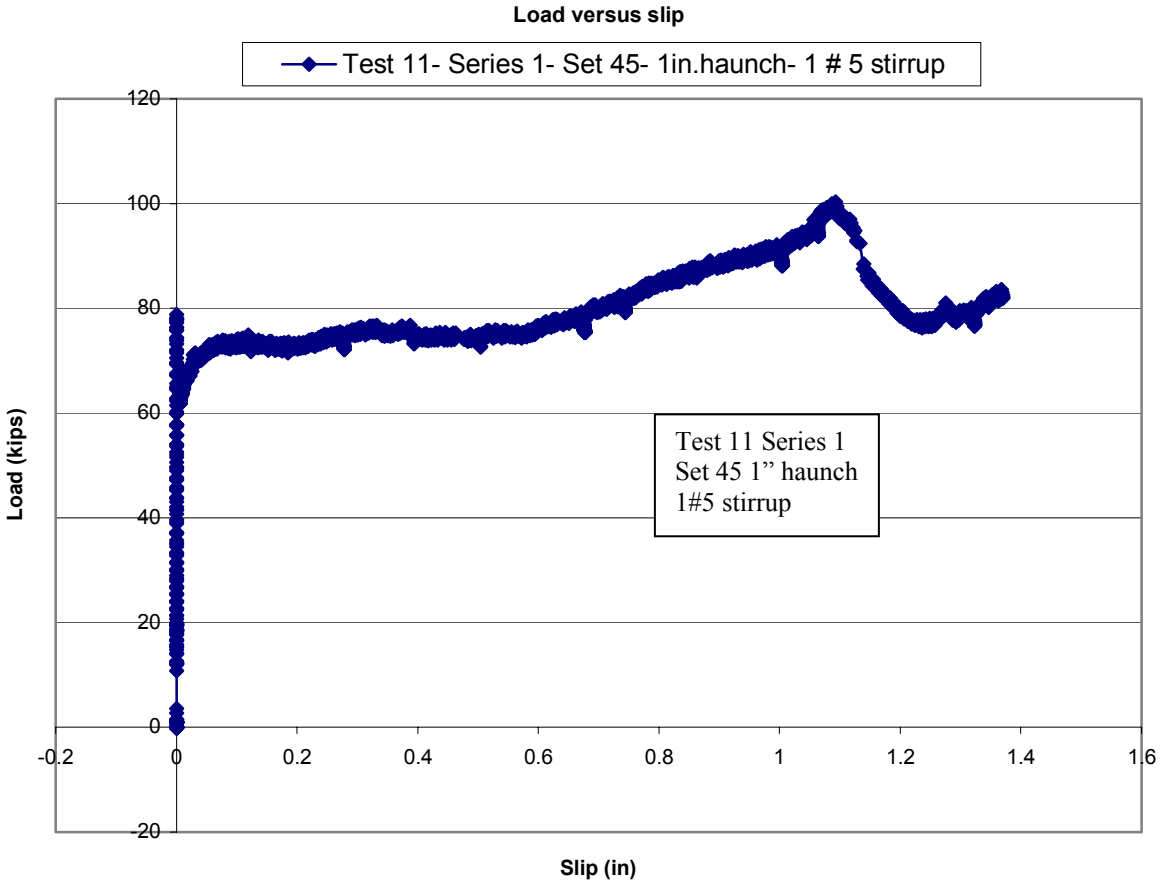
Load versus slip
Test 11- Series 1- Set 45- 1in.haunch- 1 # 5 stirrup
Load (kips)
120
100
80
60
40
20
0
-20
-0.2
0
0.2
0.4
0.6
0.8
1
1.2
1.4
1.6
Slip (in)
Test 11 Series 1
Set 45 1” haunch
1#5 stirrup

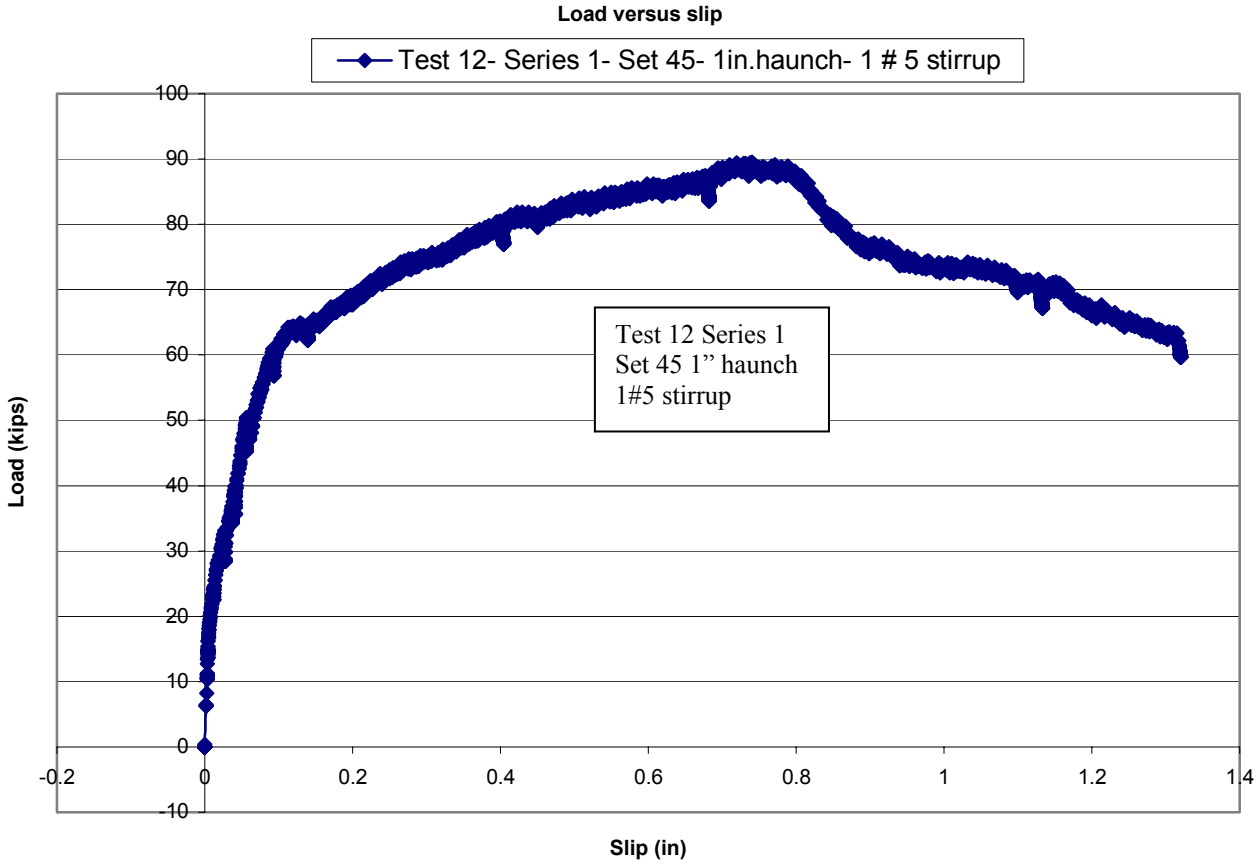
Load versus slip
Test 12- Series 1- Set 45- 1in.haunch- 1 # 5 stirrup
Test 12 Series 1
Set 45 1" haunch
1#5 stirrup
Load (kips)
Slip (in)
100
90
80
70
60
50
40
30
20
10
0
-10
-0.2
0
0.2
0.4
0.6
0.8
1
1.2
1.4

Series 2

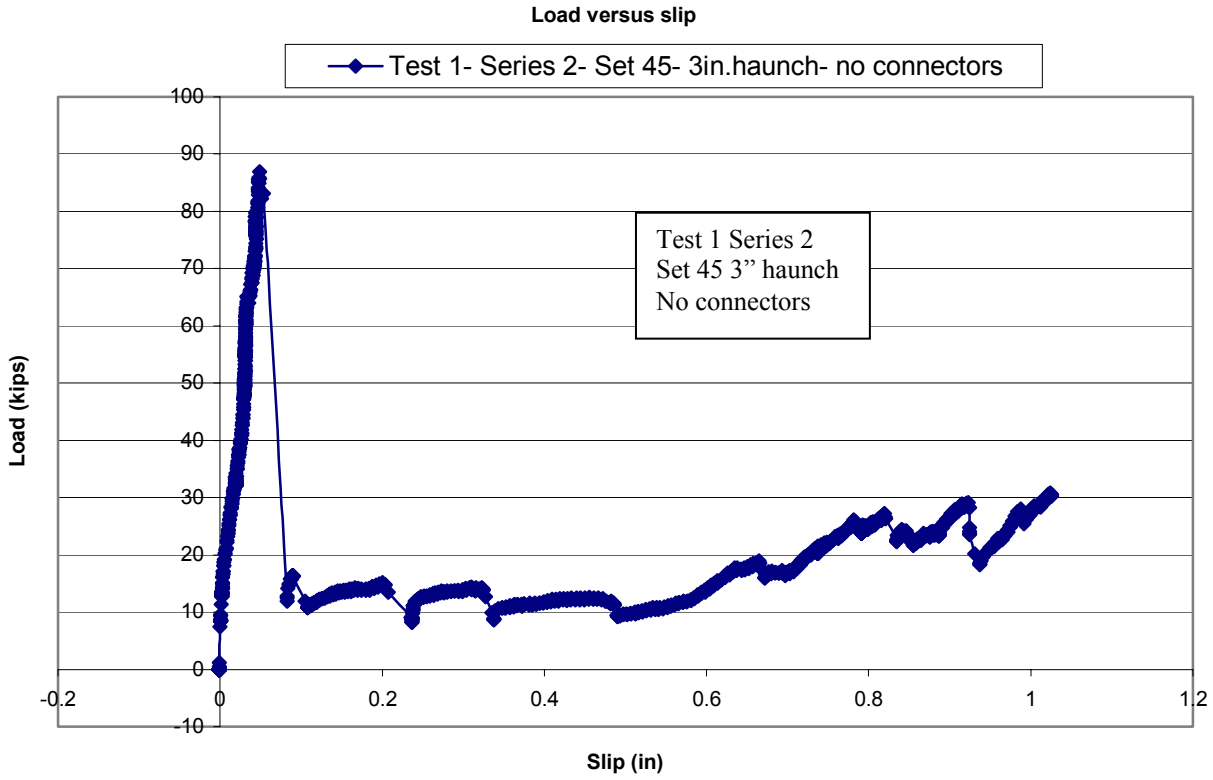
Load versus slip
Test 1- Series 2- Set 45- 3in.haunch- no connectors
Test 1 Series 2
Set 45 3" haunch
No connectors
Load (kips)
Slip (in)
100
90
80
70
60
50
40
30
20
10
0
-10
-0.2
0
0.2
0.4
0.6
0.8
1
1.2

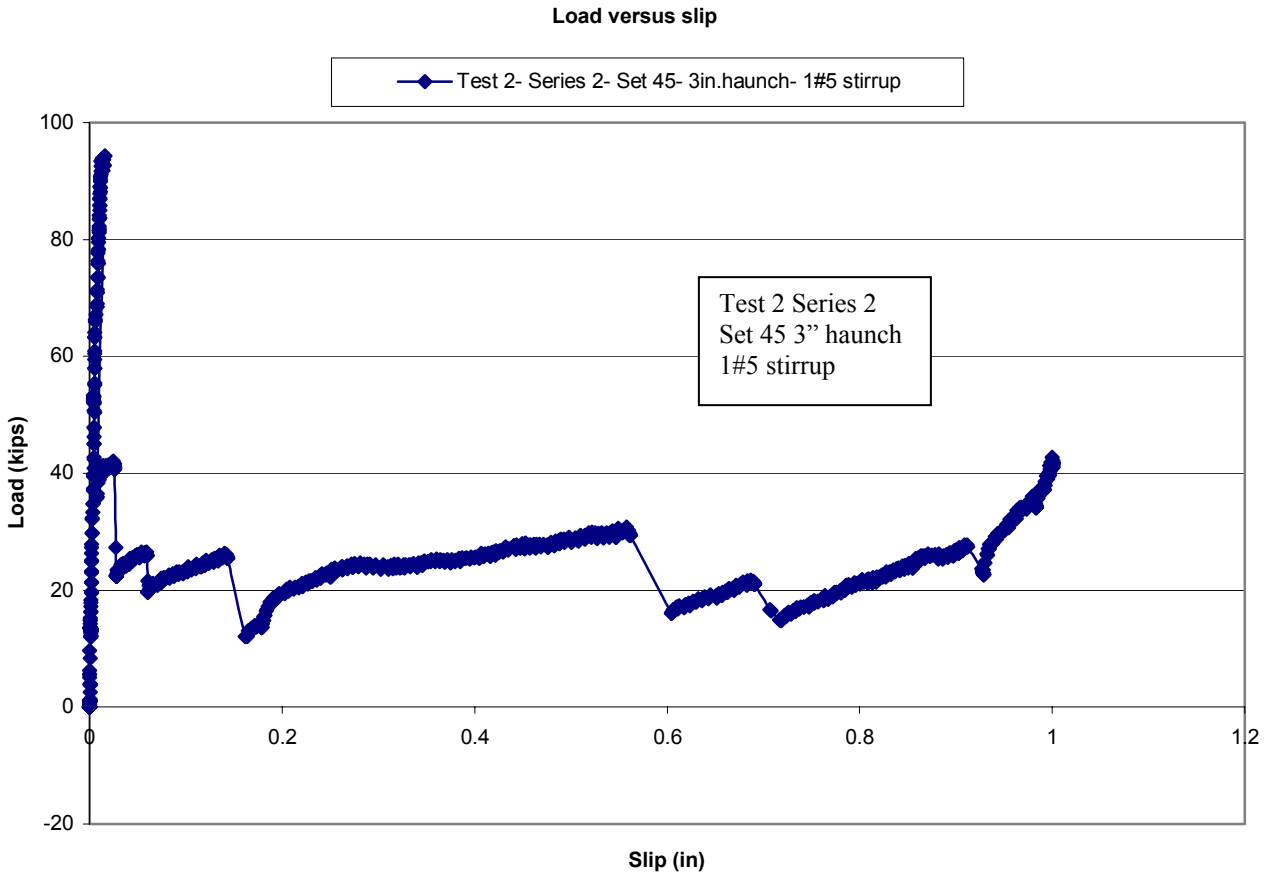
Load versus slip
Test 2- Series 2- Set 45- 3in.haunch- 1#5 stirrup
Test 2 Series 2
Set 45 3" haunch
1#5 stirrup
Load (kips)
Slip (in)
100
80
60
40
20
0
-20
0
0.2
0.4
0.6
0.8
1
1.2

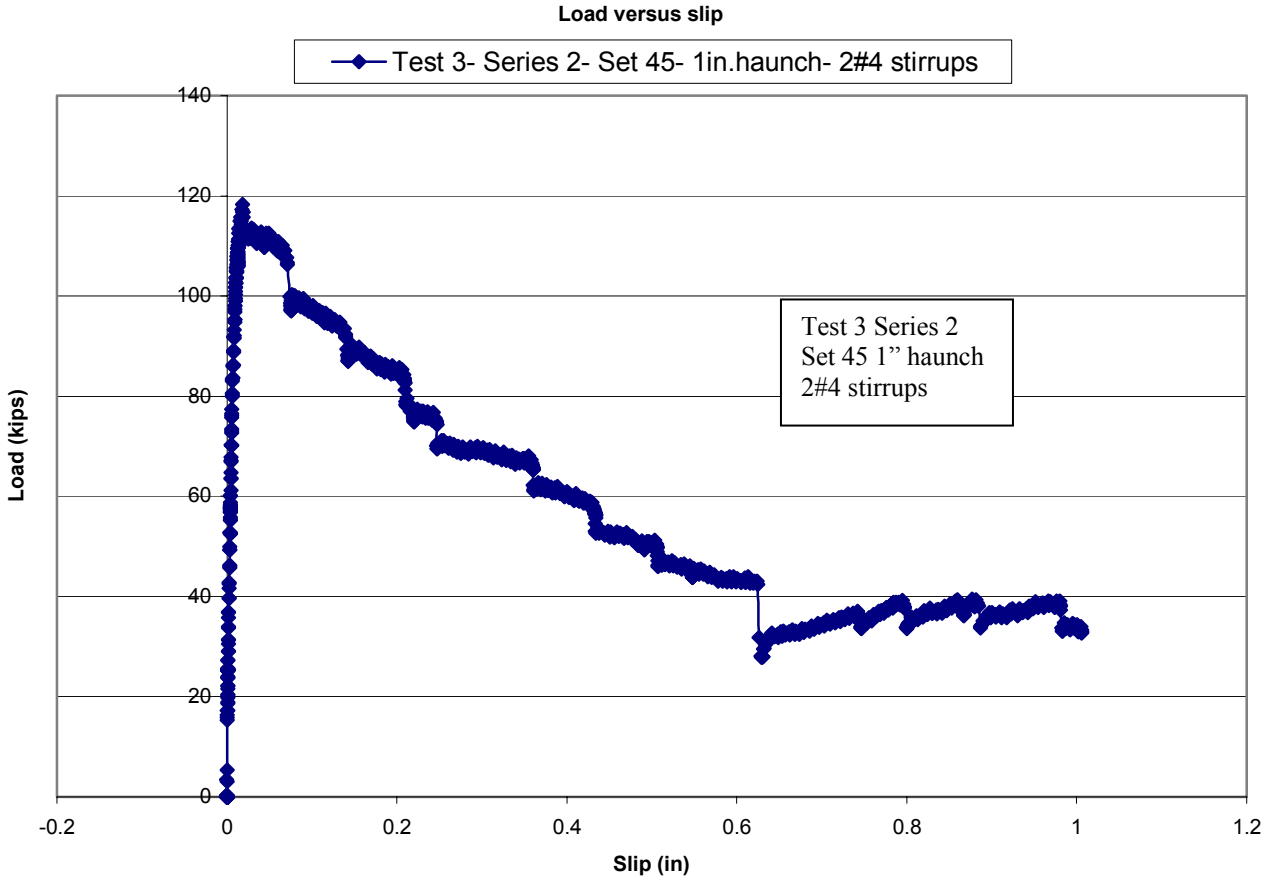
Load versus slip
Test 3- Series 2- Set 45- 1in.haunch- 2#4 stirrups
Load (kips)
140
120
100
80
60
40
20
0
-0.2
0
0.2
0.4
0.6
0.8
1
1.2
Slip (in)
Test 3 Series 2
Set 45 1” haunch
2#4 stirrups

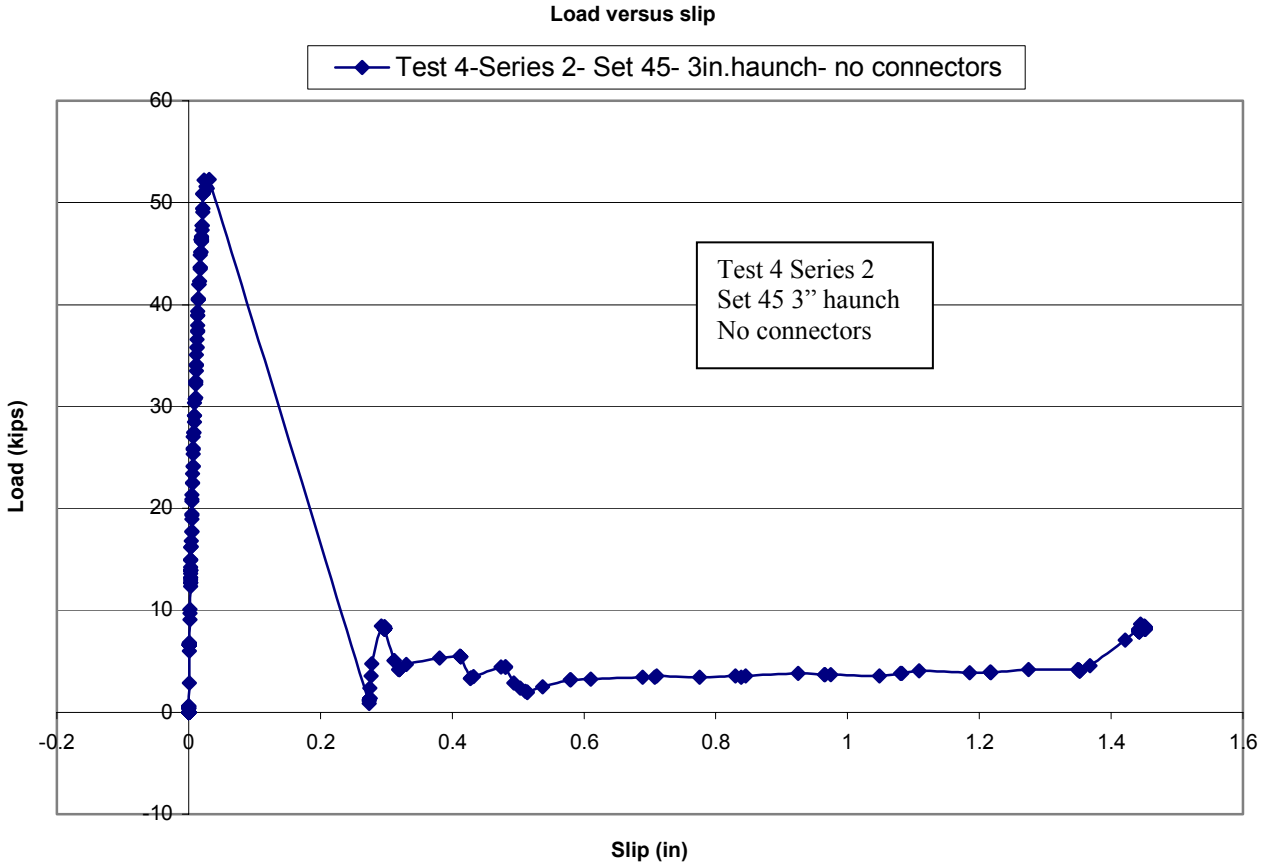
Load versus slip
Test 4-Series 2- Set 45- 3in.haunch- no connectors
Test 4 Series 2
Set 45 3" haunch
No connectors
Load (kips)
60
50
40
30
20
10
0
-10
-0.2
0
0.2
0.4
0.6
0.8
1
1.2
1.4
1.6
Slip (in)

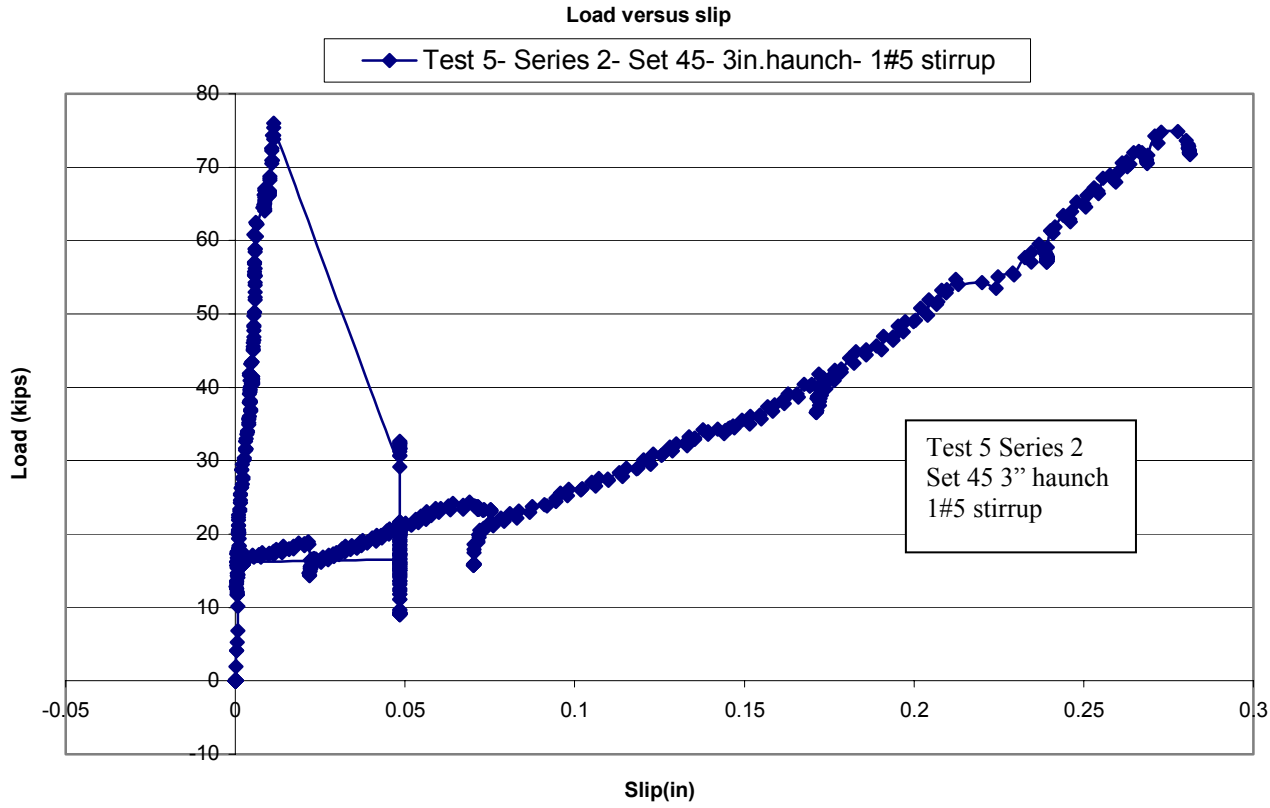
Load versus slip
Test 5- Series 2- Set 45- 3in.haunch- 1#5 stirrup
Load (kips)
80
70
60
50
40
30
20
10
0
-10
-0.05
0
0.05
0.1
0.15
0.2
0.25
0.3
Slip(in)
Test 5 Series 2
Set 45 3" haunch
1#5 stirrup

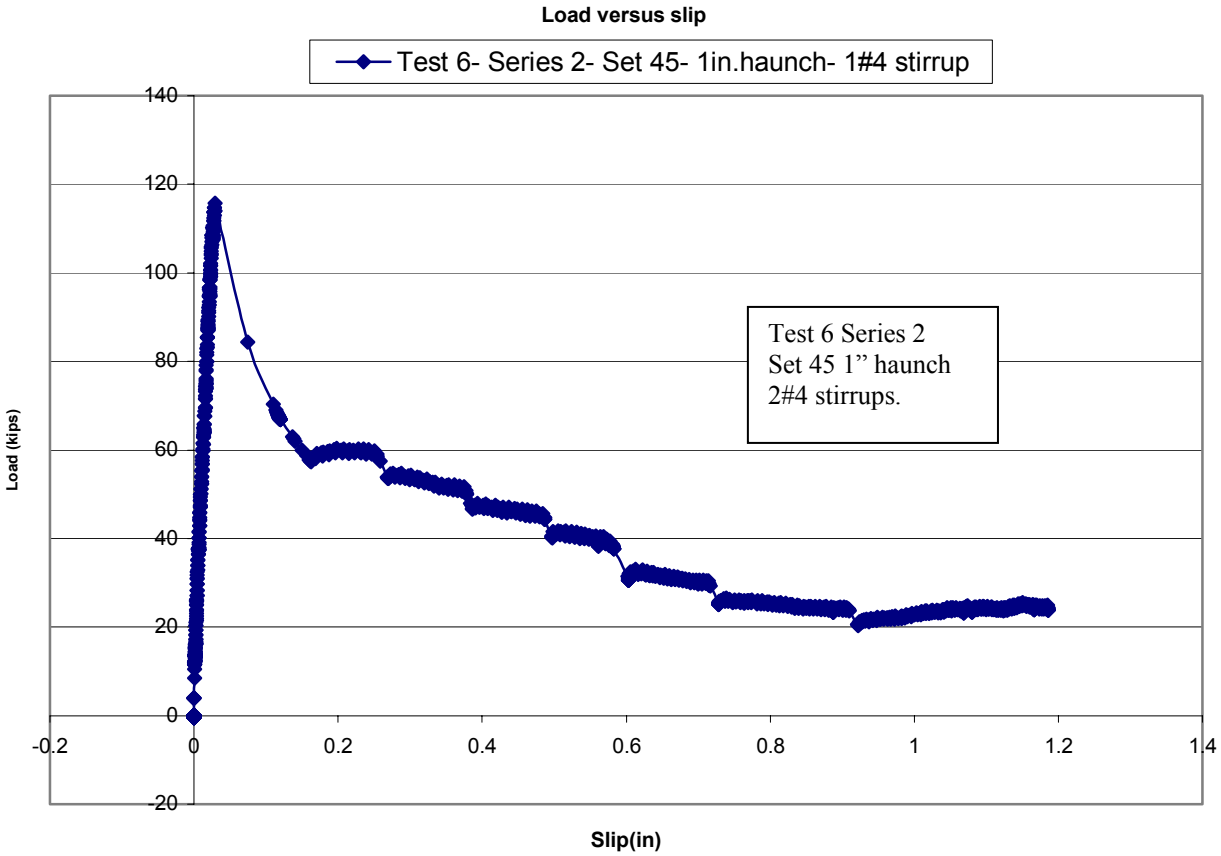
Load versus slip
Test 6- Series 2- Set 45- 1in.haunch- 1#4 stirrup
Test 6 Series 2
Set 45 1" haunch
2#4 stirrups.
Load (kips)
Slip(in)
140
120
100
80
60
40
20
0
-20
-0.2
0
0.2
0.4
0.6
0.8
1
1.2
1.4

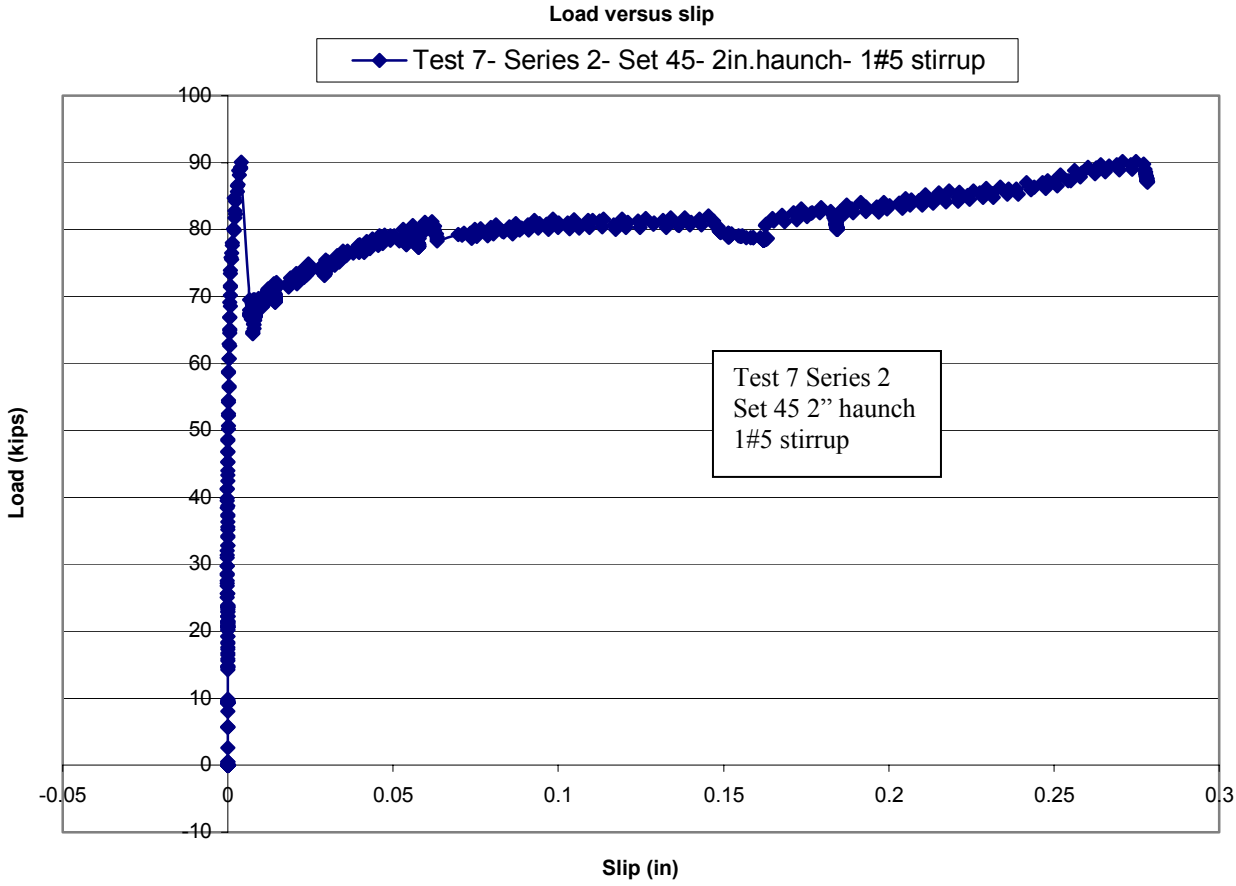
Load versus slip
Test 7- Series 2- Set 45- 2in.haunch- 1#5 stirrup
Test 7 Series 2
Set 45 2" haunch
1#5 stirrup
Load (kips)
Slip (in)
100
90
80
70
60
50
40
30
20
10
0
-10
-0.05
0
0.05
0.1
0.15
0.2
0.25
0.3

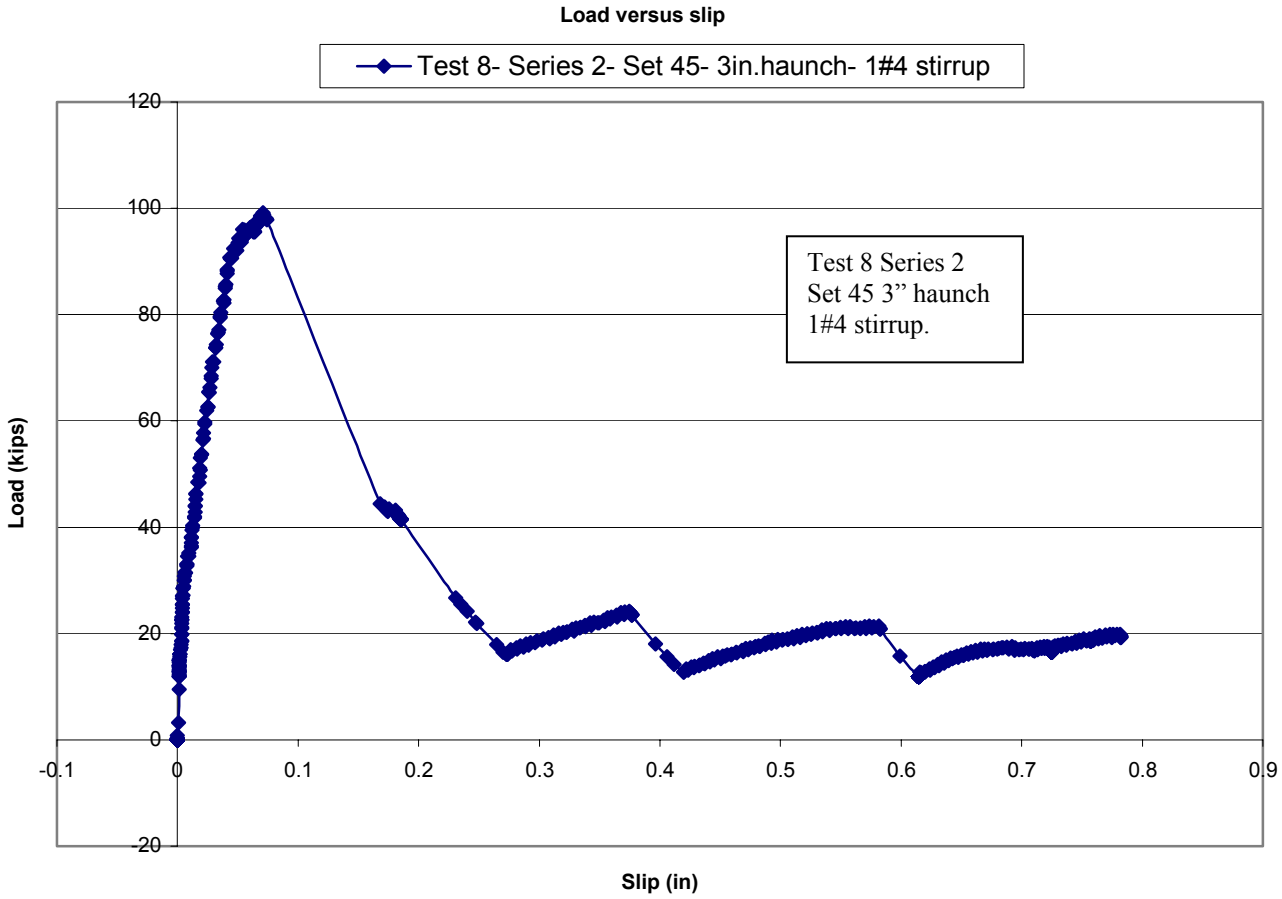
Load versus slip
Test 8- Series 2- Set 45- 3in.haunch- 1#4 stirrup
Test 8 Series 2
Set 45 3" haunch
1#4 stirrup.
Load (kips)
120
100
80
60
40
20
0
-20
-0.1
0
0.1
0.2
0.3
0.4
0.5
0.6
0.7
0.8
0.9
Slip (in)

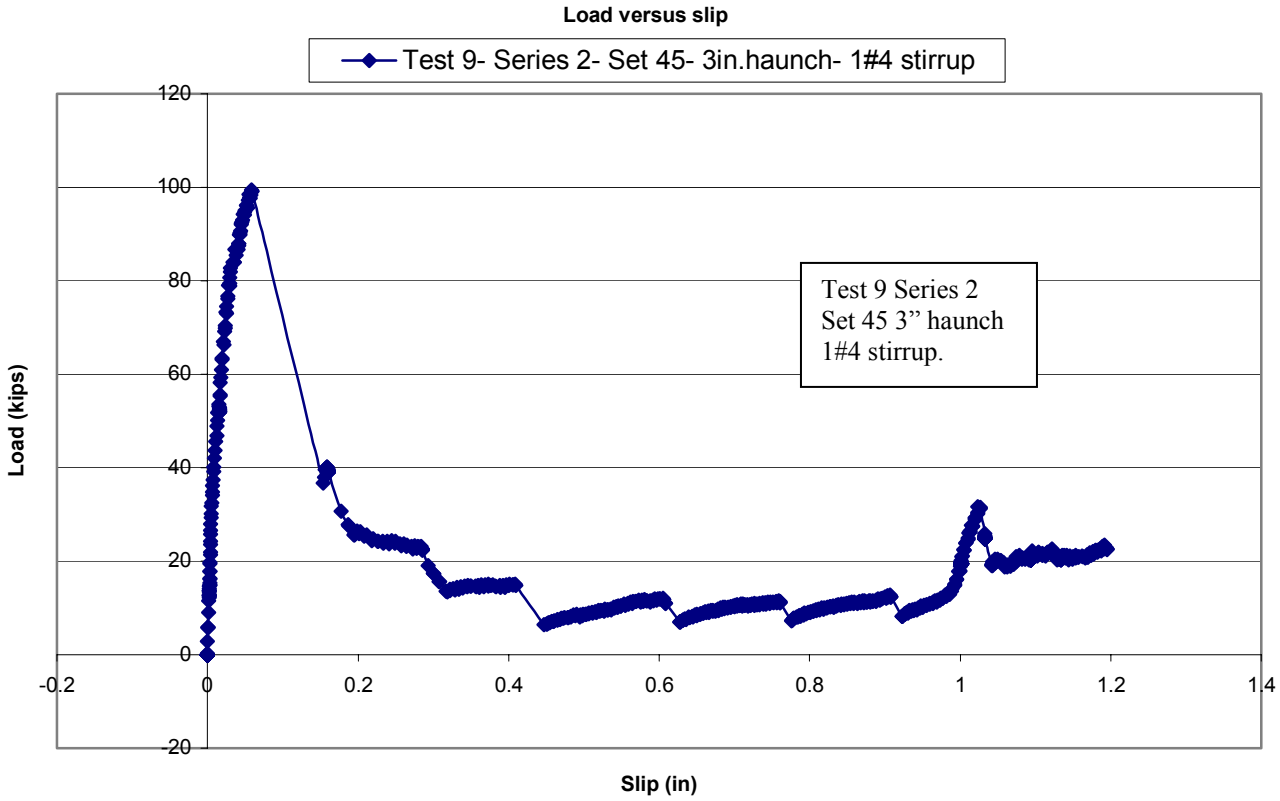
Load versus slip
Test 9- Series 2- Set 45- 3in.haunch- 1#4 stirrup
Test 9 Series 2
Set 45 3" haunch
1#4 stirrup.
Load (kips)
120
100
80
60
40
20
0
-20
-0.2
0
0.2
0.4
0.6
0.8
1
1.2
1.4
Slip (in)

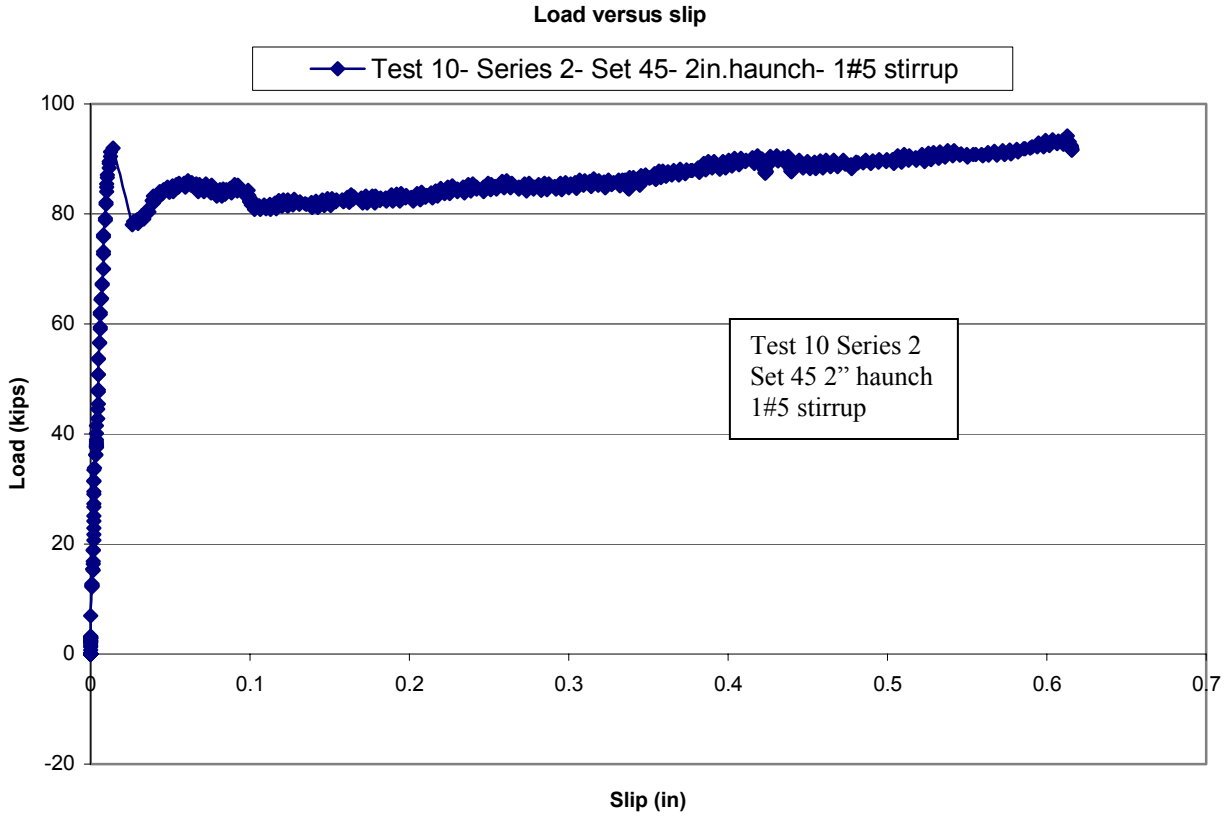
Load versus slip
Test 10- Series 2- Set 45- 2in.haunch- 1#5 stirrup
100
80
60
40
20
0
-20
0
0.1
0.2
0.3
0.4
0.5
0.6
0.7
Load (kips)
Slip (in)
Test 10 Series 2
Set 45 2" haunch
1#5 stirrup

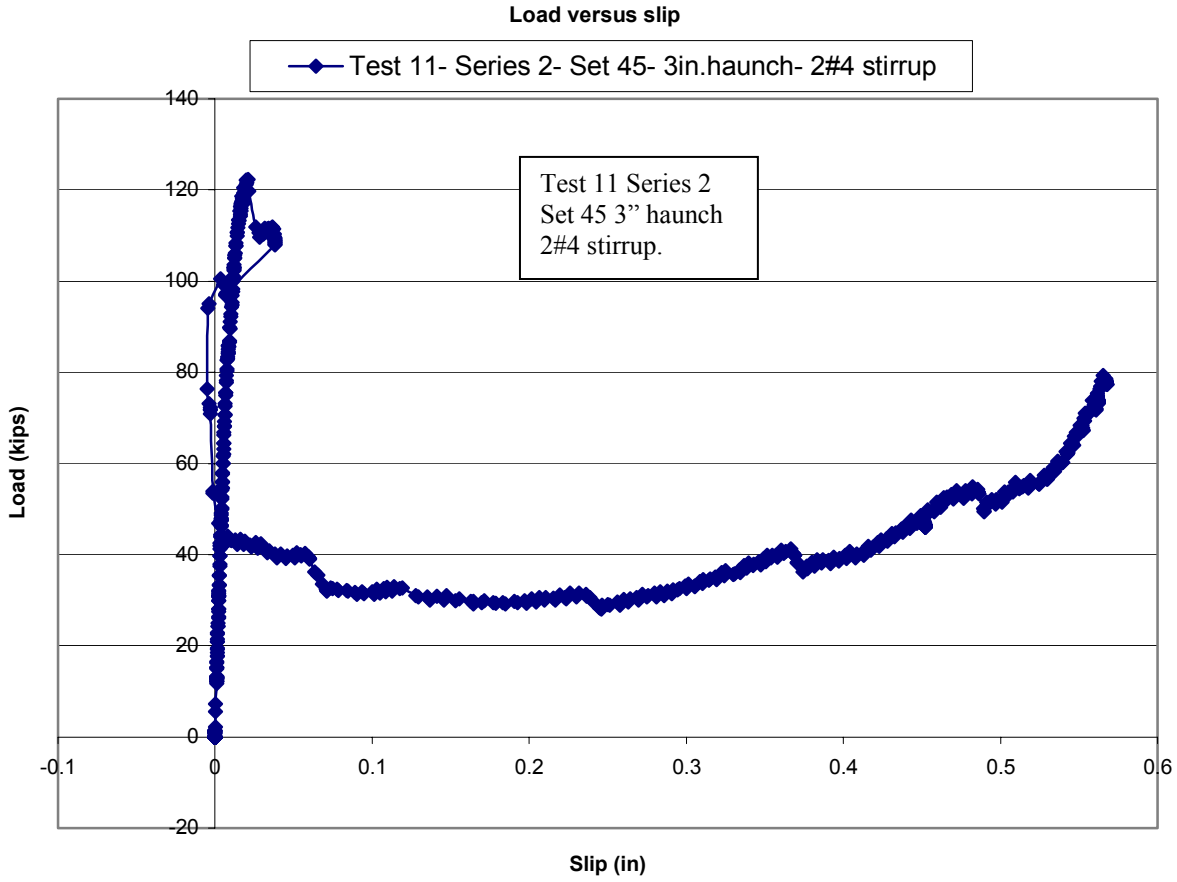
Load versus slip
Test 11- Series 2- Set 45- 3in.haunch- 2#4 stirrup
Test 11 Series 2
Set 45 3" haunch
2#4 stirrup.
Load (kips)
140
120
100
80
60
40
20
0
-20
-0.1
0
0.1
0.2
0.3
0.4
0.5
0.6
Slip (in)

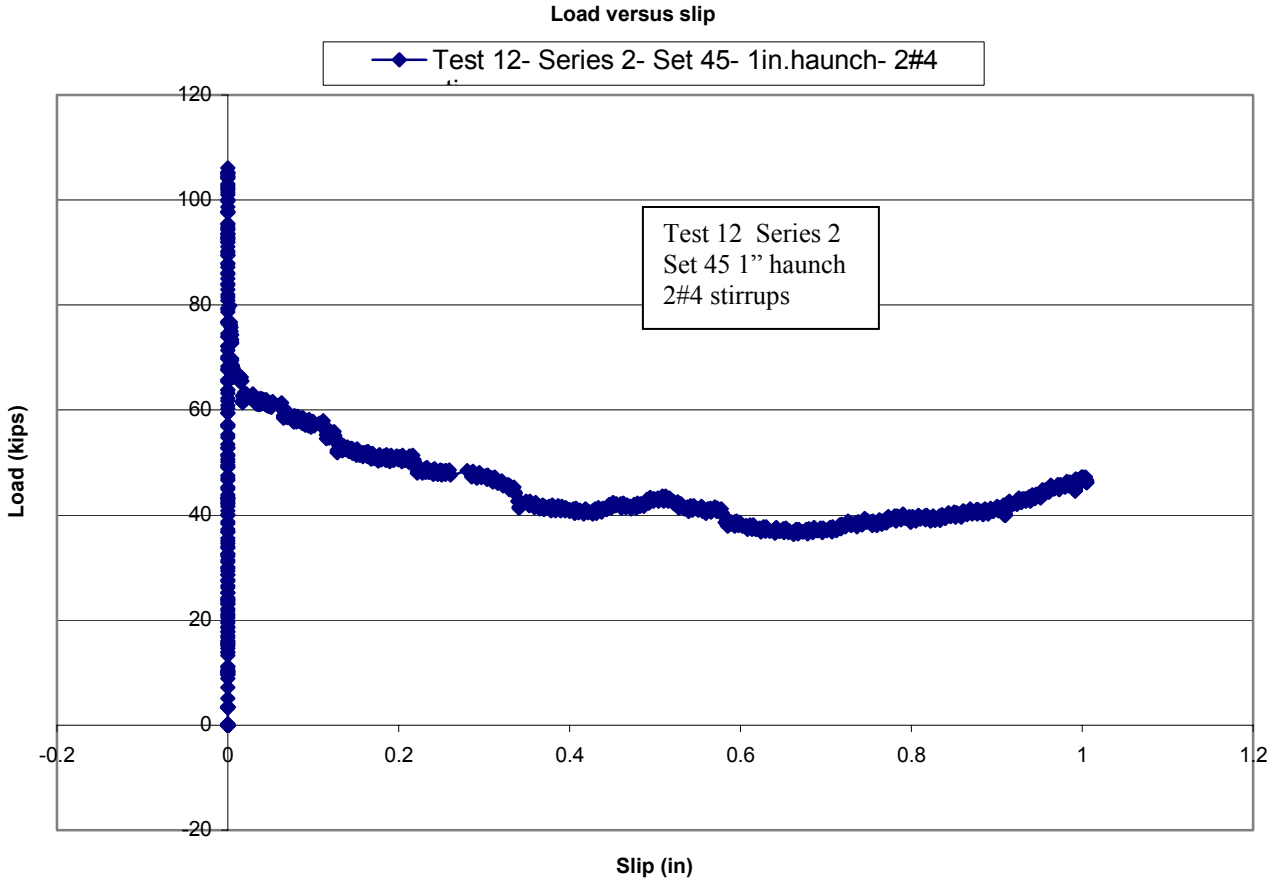
Load versus slip
Test 12- Series 2- Set 45- 1in.haunch- 2#4
Test 12 Series 2
Set 45 1" haunch
2#4 stirrups
Load (kips)
120
100
80
60
40
20
0
-20
-0.2
0
0.2
0.4
0.6
0.8
1
1.2
Slip (in)

Series 3

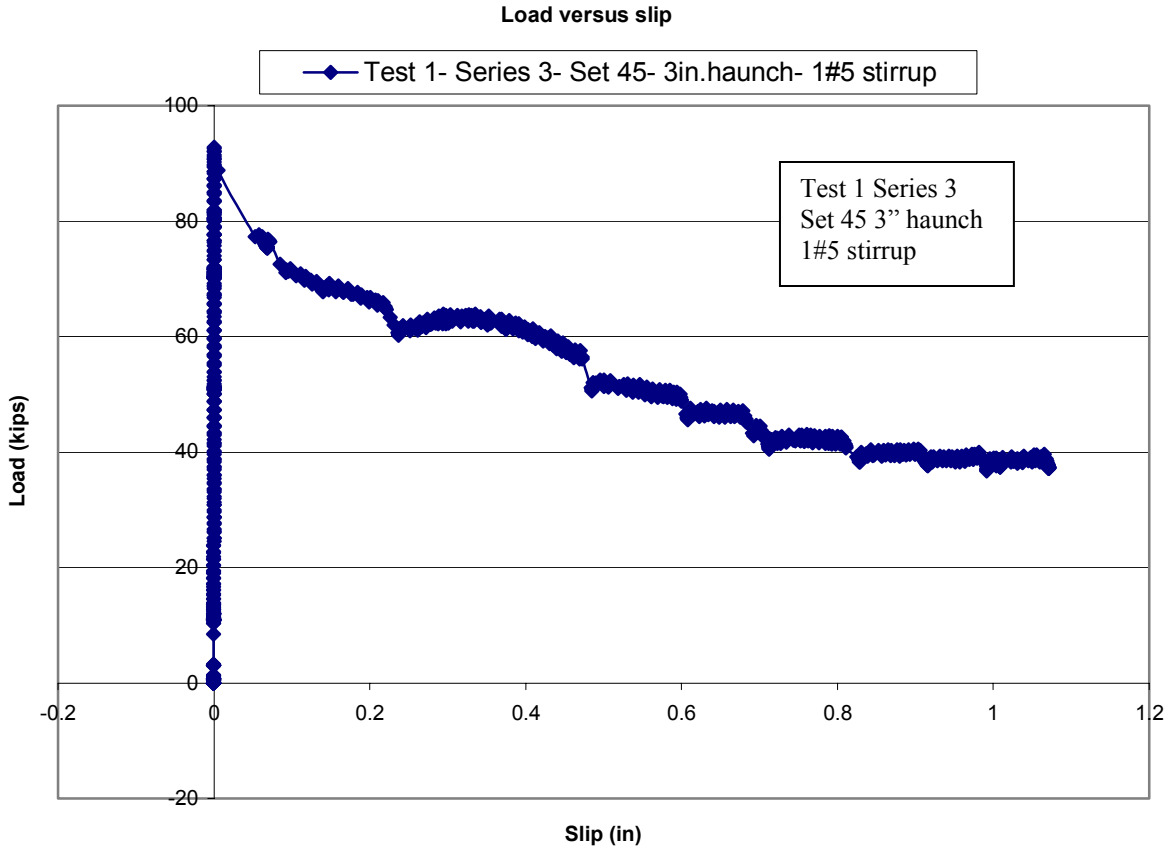
Load versus slip
Test 1- Series 3- Set 45- 3in.haunch- 1#5 stirrup
Test 1 Series 3
Set 45 3" haunch
1#5 stirrup
Load (kips)
100
80
60
40
20
0
-20
-0.2
0
0.2
0.4
0.6
0.8
1
1.2
Slip (in)

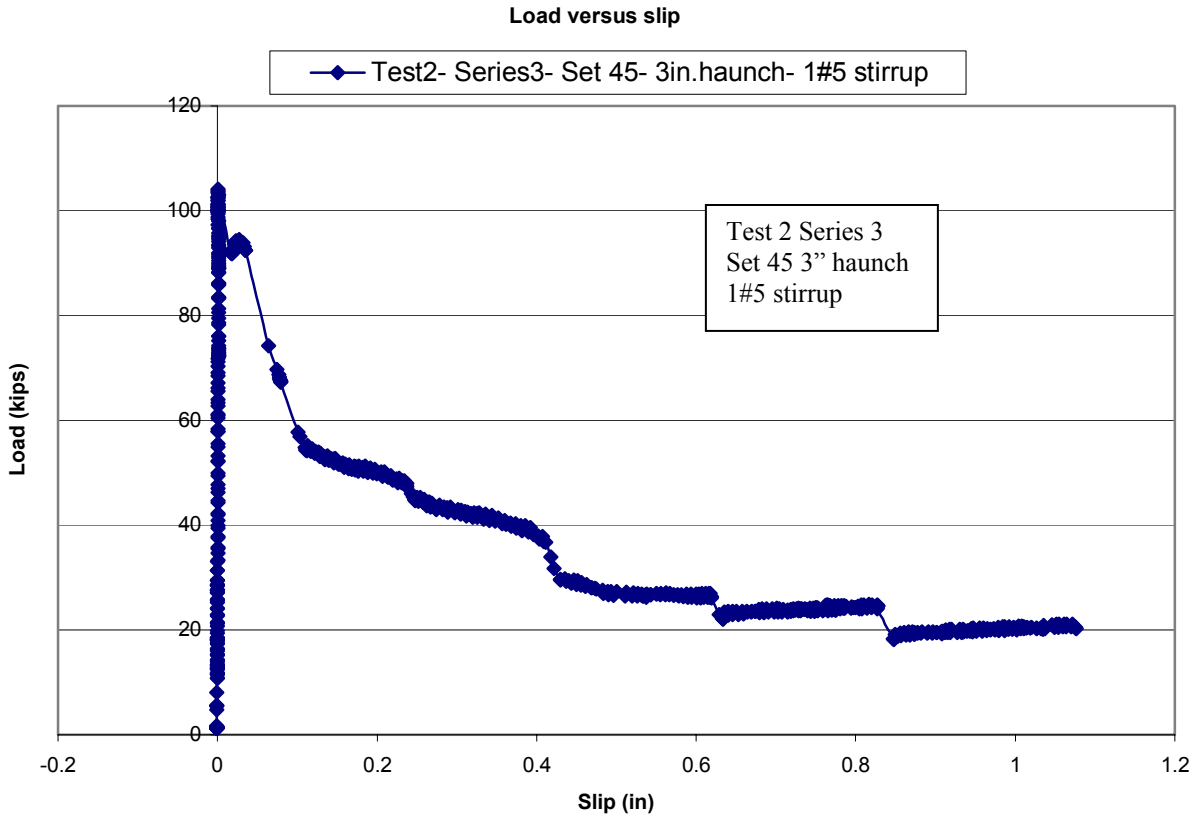
Load versus slip
Test2- Series3- Set 45- 3in.haunch- 1#5 stirrup
Test 2 Series 3
Set 45 3" haunch
1#5 stirrup
Load (kips)
Slip (in)
120
100
80
60
40
20
0
-0.2
0
0.2
0.4
0.6
0.8
1
1.2

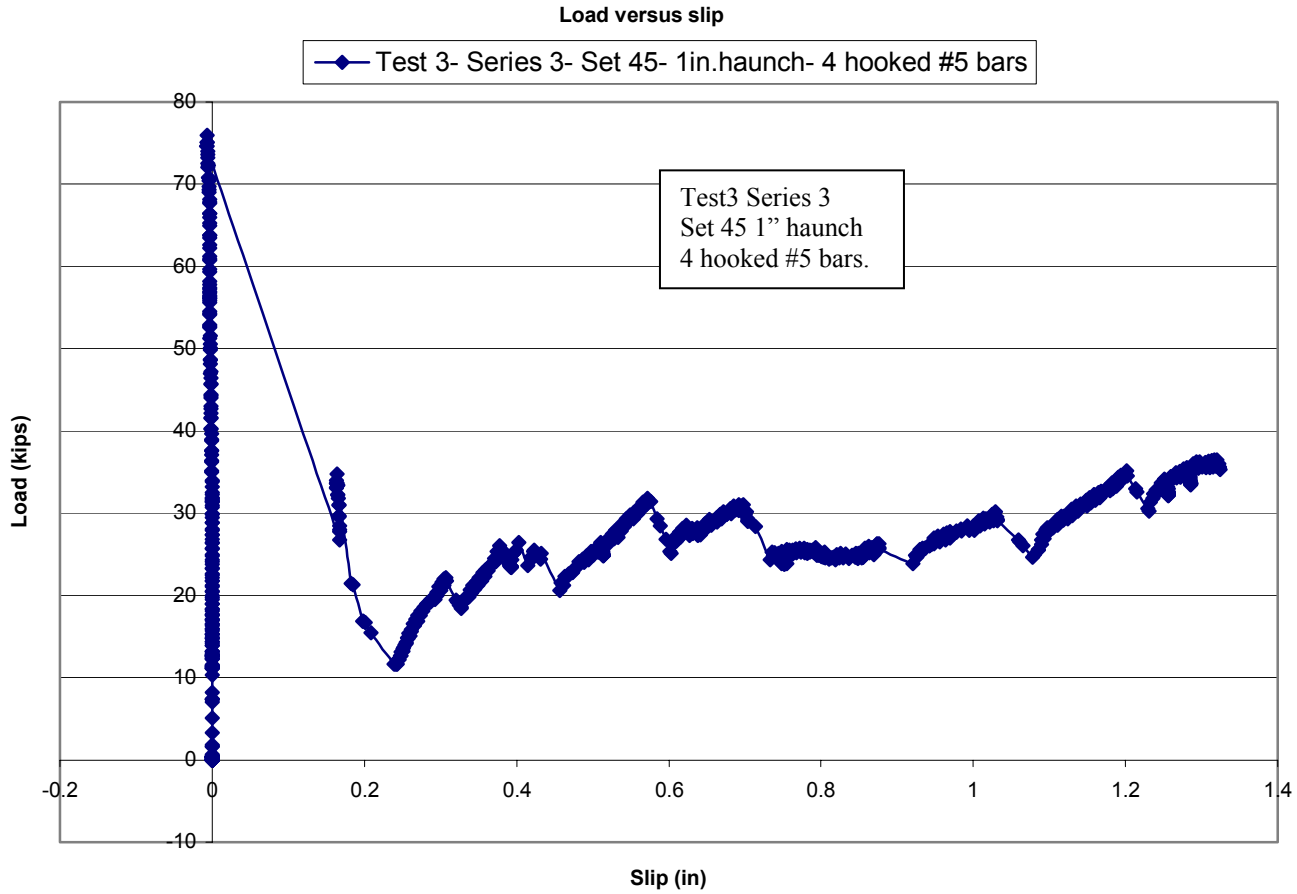
Load versus slip
Test 3- Series 3- Set 45- 1in.haunch- 4 hooked #5 bars
Test3 Series 3
Set 45 1" haunch
4 hooked #5 bars.
Load (kips)
Slip (in)
80
70
60
50
40
30
20
10
0
-10
-0.2
0
0.2
0.4
0.6
0.8
1
1.2
1.4

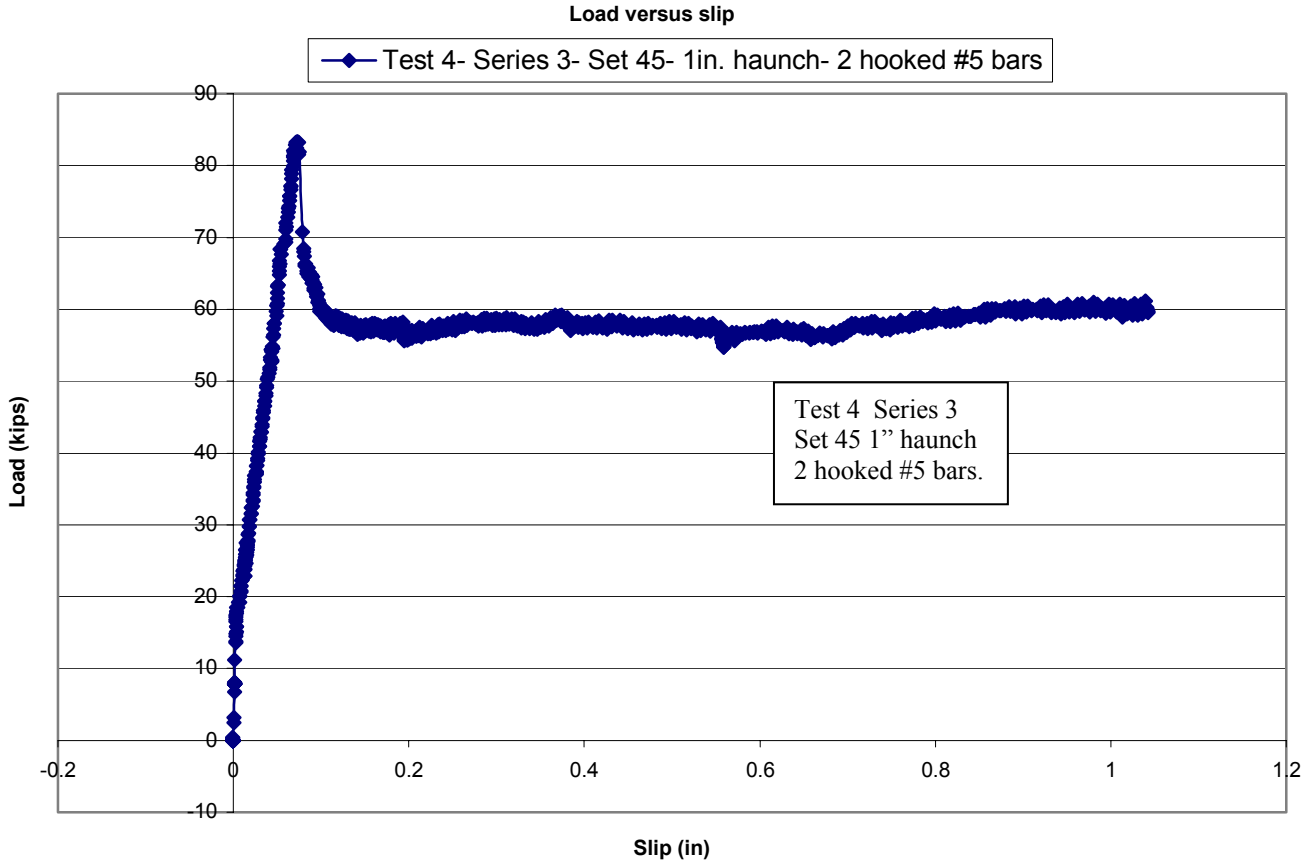
Load versus slip
Test 4- Series 3- Set 45- 1in. haunch- 2 hooked #5 bars
Load (kips)
90
80
70
60
50
40
30
20
10
0
-10
-0.2
0
0.2
0.4
0.6
0.8
1
1.2
Slip (in)
Test 4 Series 3
Set 45 1" haunch
2 hooked #5 bars.

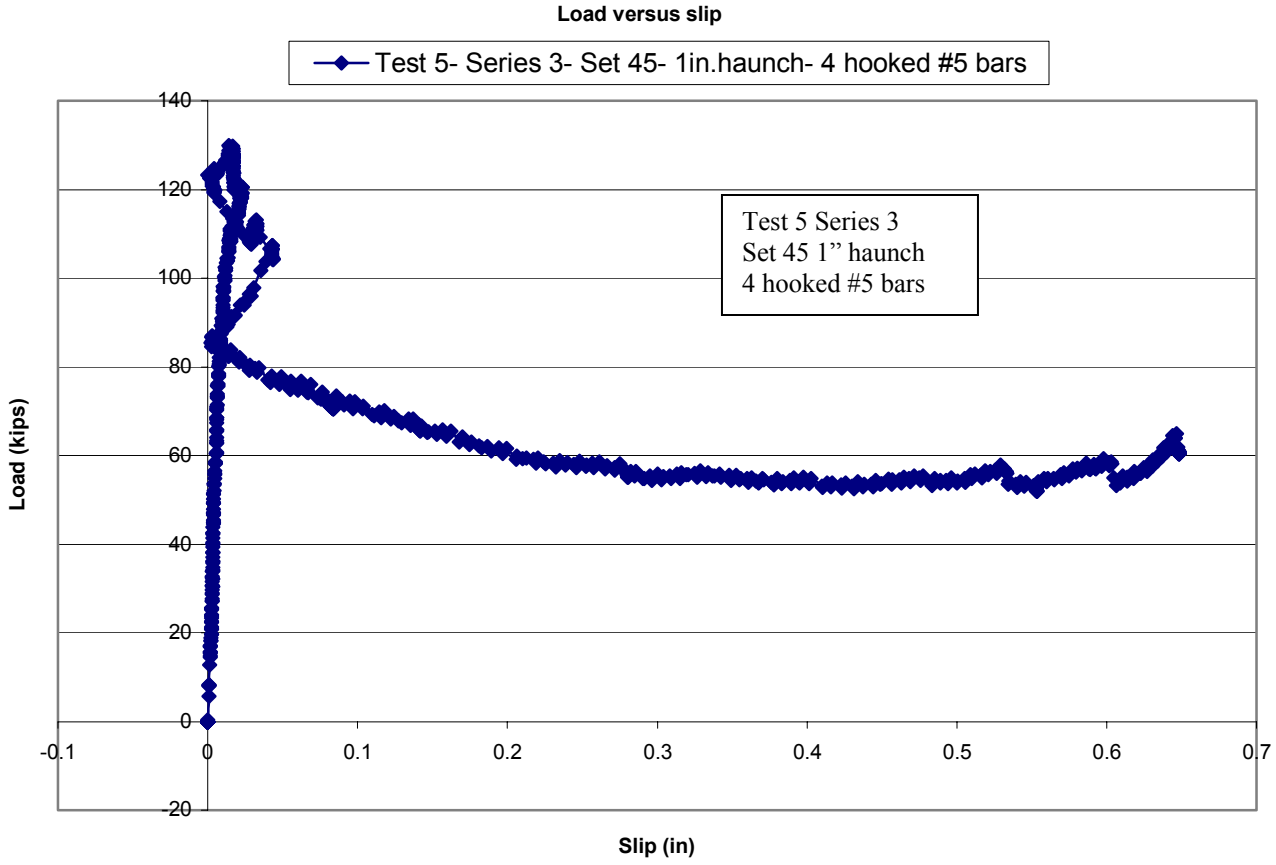
Load versus slip
Test 5- Series 3- Set 45- 1in.haunch- 4 hooked #5 bars
Test 5 Series 3
Set 45 1" haunch
4 hooked #5 bars
Load (kips)
Slip (in)
140
120
100
80
60
40
20
0
-20
-0.1
0
0.1
0.2
0.3
0.4
0.5
0.6
0.7

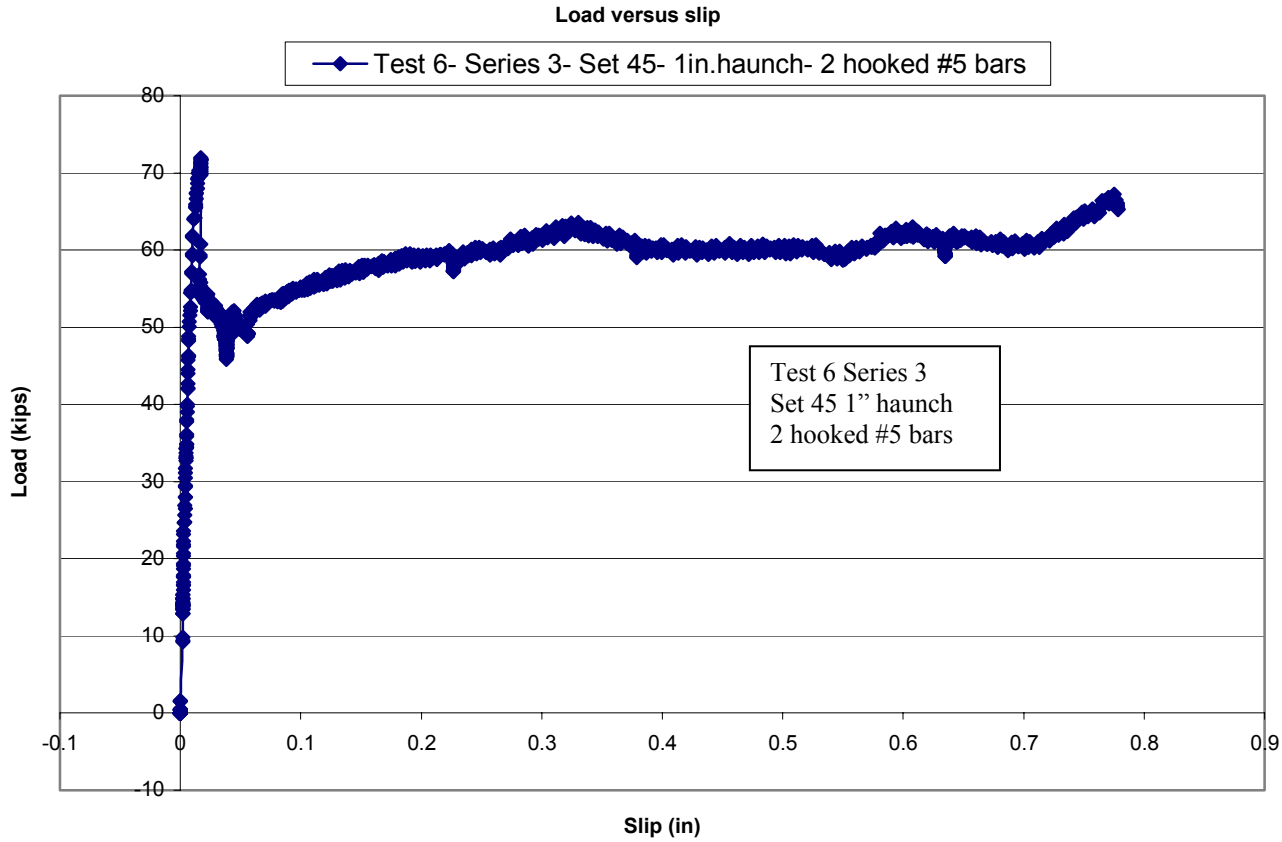
Load versus slip
Test 6- Series 3- Set 45- 1in.haunch- 2 hooked #5 bars
Load (kips)
80
70
60
50
40
30
20
10
0
-10
-0.1
0
0.1
0.2
0.3
0.4
0.5
0.6
0.7
0.8
0.9
Slip (in)
Test 6 Series 3
Set 45 1" haunch
2 hooked #5 bars

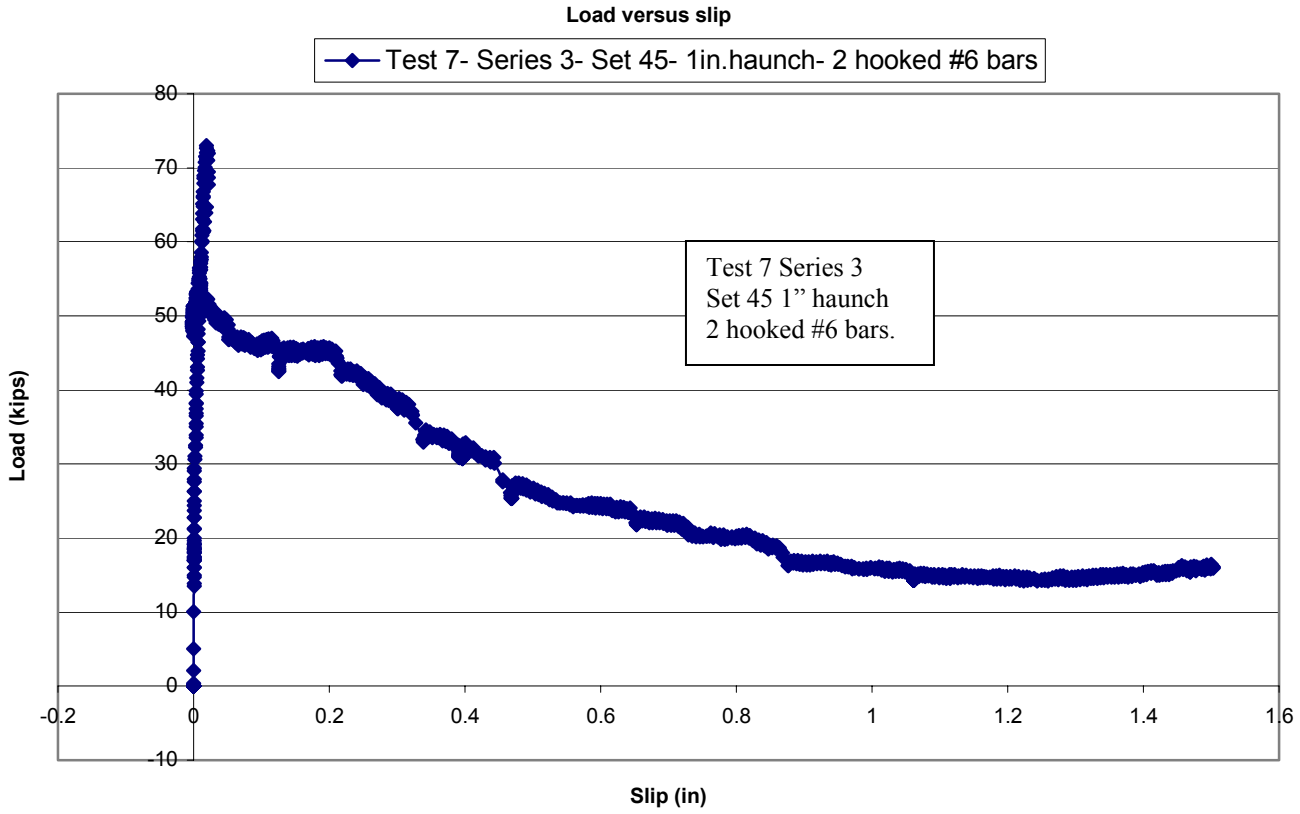
Load versus slip
Test 7- Series 3- Set 45- 1in.haunch- 2 hooked #6 bars
Test 7 Series 3
Set 45 1" haunch
2 hooked #6 bars.
Load (kips)
Slip (in)
80
70
60
50
40
30
20
10
0
-10
-0.2
0
0.2
0.4
0.6
0.8
1
1.2
1.4
1.6

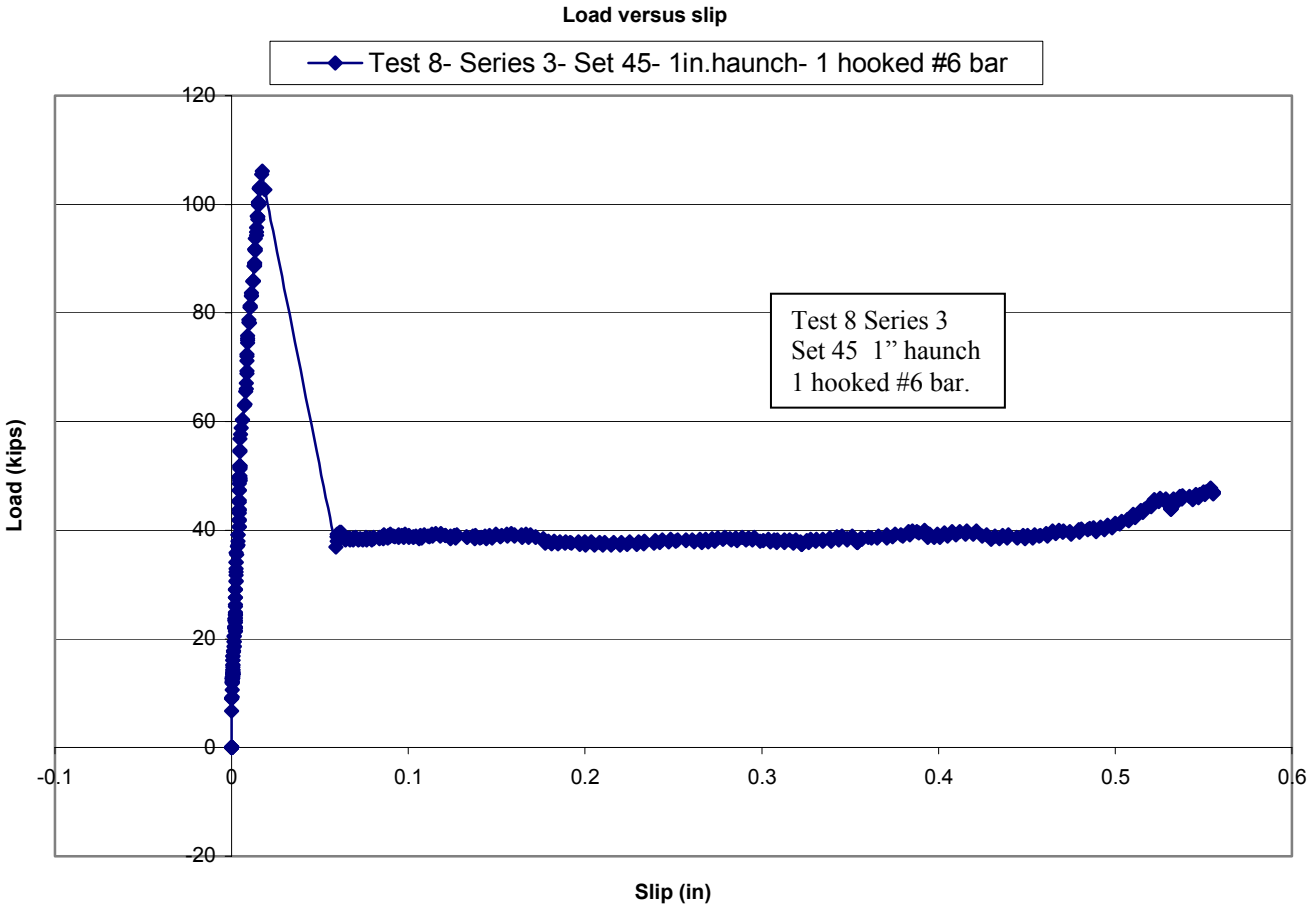
Load versus slip
Test 8- Series 3- Set 45- 1in.haunch- 1 hooked #6 bar
Test 8 Series 3
Set 45 1" haunch
1 hooked #6 bar.
Load (kips)
Slip (in)
120
100
80
60
40
20
0
-20
-0.1
0
0.1
0.2
0.3
0.4
0.5
0.6

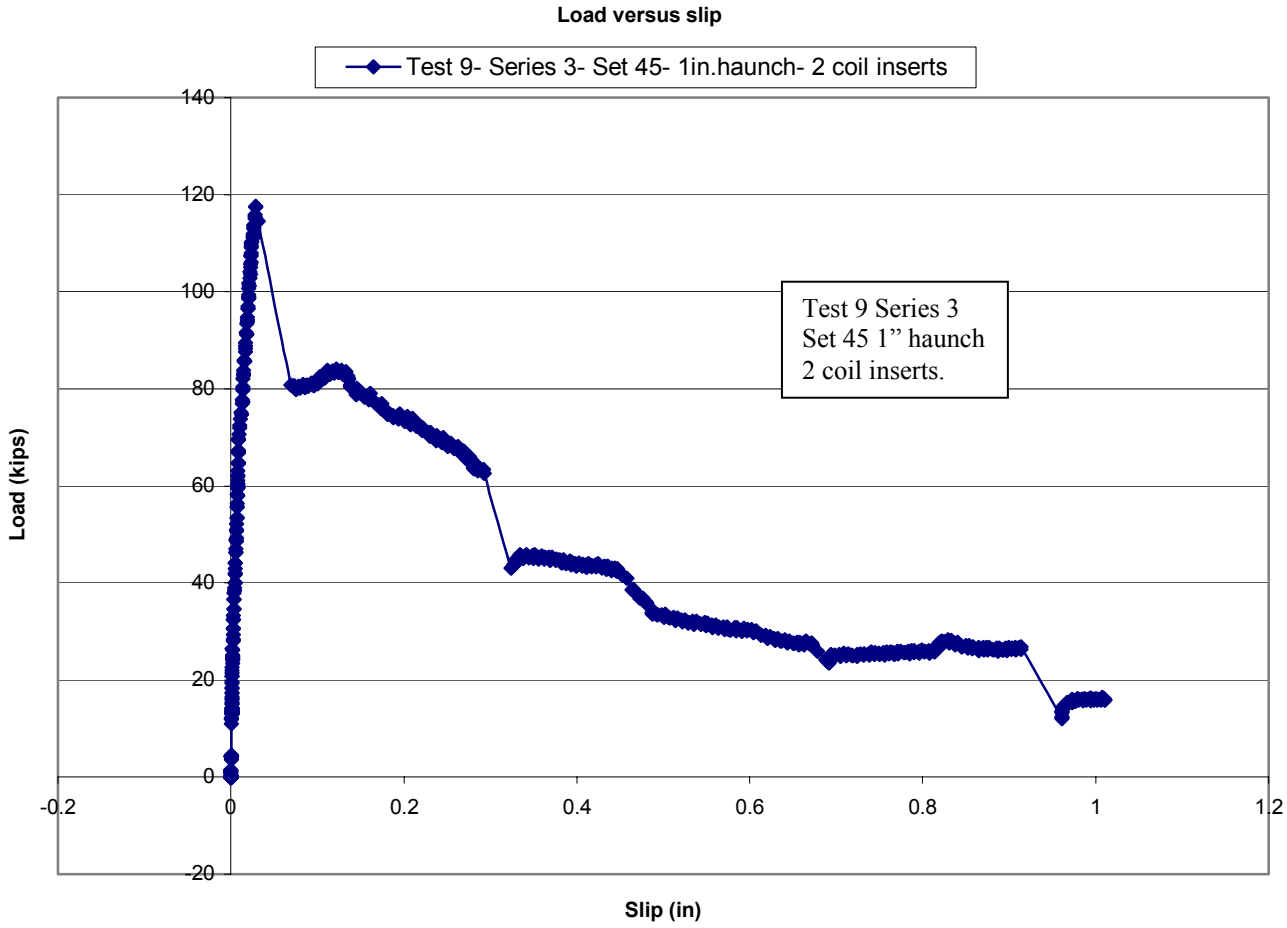
Load versus slip
Test 9- Series 3- Set 45- 1in.haunch- 2 coil inserts
Test 9 Series 3
Set 45 1" haunch
2 coil inserts.
Load (kips)
Slip (in)
140
120
100
80
60
40
20
0
-20
-0.2
0
0.2
0.4
0.6
0.8
1
1.2

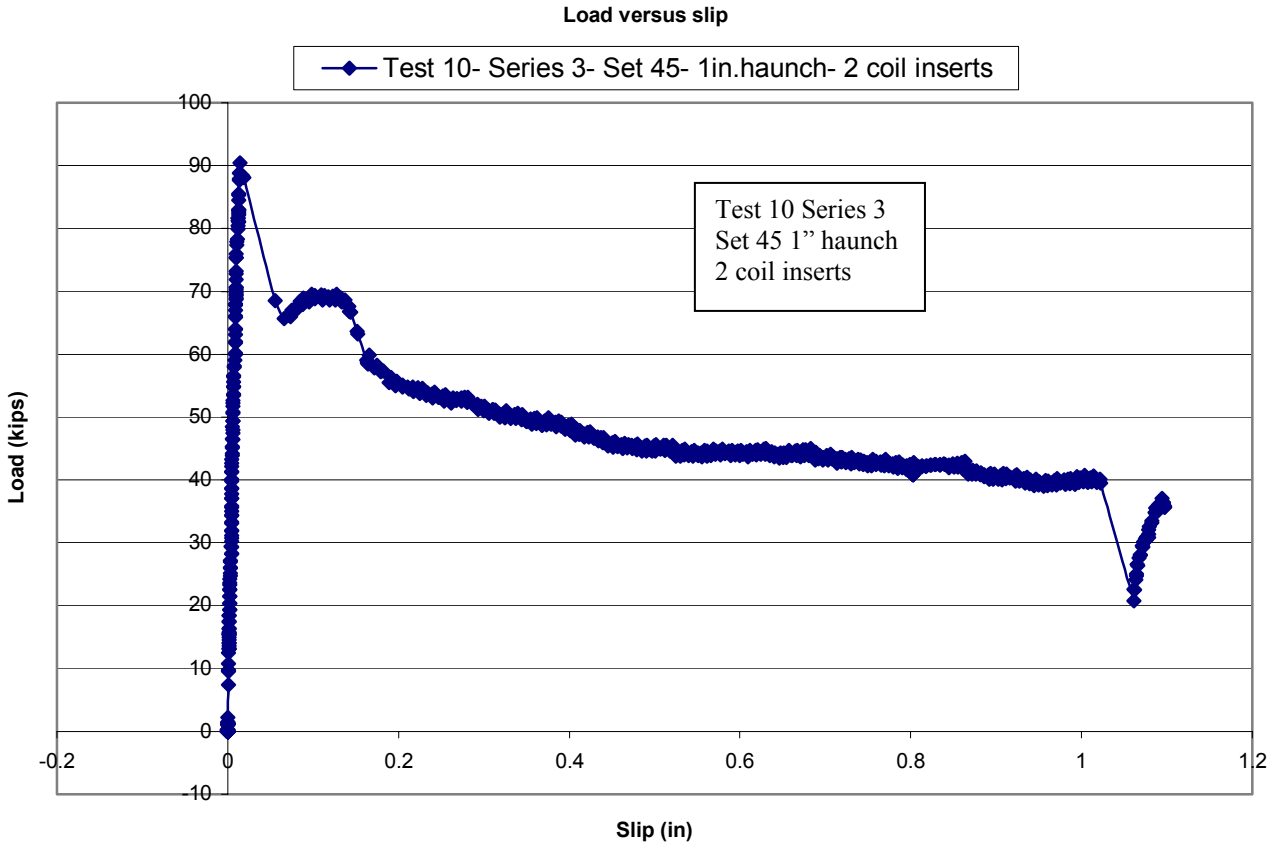
Load versus slip
Test 10- Series 3- Set 45- 1in.haunch- 2 coil inserts
Test 10 Series 3
Set 45 1" haunch
2 coil inserts
Load (kips)
Slip (in)
100
90
80
70
60
50
40
30
20
10
0
-10
-0.2
0
0.2
0.4
0.6
0.8
1
1.2

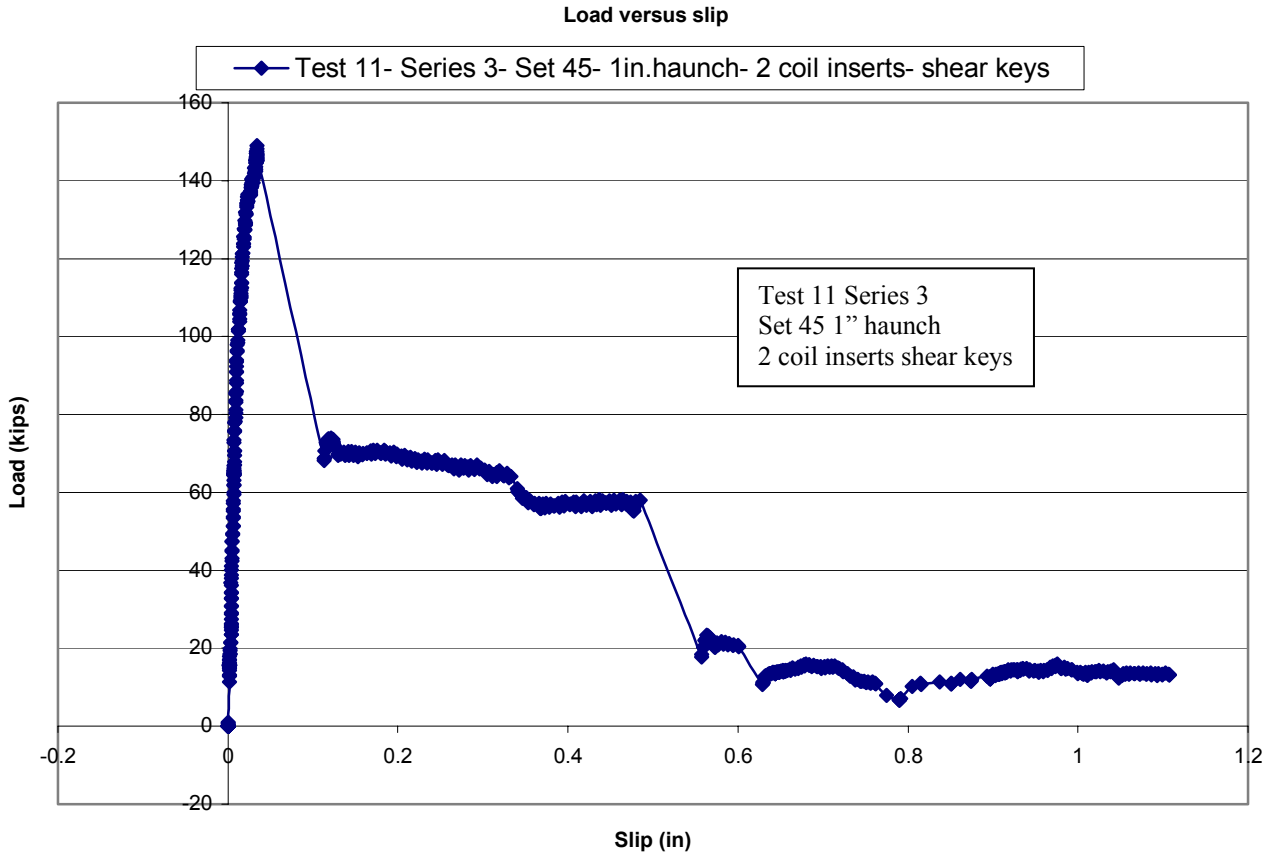
Load versus slip
Test 11- Series 3- Set 45- 1in.haunch- 2 coil inserts- shear keys
Test 11 Series 3
Set 45 1" haunch
2 coil inserts shear keys
Load (kips)
160
140
120
100
80
60
40
20
0
-20
-0.2
0
0.2
0.4
0.6
0.8
1
1.2
Slip (in)

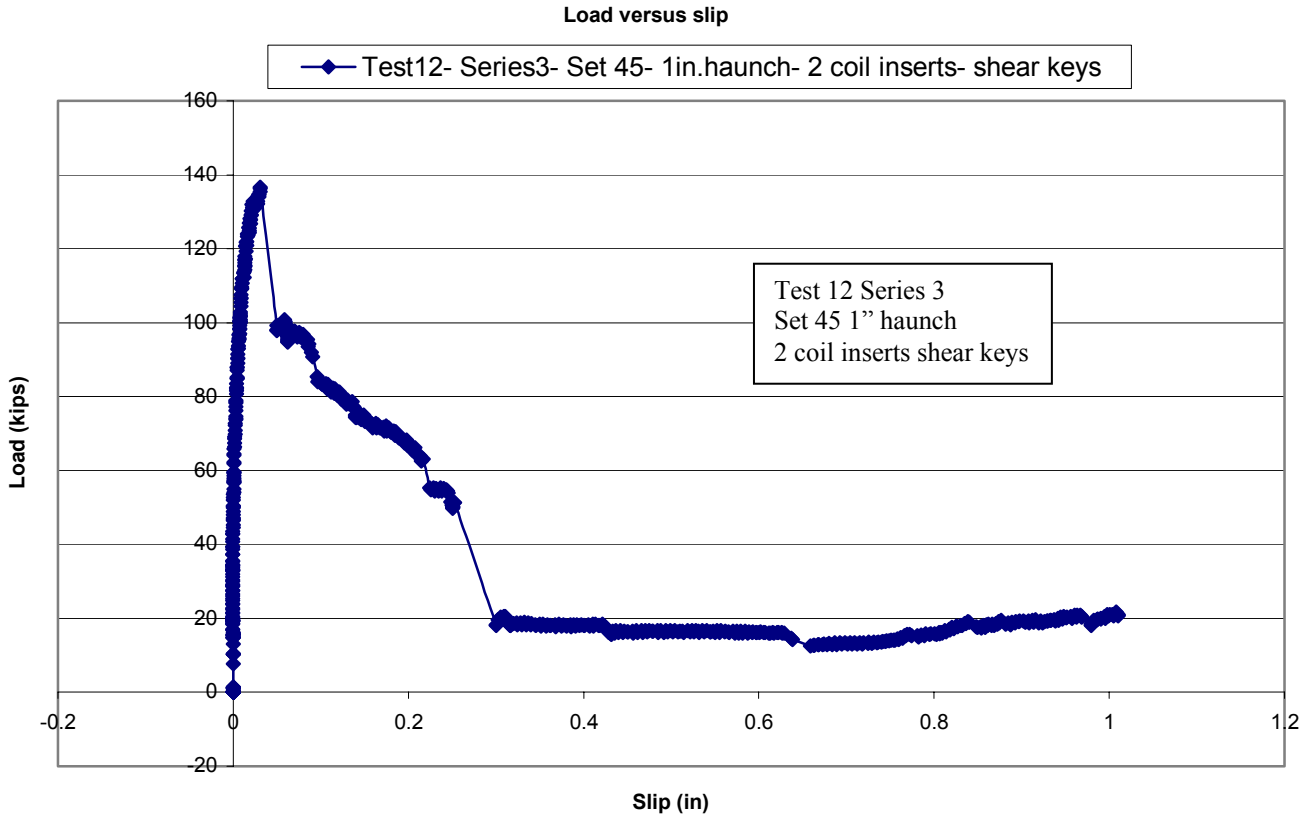
Load versus slip
Test12- Series3- Set 45- 1in.haunch- 2 coil inserts- shear keys
Test 12 Series 3
Set 45 1" haunch
2 coil inserts shear keys
Load (kips)
160
140
120
100
80
60
40
20
0
-20
-0.2
0
0.2
0.4
0.6
0.8
1
1.2
Slip (in)

APPENDIX B

Load versus strain diagrams before crack

Series 1

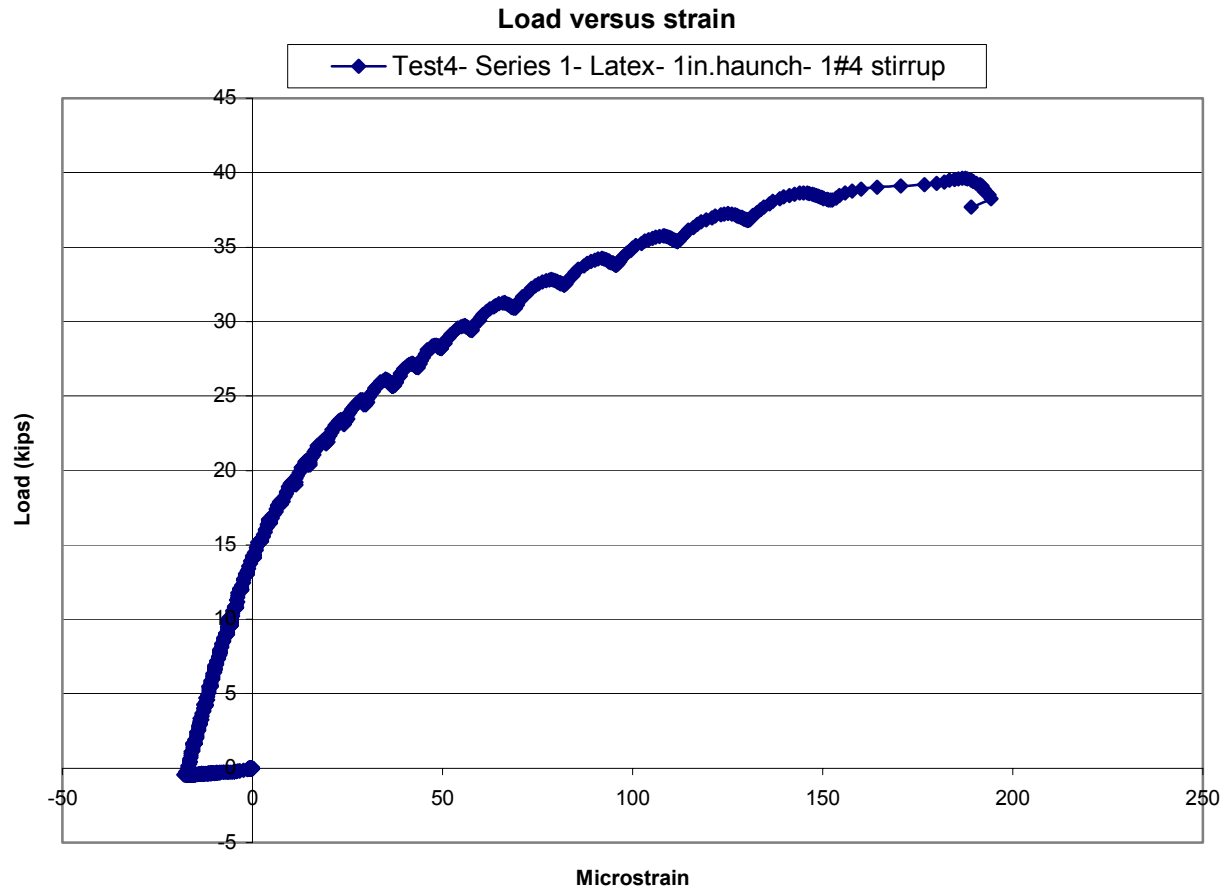

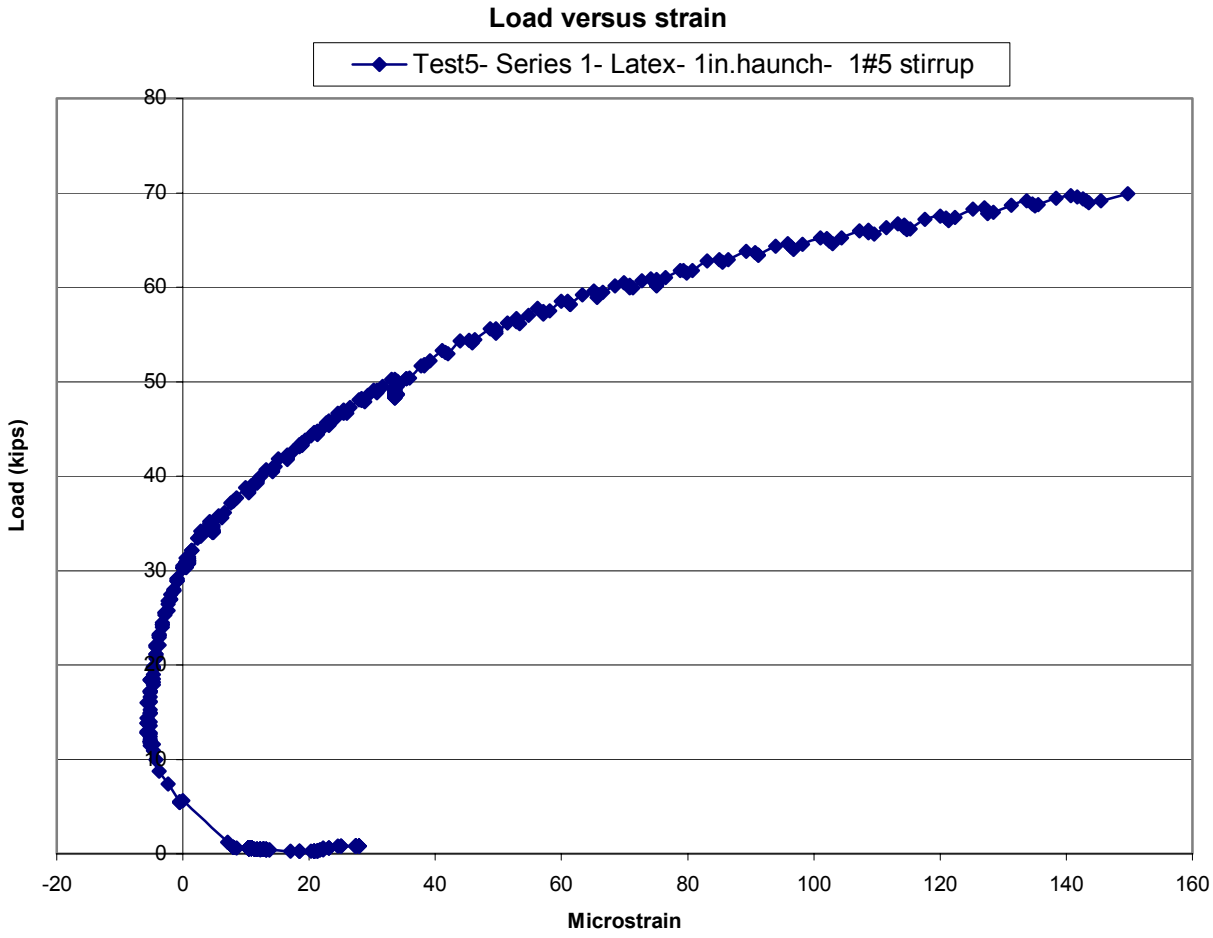
Load versus strain
Test5- Series 1- Latex- 1in.haunch- 1#5 stirrup
Load (kips)
80
70
60
50
40
30
20
10
0
-20
0
20
40
60
80
100
120
140
160
Microstrain

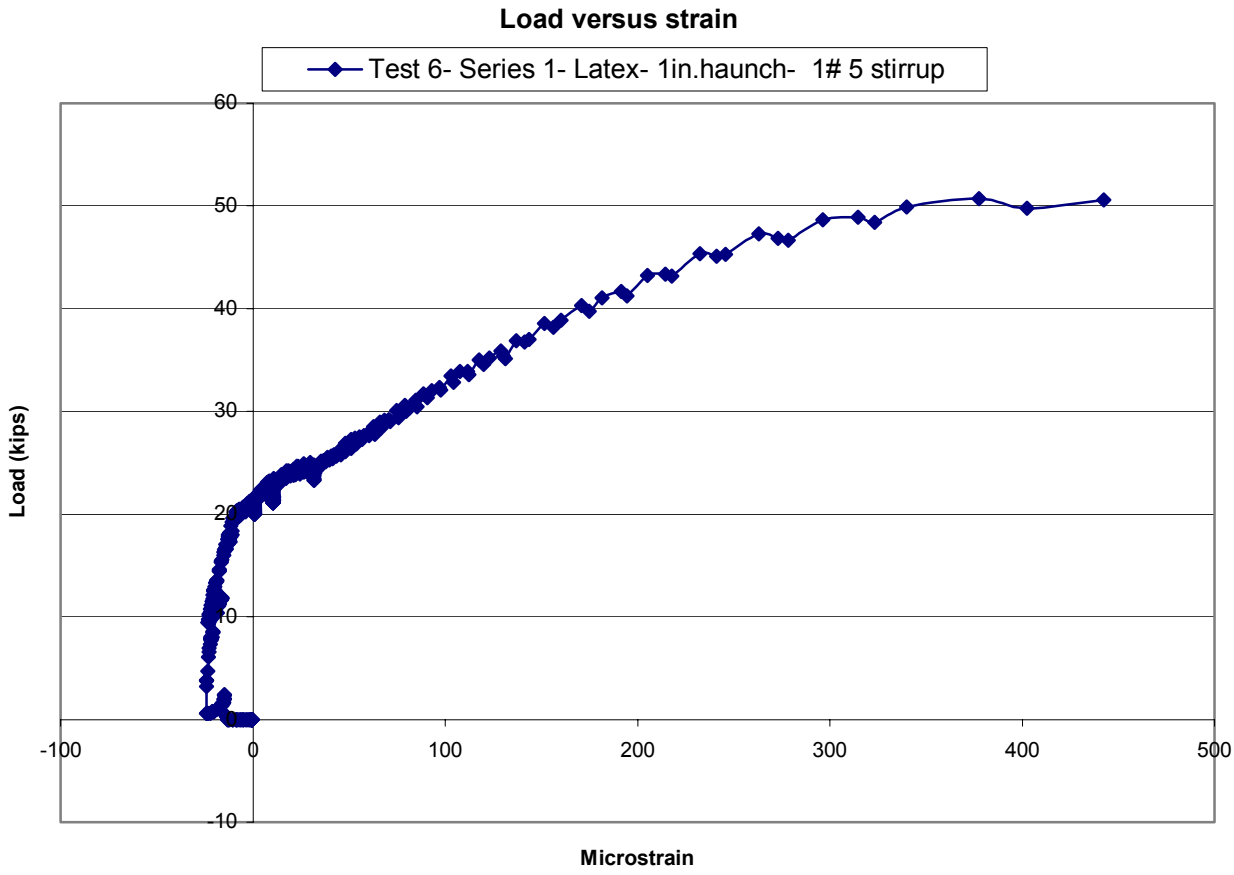
Load versus strain
Test 6- Series 1- Latex- 1in.haunch- 1# 5 stirrup
Load (kips)
60
50
40
30
20
10
0
-10
-100
0
100
200
300
400
500
Microstrain

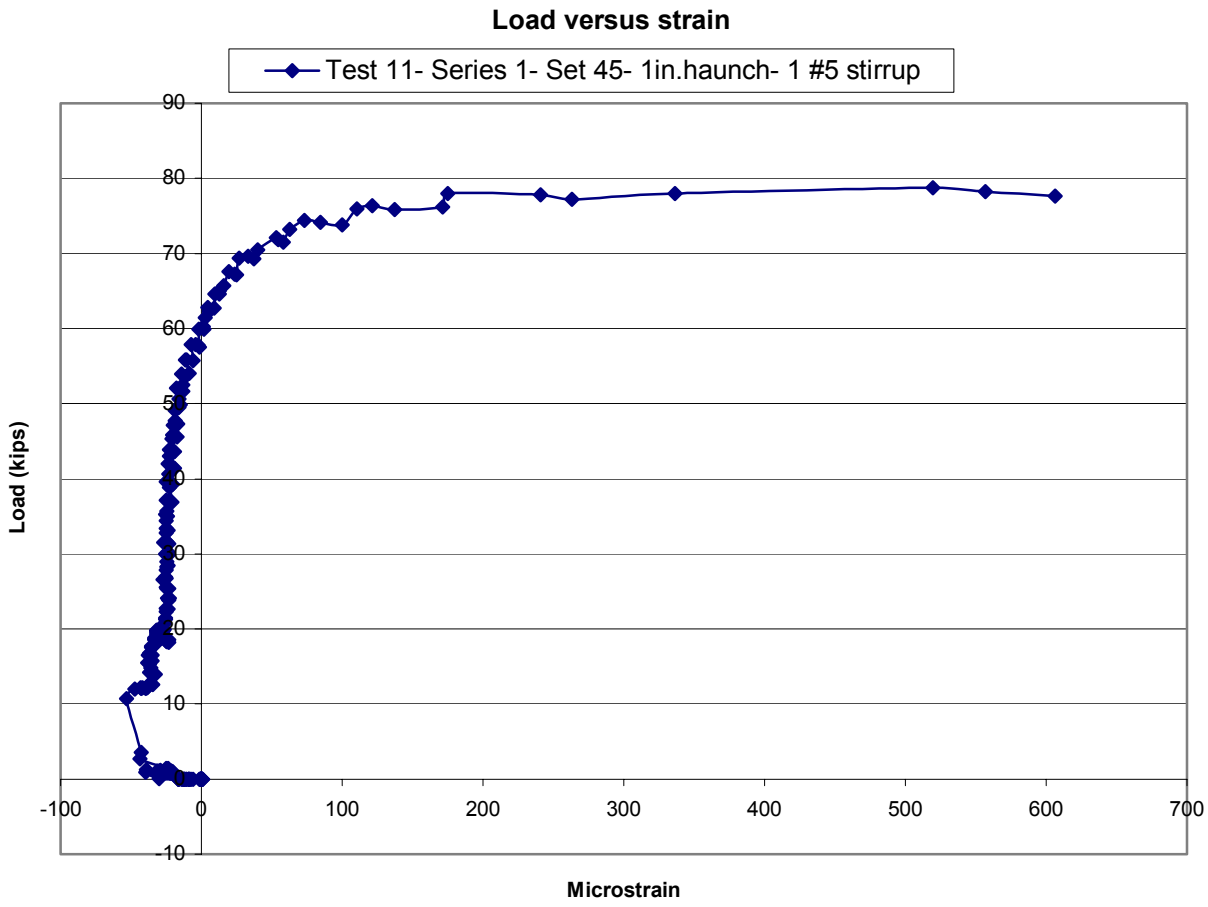
Load versus strain
Test 11- Series 1- Set 45- 1in.haunch- 1 #5 stirrup
Load (kips)
90
80
70
60
50
40
30
20
10
0
-10
-100
0
100
200
300
400
500
600
700
Microstrain

Series 2

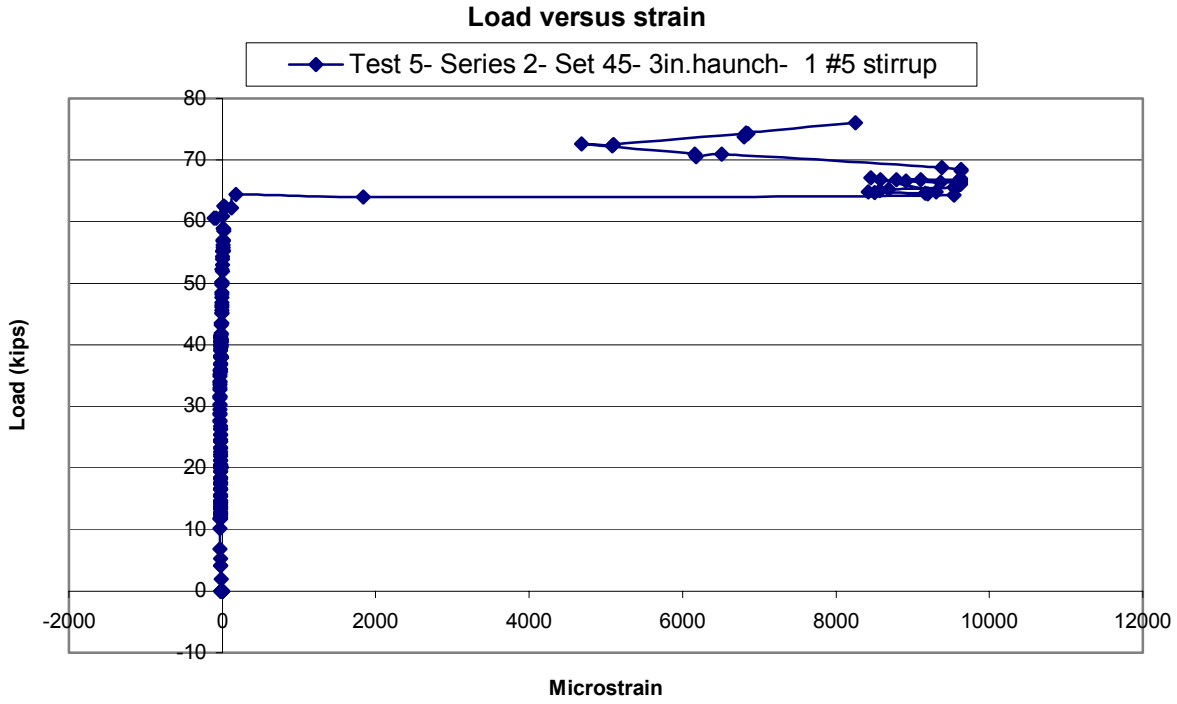
Load versus strain
Test 5- Series 2- Set 45- 3in.haunch- 1 #5 stirrup
Load (kips)
80
70
60
50
40
30
20
10
0
-10
-2000
0
2000
4000
6000
8000
10000
12000
Microstrain

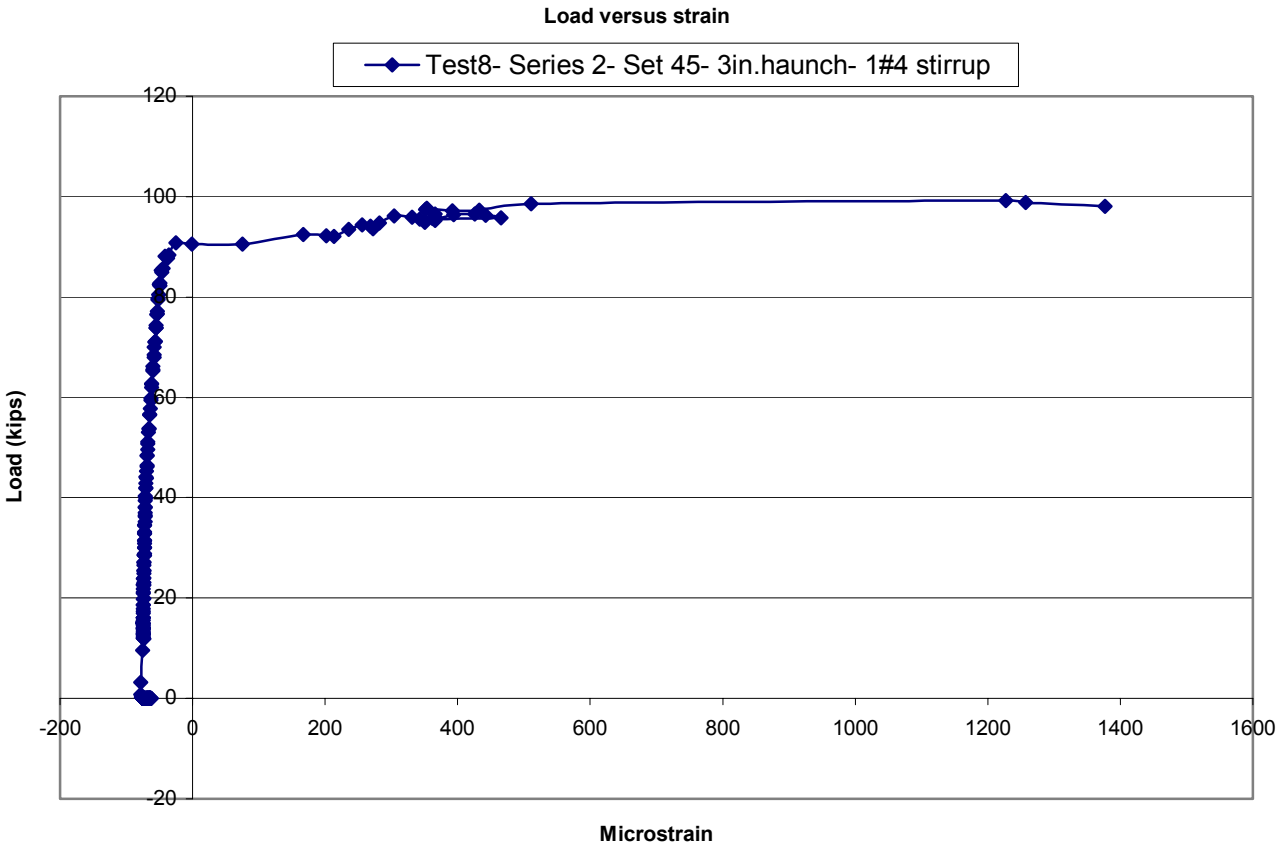
Load versus strain
Test8- Series 2- Set 45- 3in.haunch- 1#4 stirrup
Load (kips)
120
100
80
60
40
20
0
-20
-200
0
200
400
600
800
1000
1200
1400
1600
Microstrain

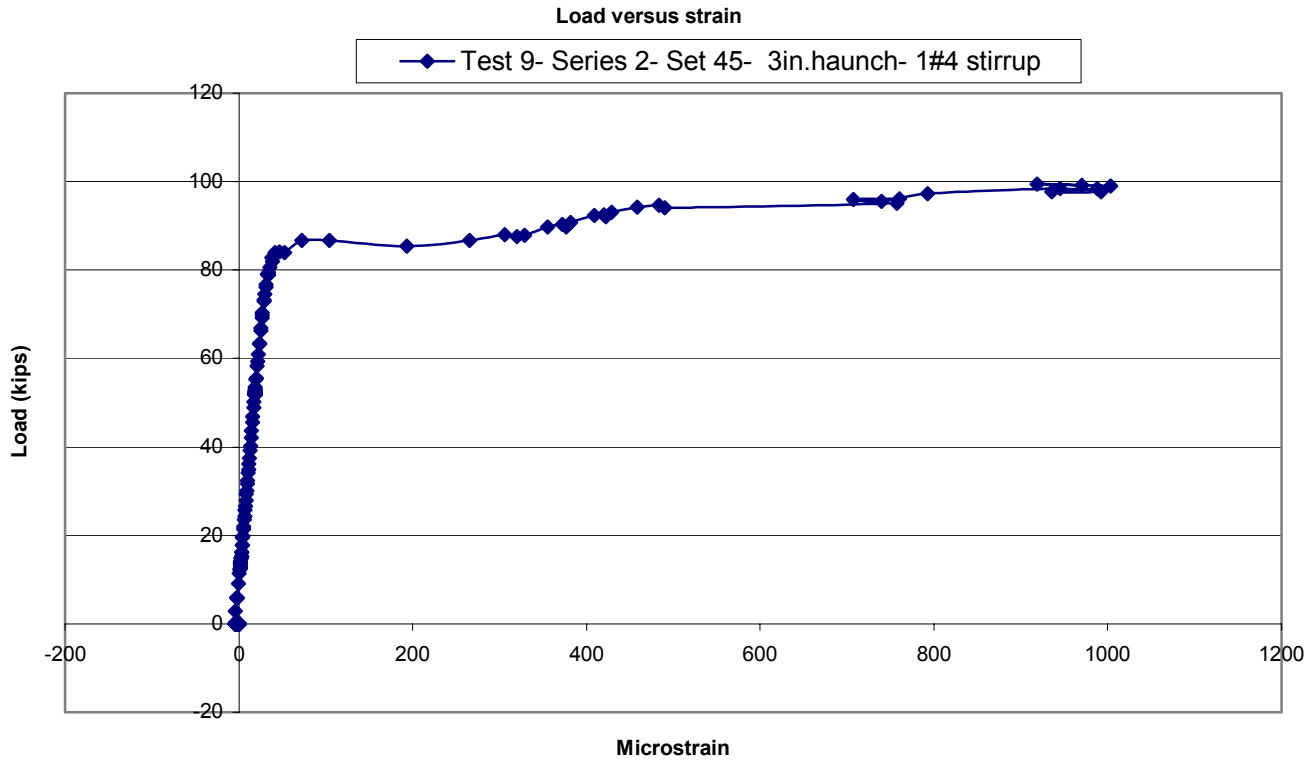
Load versus strain
Test 9- Series 2- Set 45- 3in.haunch- 1#4 stirrup
Load (kips)
120
100
80
60
40
20
0
-20
-200
0
200
400
600
800
1000
1200
Microstrain

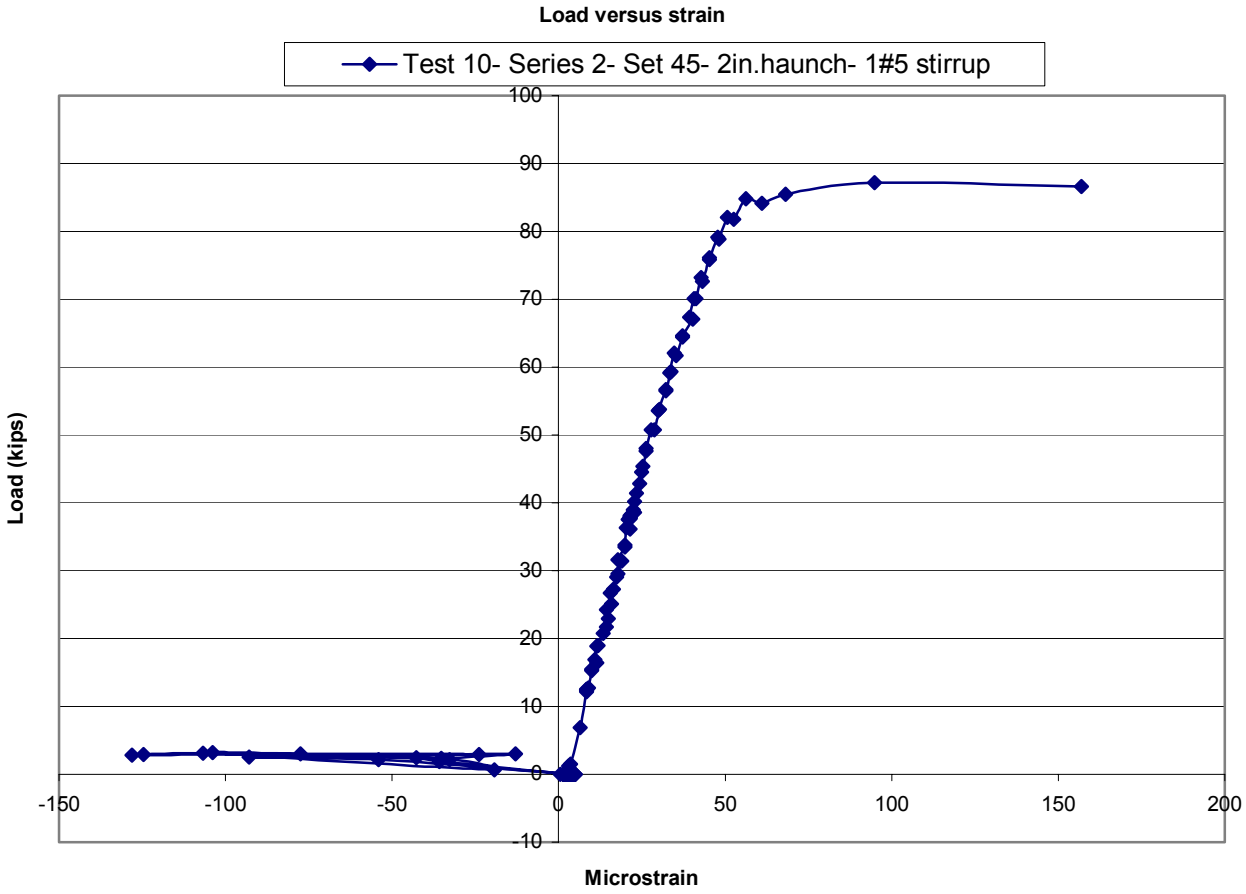
Load versus strain
Test 10- Series 2- Set 45- 2in.haunch- 1#5 stirrup
Load (kips)
100
90
80
70
60
50
40
30
20
10
0
-10
-150
-100
-50
0
50
100
150
200
Microstrain

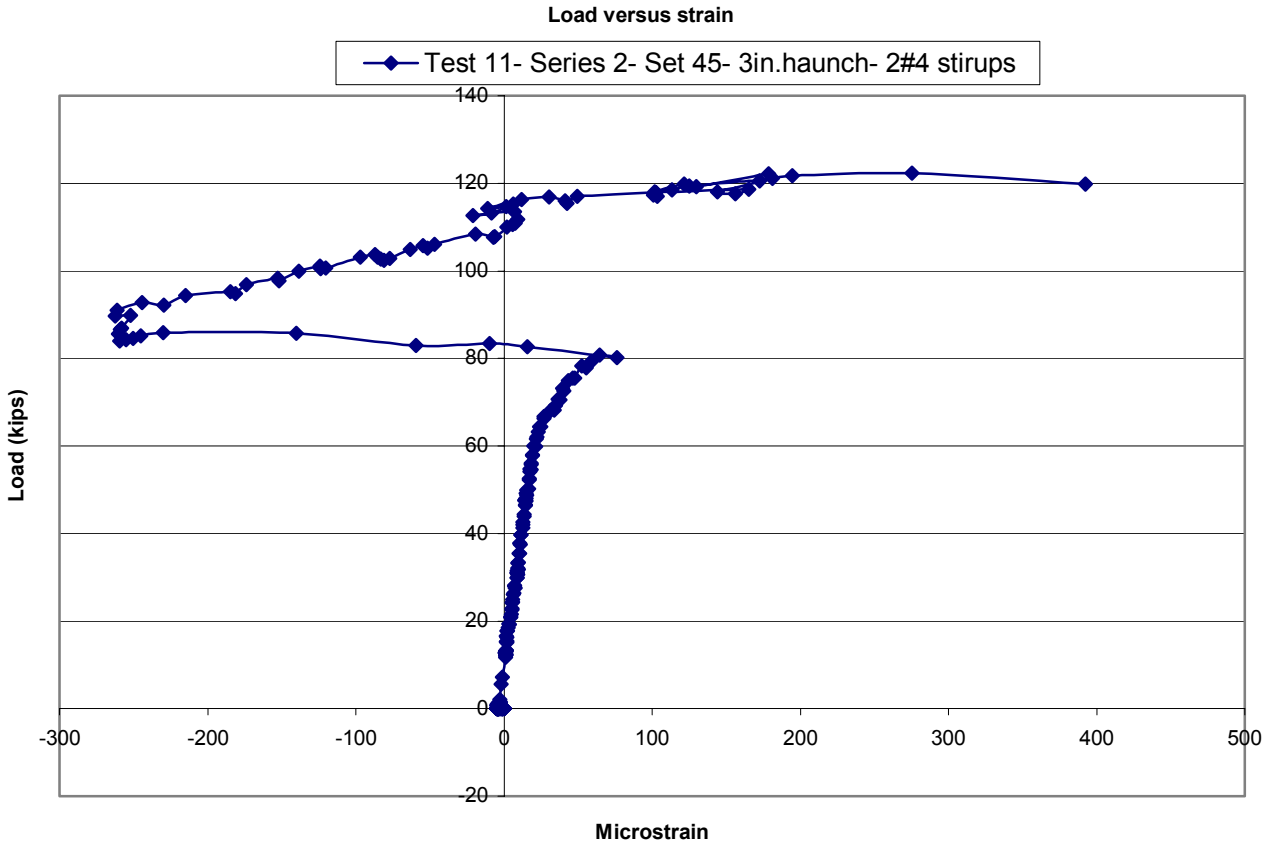
Load versus strain
Test 11- Series 2- Set 45- 3in.haunch- 2#4 stirups
Load (kips)
140
120
100
80
60
40
20
0
-20
-300
-200
-100
0
100
200
300
400
500
Microstrain

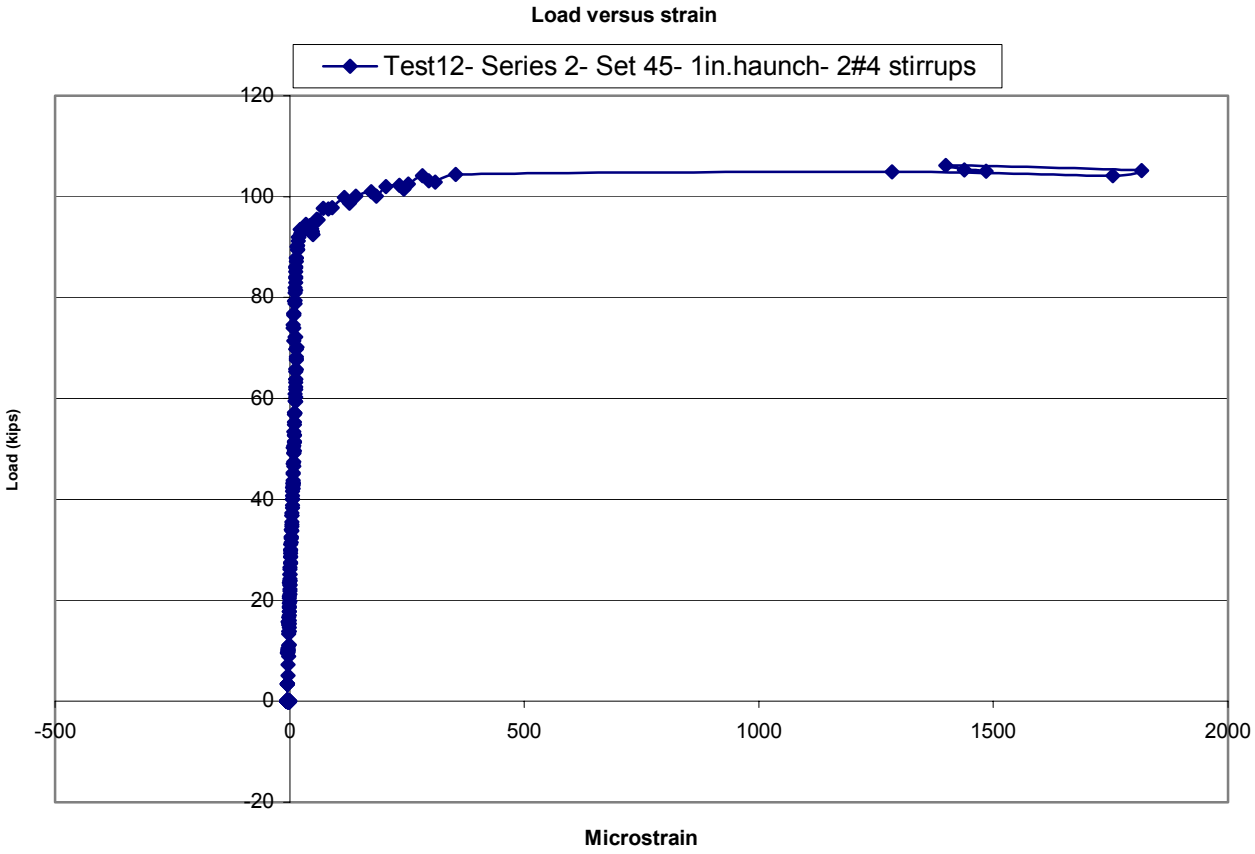
Load versus strain
Test12- Series 2- Set 45- 1in.haunch- 2#4 stirrups
120
100
80
60
40
20
0
-20
Load (kips)
-500
0
500
1000
1500
2000
Microstrain

Series 3

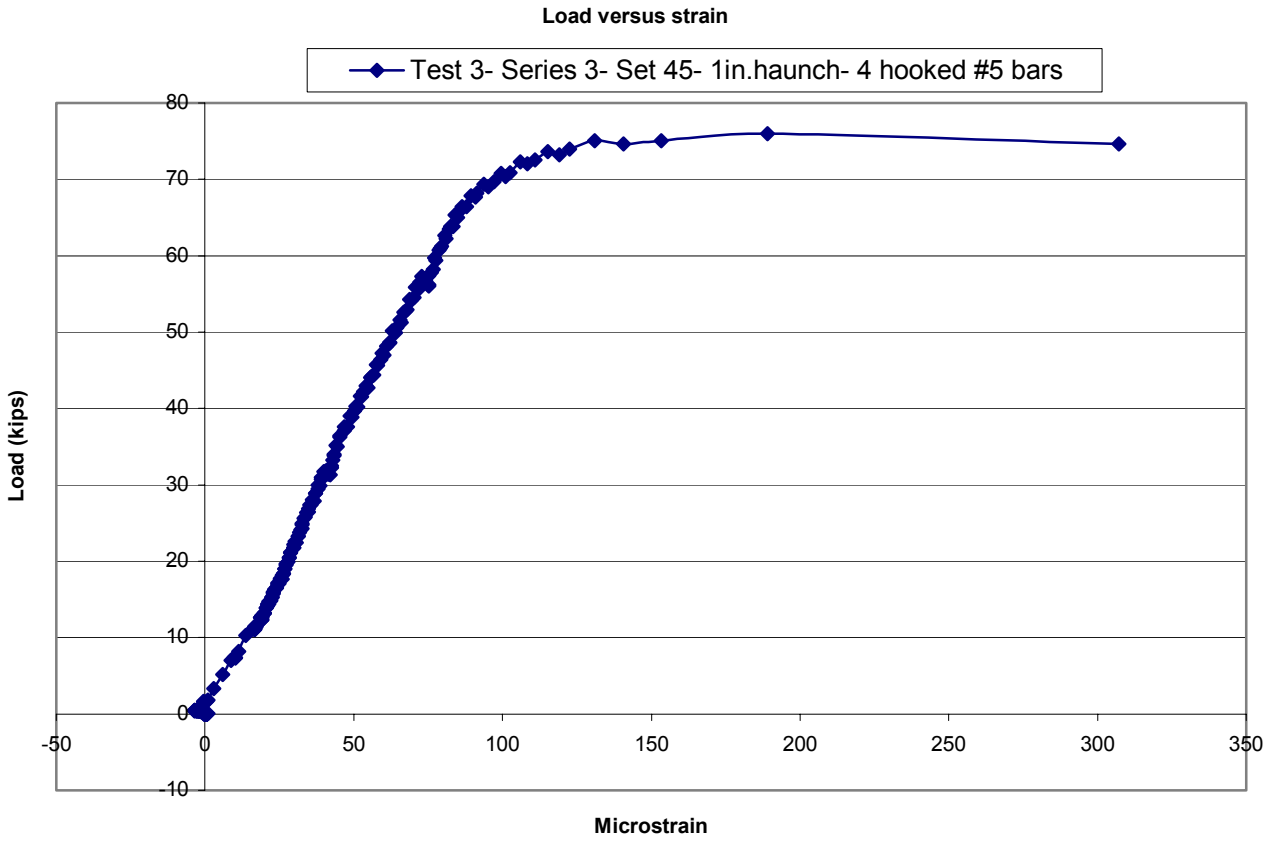
Load versus strain
Test 3- Series 3- Set 45- 1in.haunch- 4 hooked #5 bars
Load (kips)
80
70
60
50
40
30
20
10
0
-10
-50
0
50
100
150
200
250
300
350
Microstrain

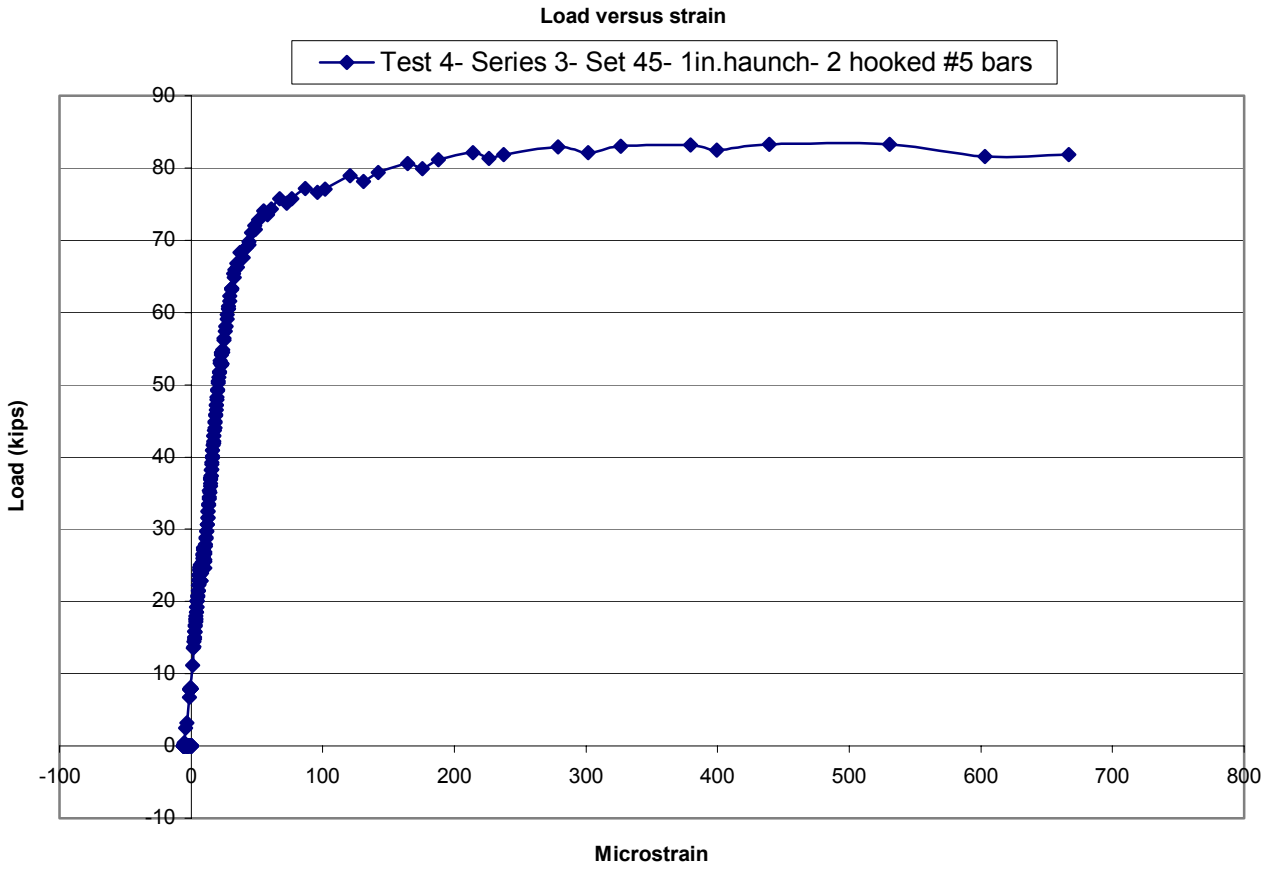
Load versus strain
Test 4- Series 3- Set 45- 1in.haunch- 2 hooked #5 bars
Load (kips)
90
80
70
60
50
40
30
20
10
0
-10
-100
0
100
200
300
400
500
600
700
800
Microstrain

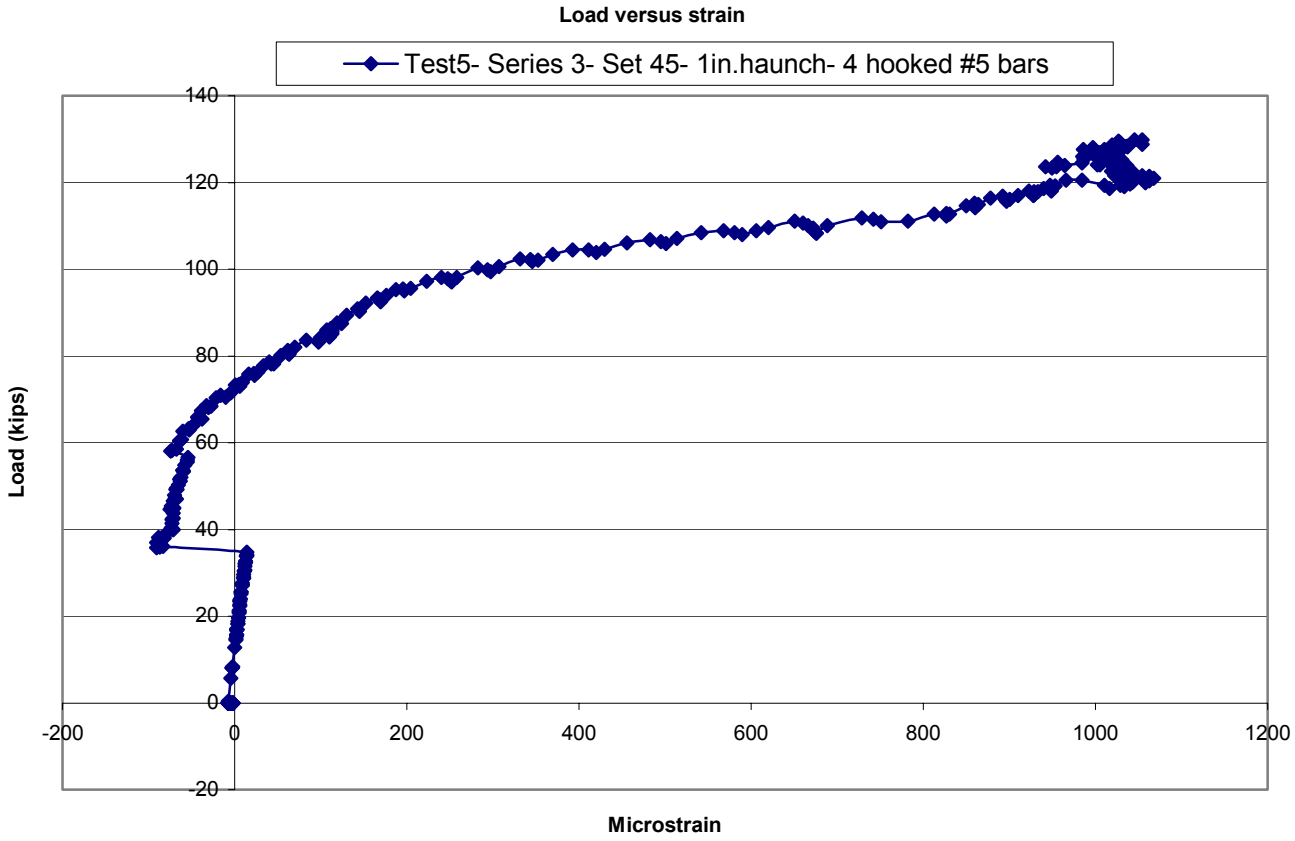
Load versus strain
Test5- Series 3- Set 45- 1in.haunch- 4 hooked #5 bars
Load (kips)
140
120
100
80
60
40
20
0
-20
-200
0
200
400
600
800
1000
1200
Microstrain

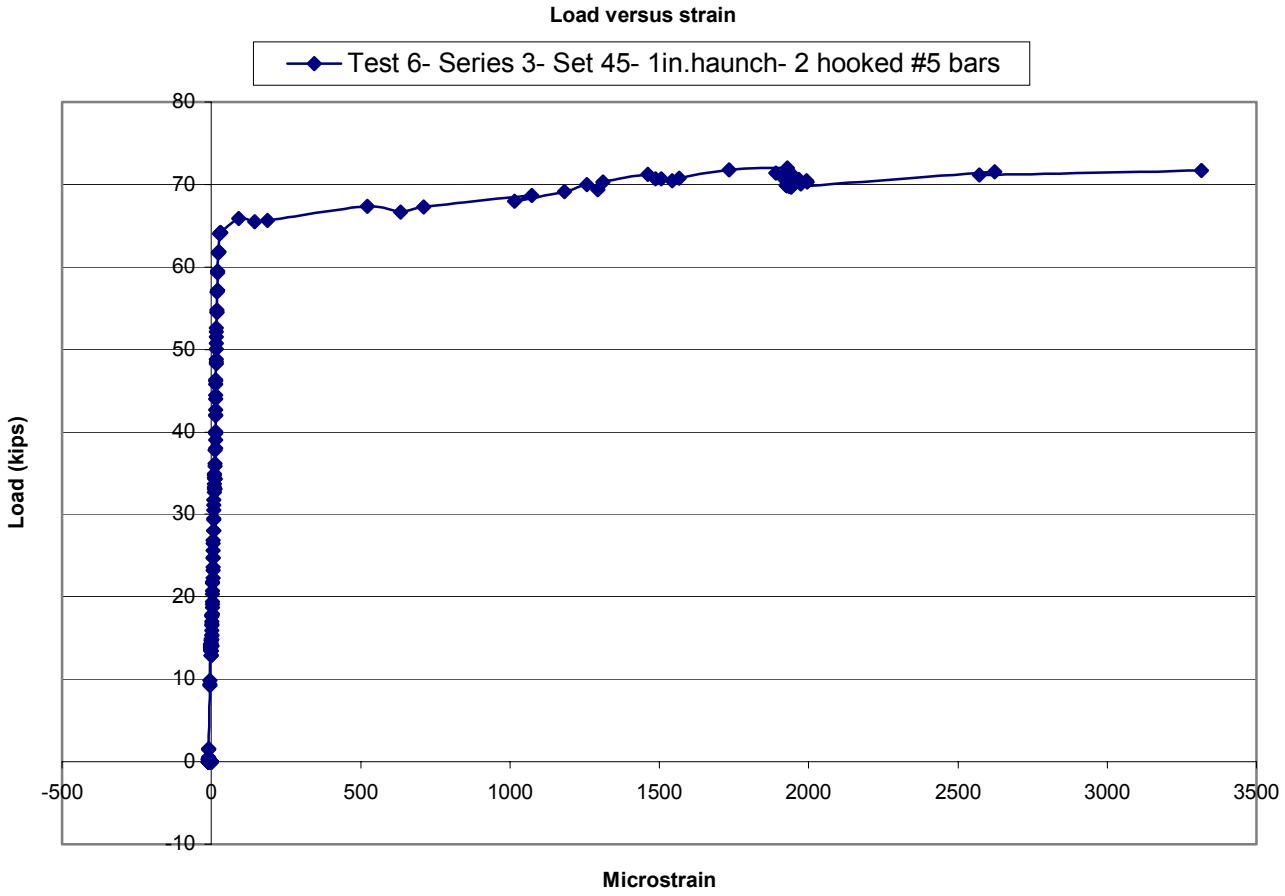
Load versus strain
Test 6- Series 3- Set 45- 1in.haunch- 2 hooked #5 bars
Load (kips)
80
70
60
50
40
30
20
10
0
-10
-500
0
500
1000
1500
2000
2500
3000
3500
Microstrain

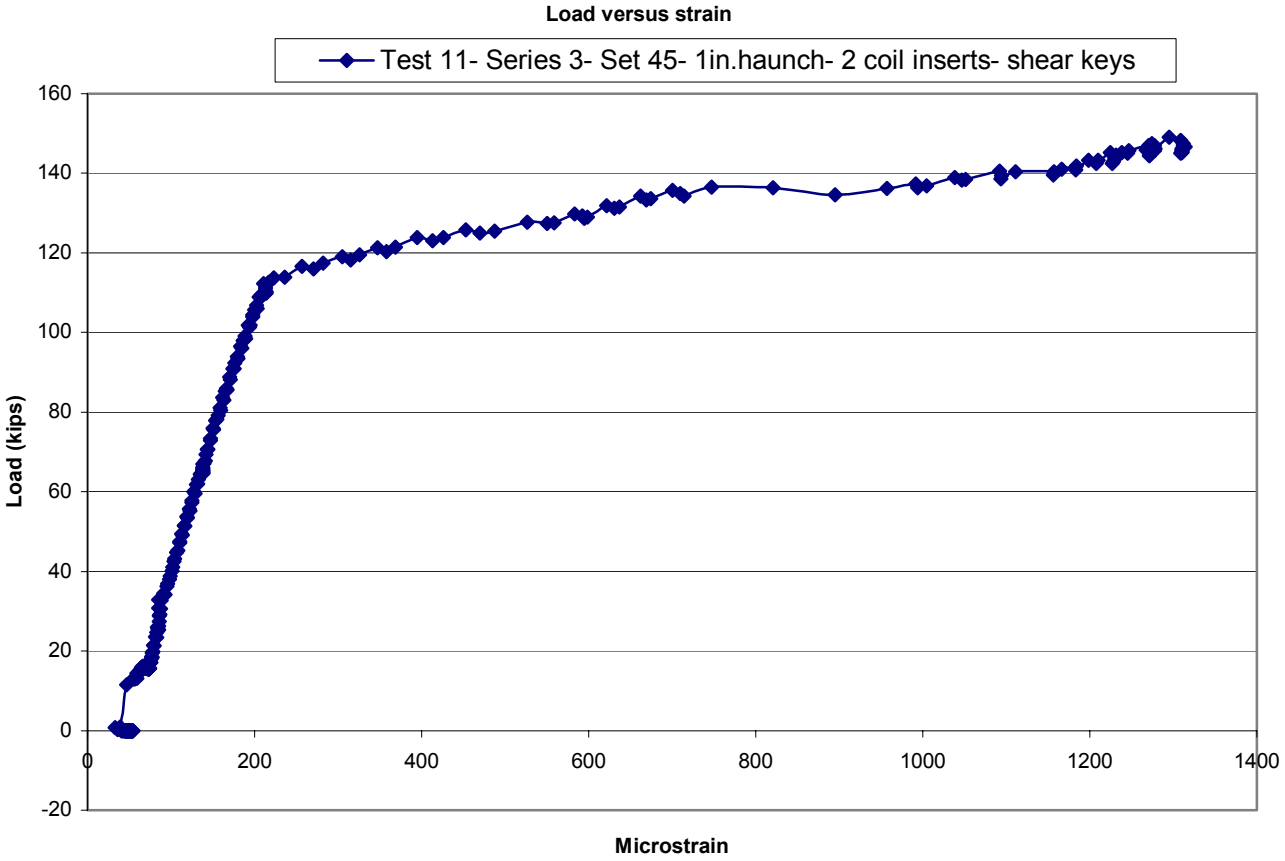
Load versus strain
Test 11- Series 3- Set 45- 1in.haunch- 2 coil inserts- shear keys
160
140
120
100
80
60
40
20
0
-20
Load (kips)
0
200
400
600
800
1000
1200
1400
Microstrain

Load versus strain diagrams before and after crack

Series 1

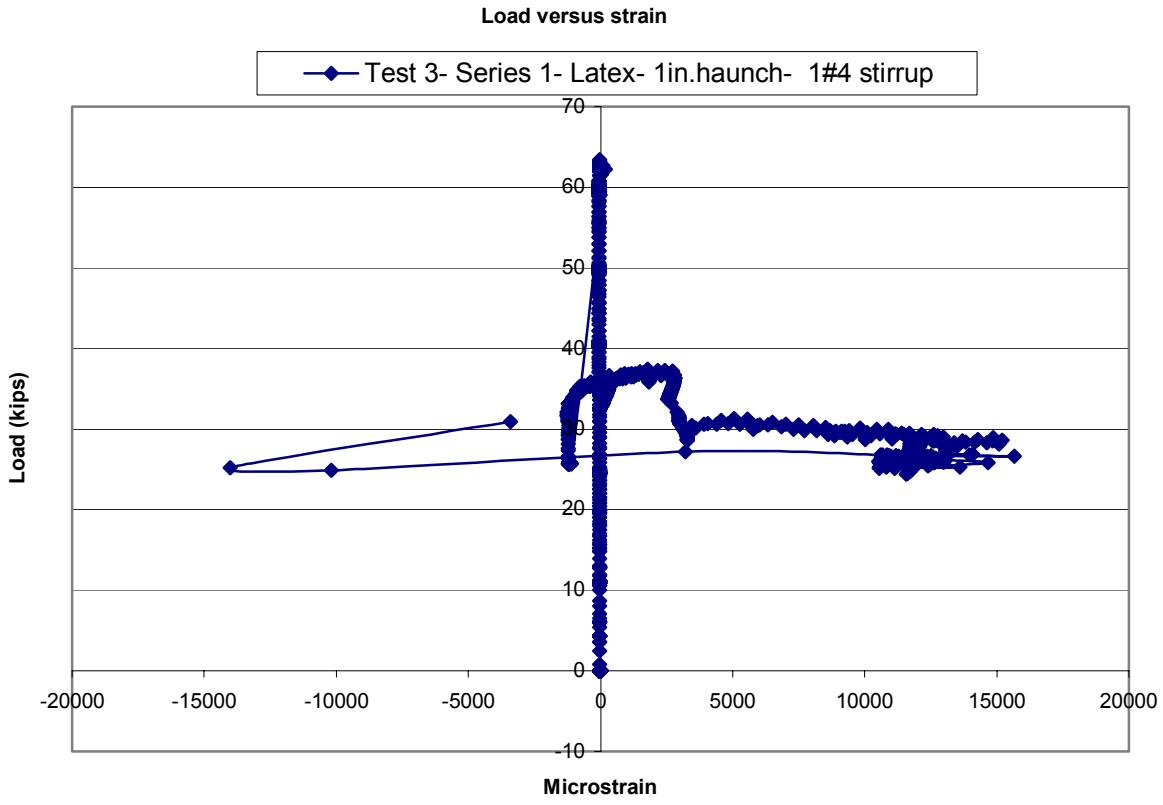

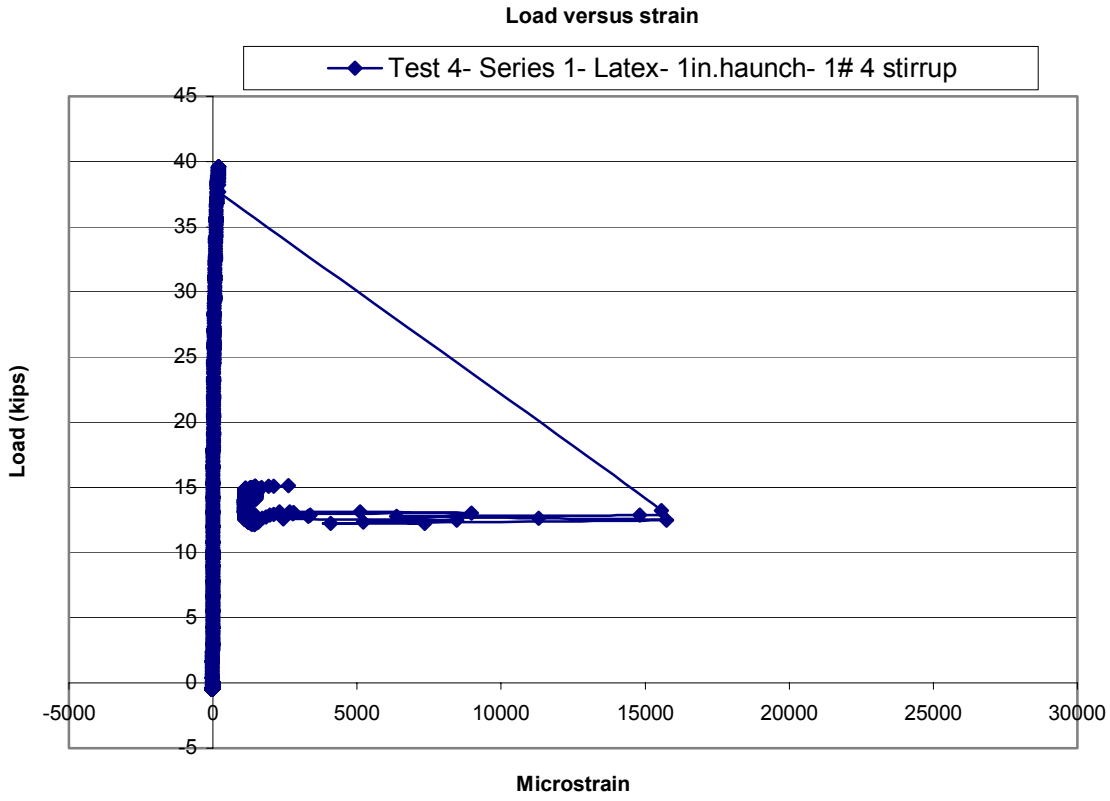
Load versus strain
Test 4- Series 1- Latex- 1in.haunch- 1# 4 stirrup
Load (kips)
45
40
35
30
25
20
15
10
5
0
-5
-5000
0
5000
10000
15000
20000
25000
30000
Microstrain

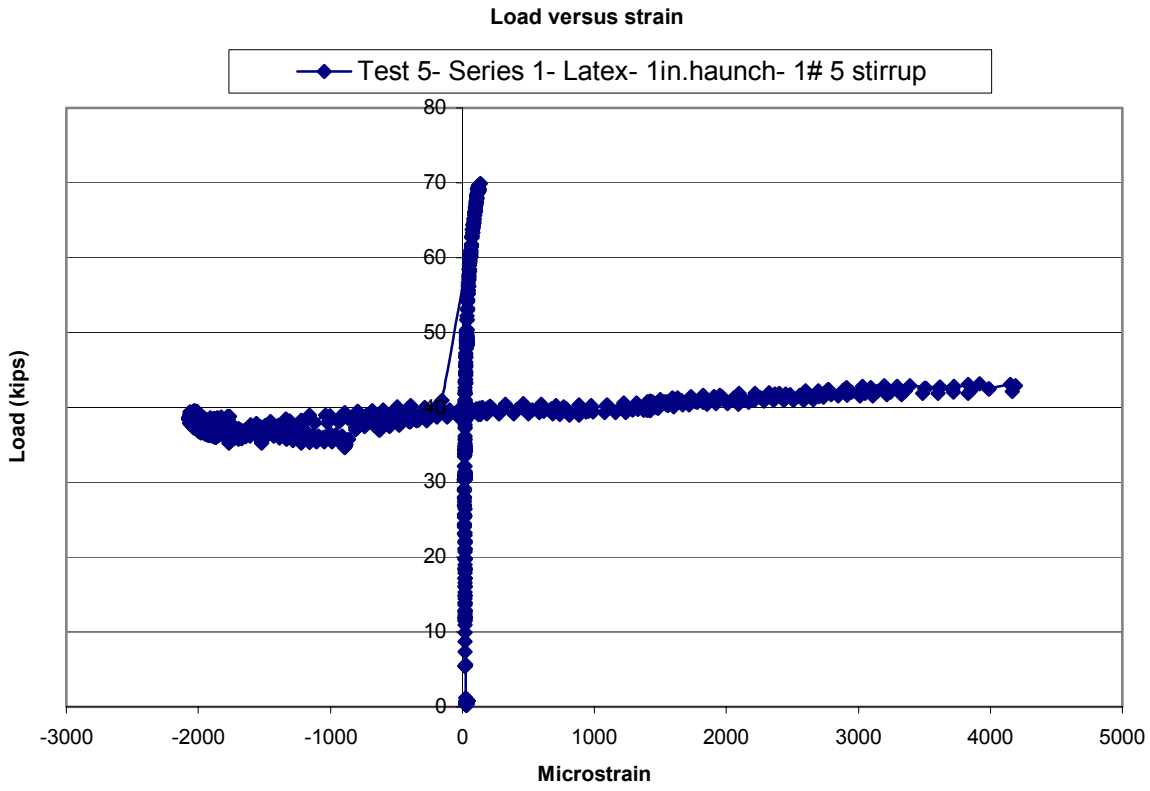
Load versus strain
Test 5- Series 1- Latex- 1in.haunch- 1# 5 stirrup
Load (kips)
80
70
60
50
40
30
20
10
0
-3000
-2000
-1000
0
1000
2000
3000
4000
5000
Microstrain

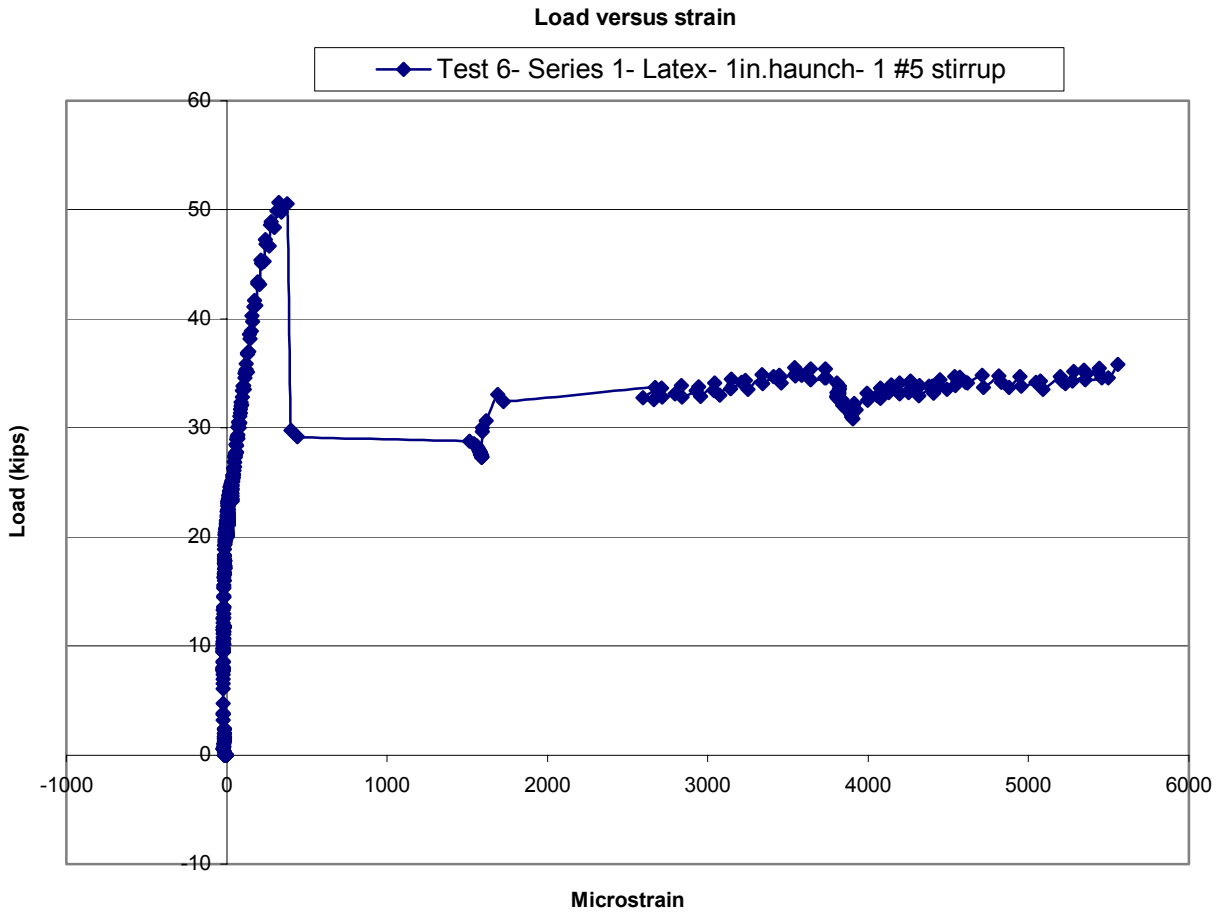
Load versus strain
Test 6- Series 1- Latex- 1in.haunch- 1 #5 stirrup
Load (kips)
60
50
40
30
20
10
0
-10
-1000
0
1000
2000
3000
4000
5000
6000
Microstrain

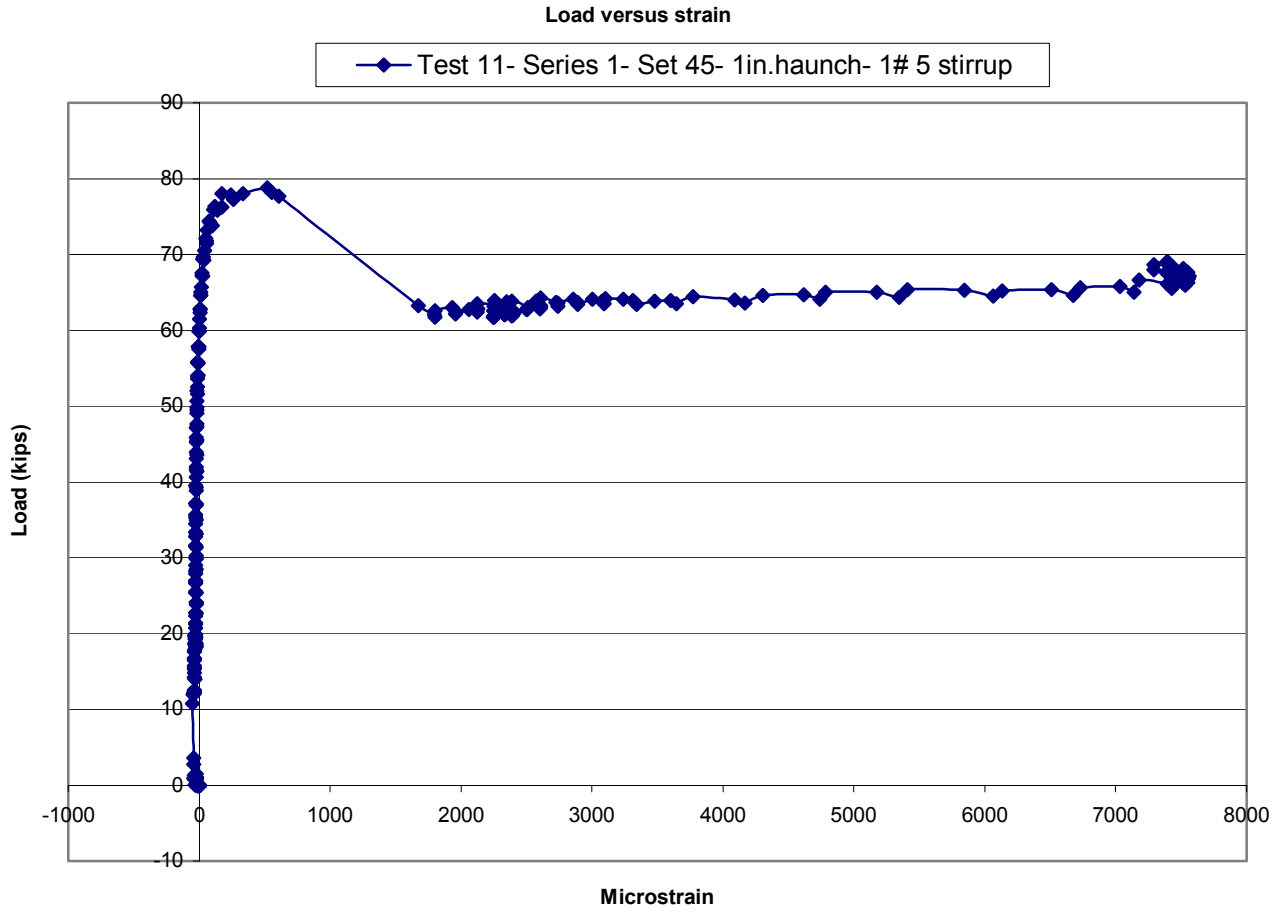
Load versus strain
Test 11- Series 1- Set 45- 1in.haunch- 1# 5 stirrup
Load (kips)
90
80
70
60
50
40
30
20
10
0
-10
-1000
0
1000
2000
3000
4000
5000
6000
7000
8000
Microstrain

Series 2

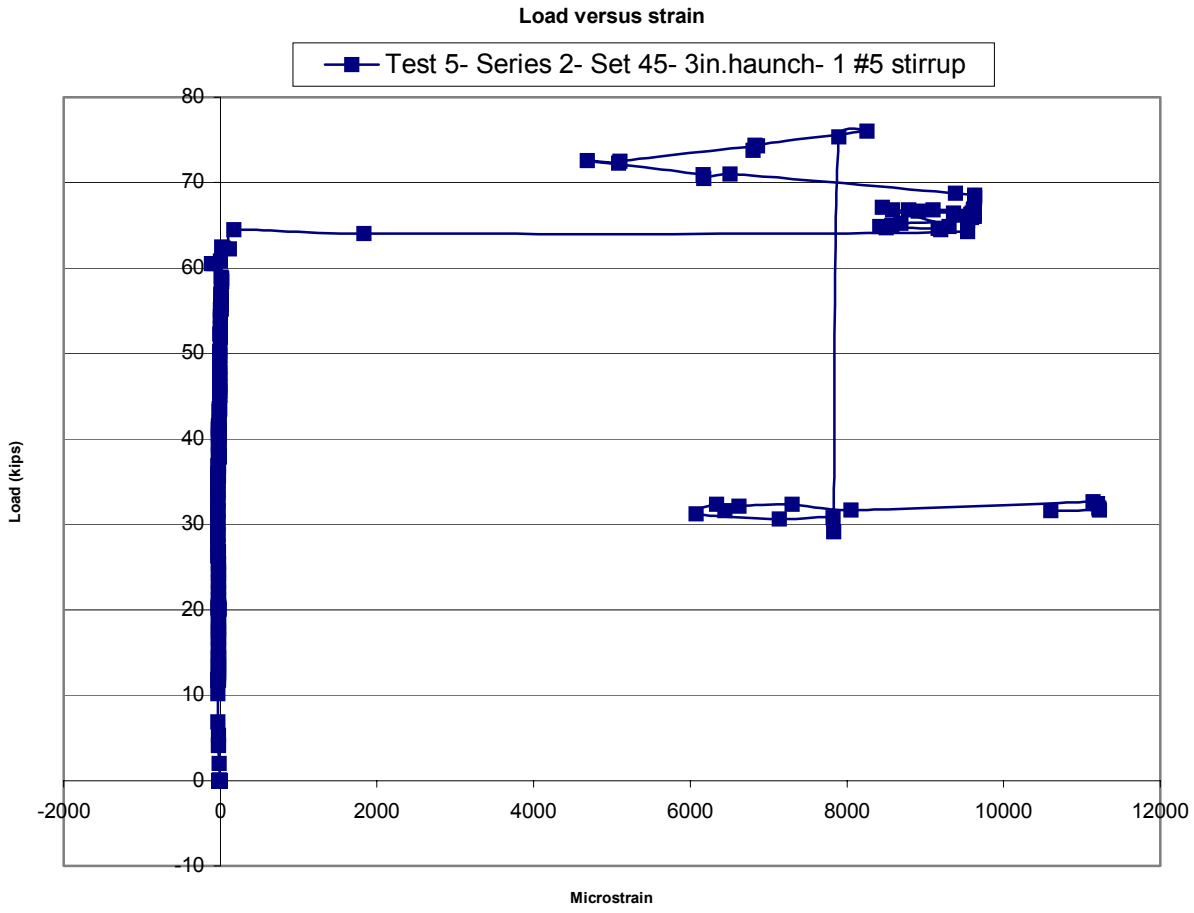
Load versus strain
Test 5- Series 2- Set 45- 3in.haunch- 1 #5 stirrup
Load (kips)
80
70
60
50
40
30
20
10
0
-10
-2000
0
2000
4000
6000
8000
10000
12000
Microstrain

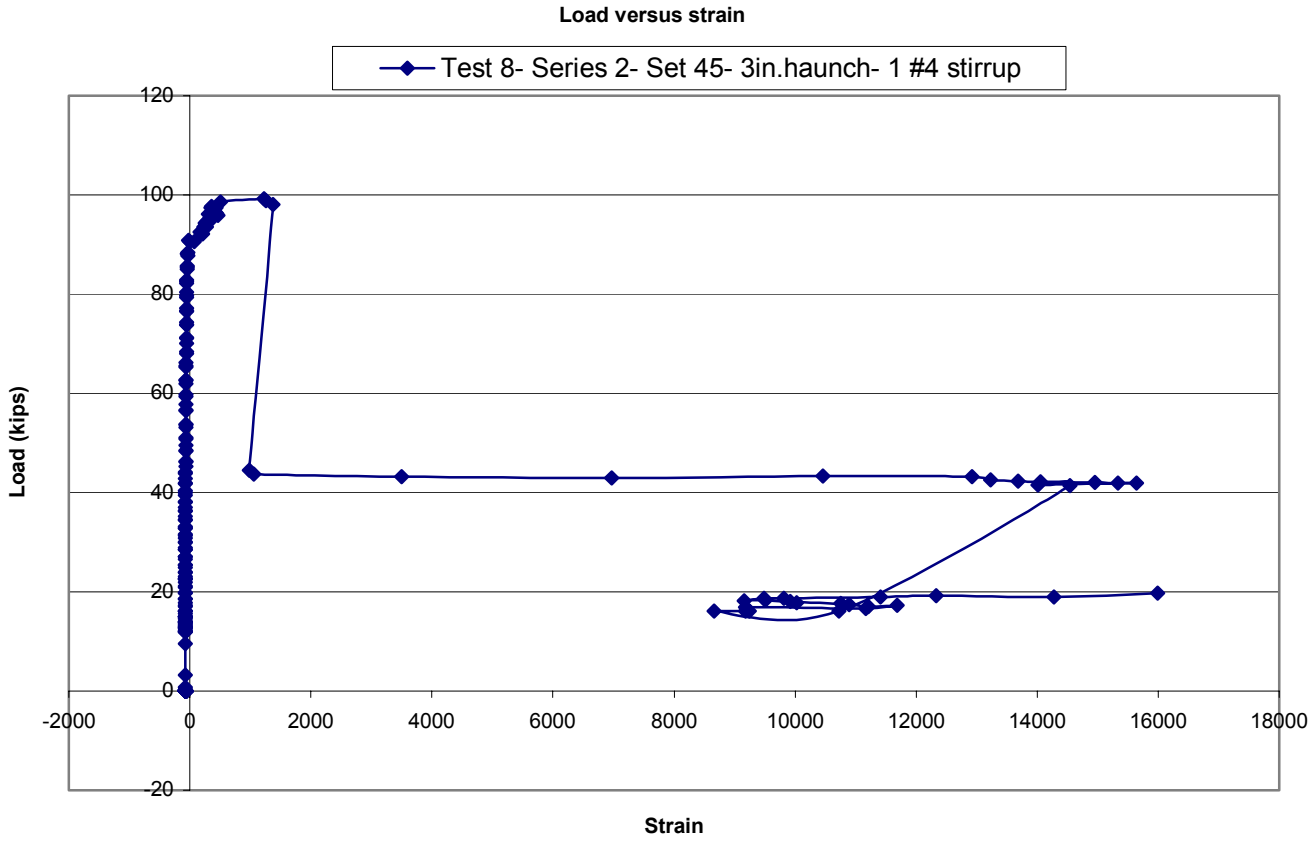
Load versus strain
Test 8- Series 2- Set 45- 3in.haunch- 1 #4 stirrup
Load (kips)
120
100
80
60
40
20
0
-20
-2000
0
2000
4000
6000
8000
10000
12000
14000
16000
18000
Strain

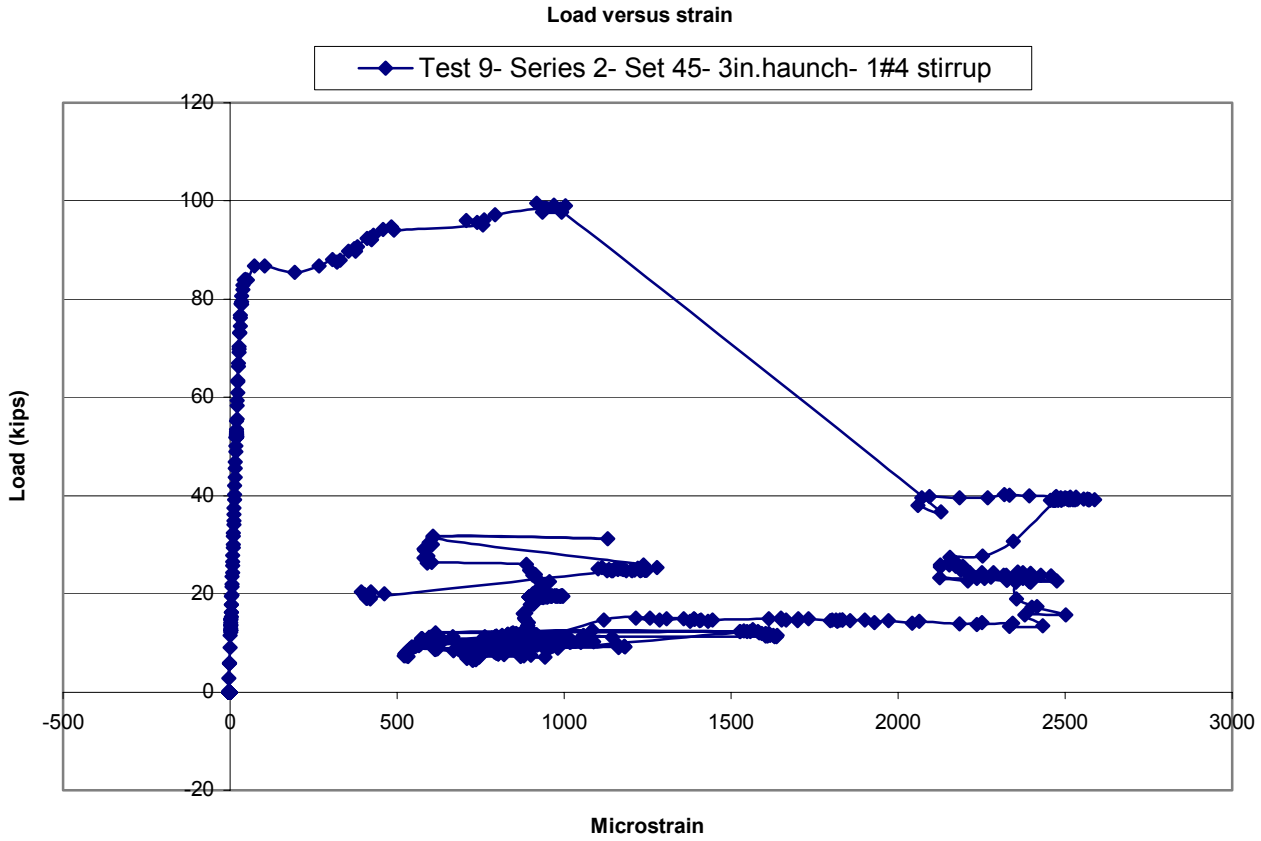
Load versus strain
Test 9- Series 2- Set 45- 3in.haunch- 1#4 stirrup
Load (kips)
120
100
80
60
40
20
0
-20
-500
0
500
1000
1500
2000
2500
3000
Microstrain

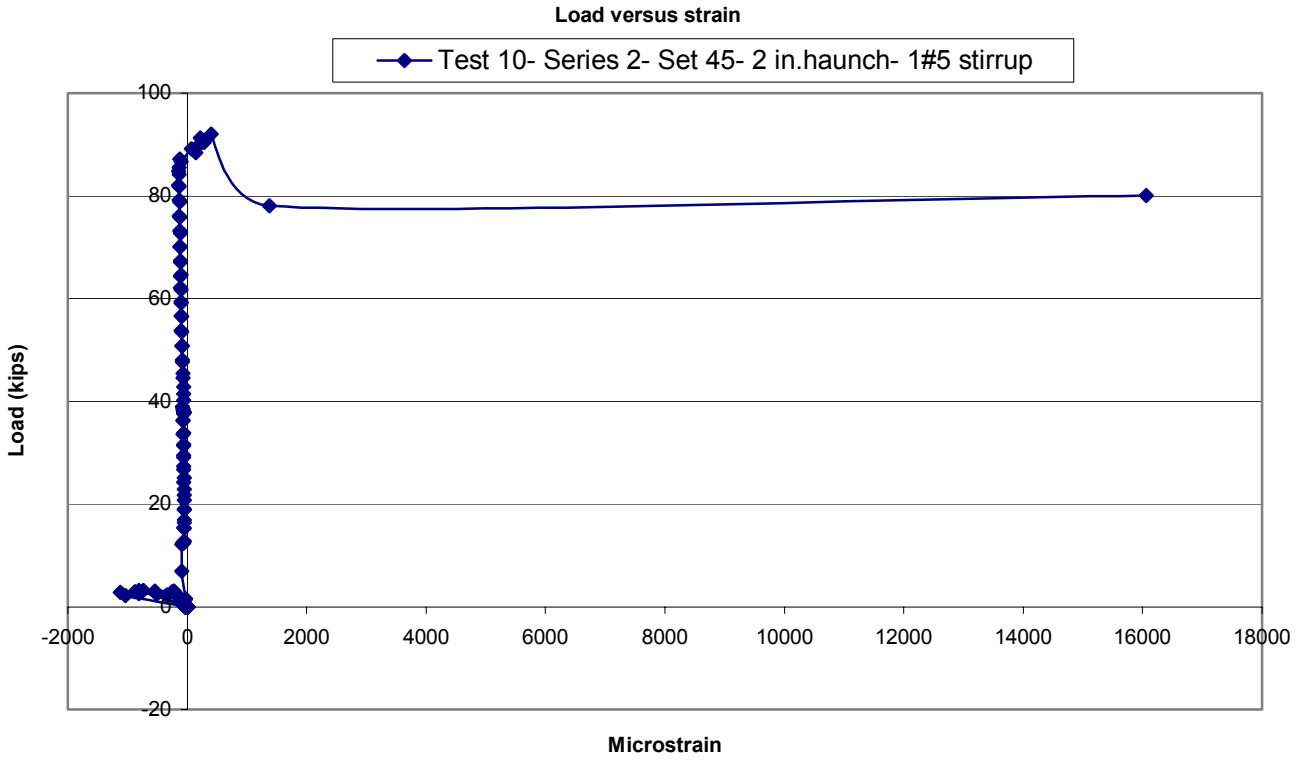
Load versus strain
Test 10- Series 2- Set 45- 2 in.haunch- 1#5 stirrup
Load (kips)
100
80
60
40
20
0
-20
-2000
0
2000
4000
6000
8000
10000
12000
14000
16000
18000
Microstrain

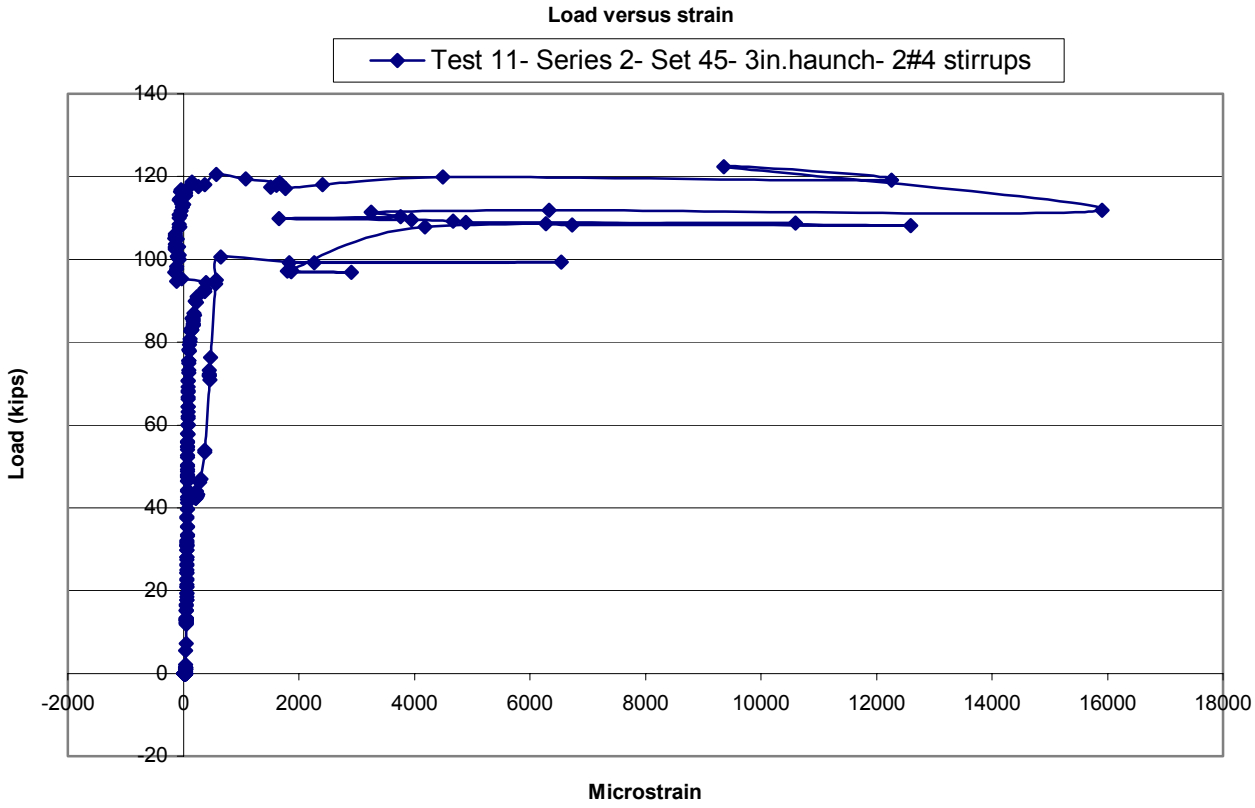
Load versus strain
Test 11- Series 2- Set 45- 3in.haunch- 2#4 stirrups
Load (kips)
140
120
100
80
60
40
20
0
-20
-2000
0
2000
4000
6000
8000
10000
12000
14000
16000
18000
Microstrain

Series 3

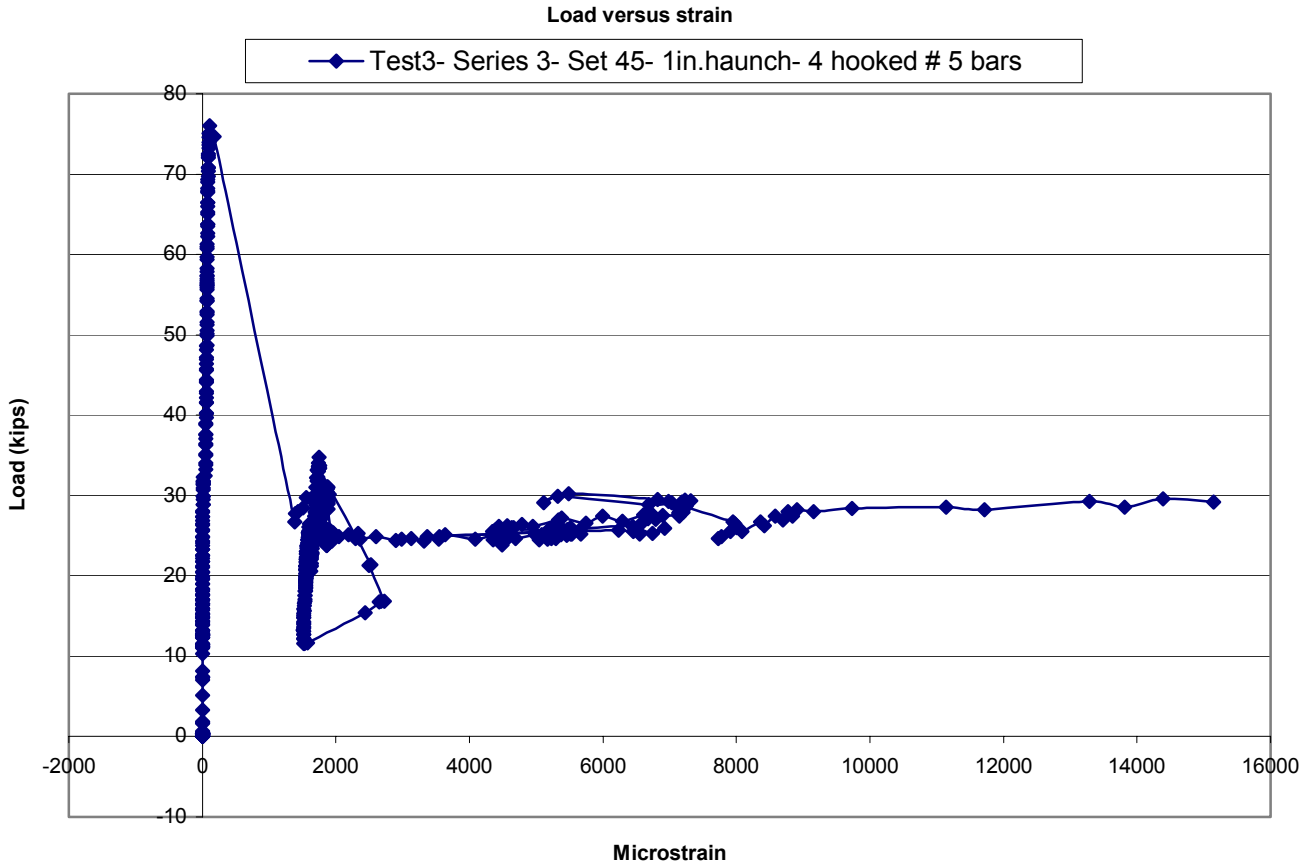
Load versus strain
Test3- Series 3- Set 45- 1in.haunch- 4 hooked # 5 bars
Load (kips)
80
70
60
50
40
30
20
10
0
-10
-2000
0
2000
4000
6000
8000
10000
12000
14000
16000
Microstrain

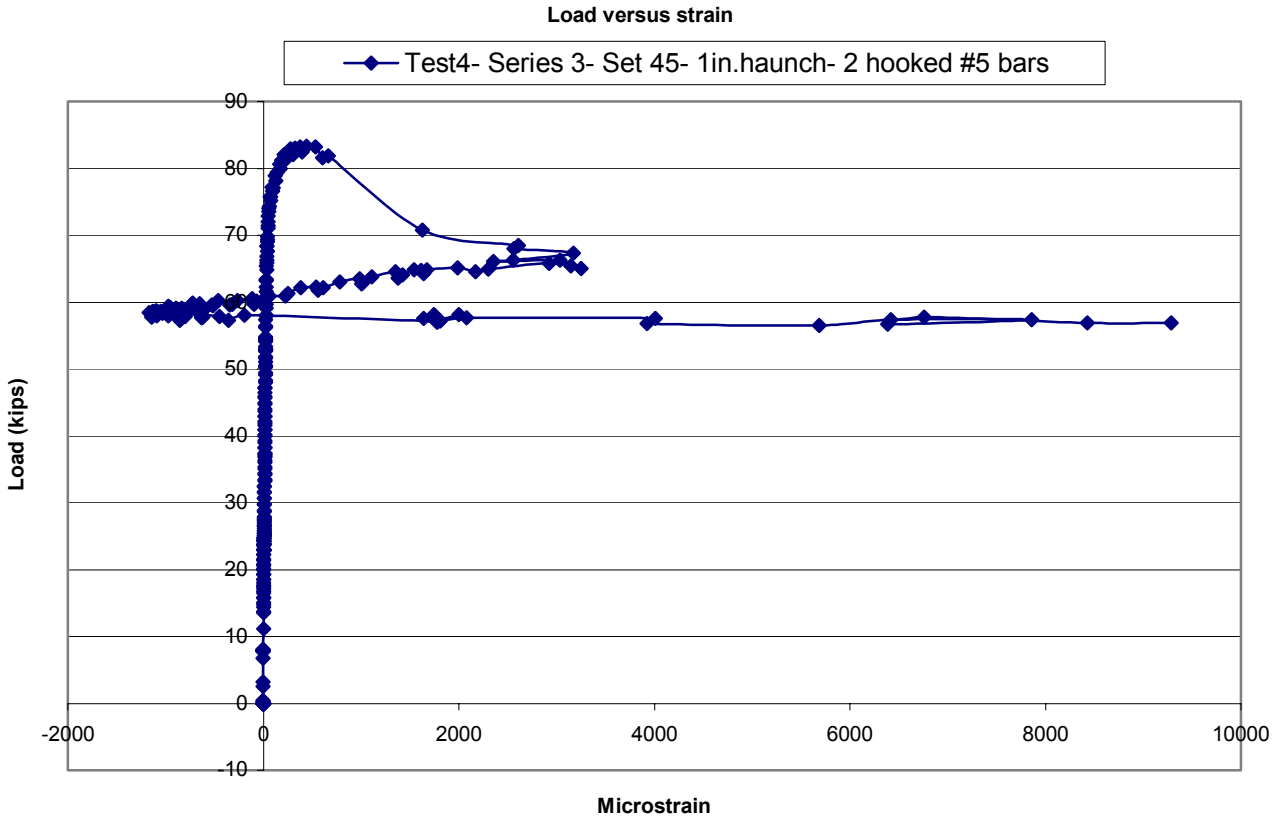
Load versus strain
Test4- Series 3- Set 45- 1in.haunch- 2 hooked #5 bars
Load (kips)
90
80
70
60
50
40
30
20
10
0
-10
-2000
0
2000
4000
6000
8000
10000
Microstrain

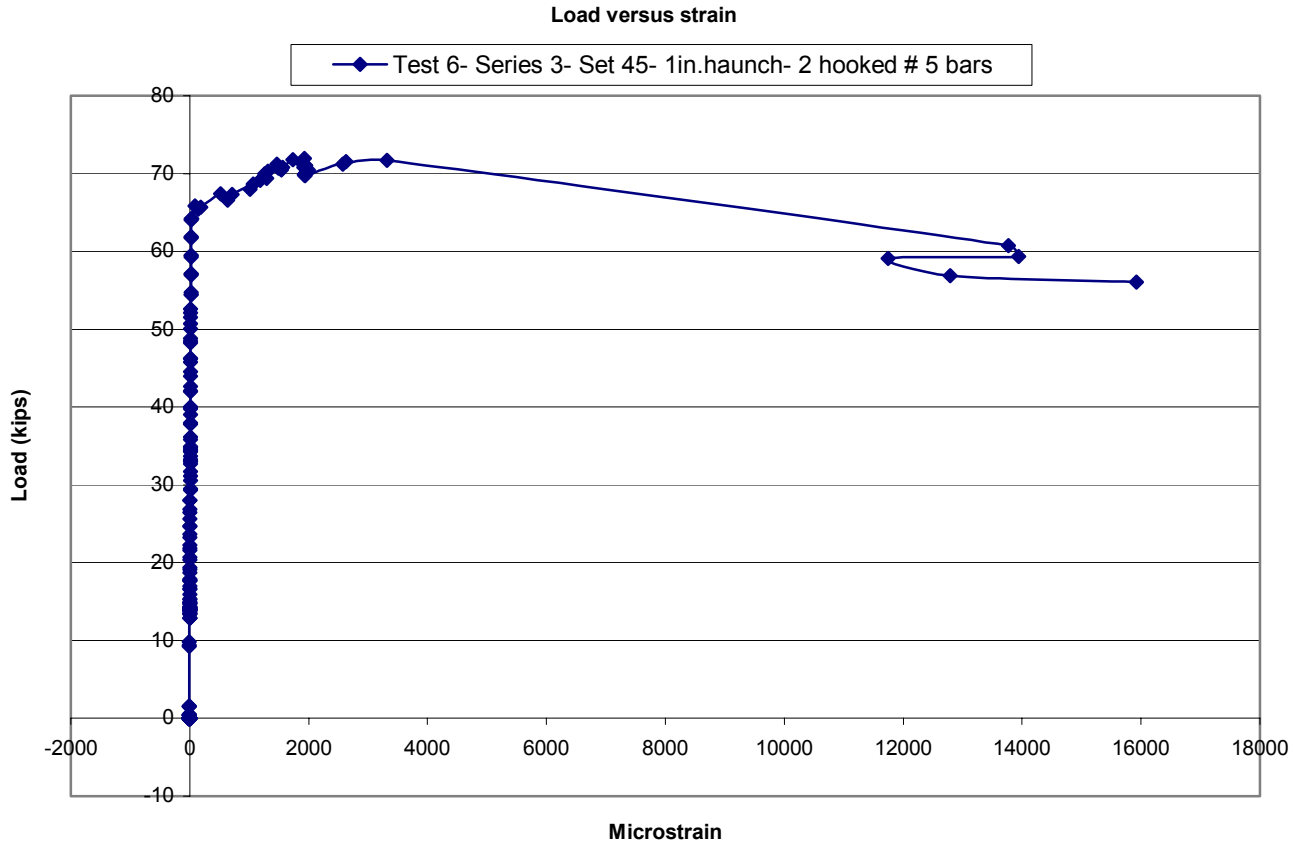
Load versus strain
Test 6- Series 3- Set 45- 1in.haunch- 2 hooked # 5 bars
Load (kips)
80
70
60
50
40
30
20
10
0
-10
-2000
0
2000
4000
6000
8000
10000
12000
14000
16000
18000
Microstrain

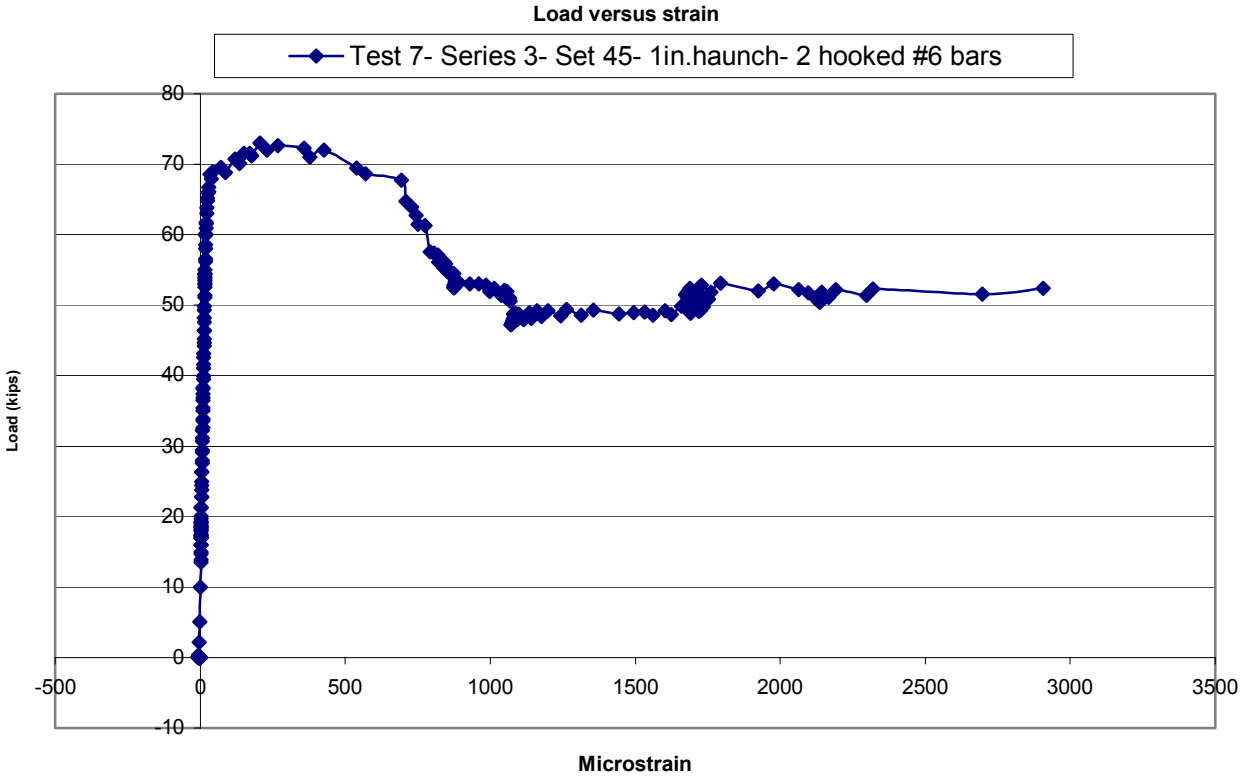
Load versus strain
Test 7- Series 3- Set 45- 1in.haunch- 2 hooked #6 bars
Load (kips)
80
70
60
50
40
30
20
10
0
-10
-500
0
500
1000
1500
2000
2500
3000
3500
Microstrain

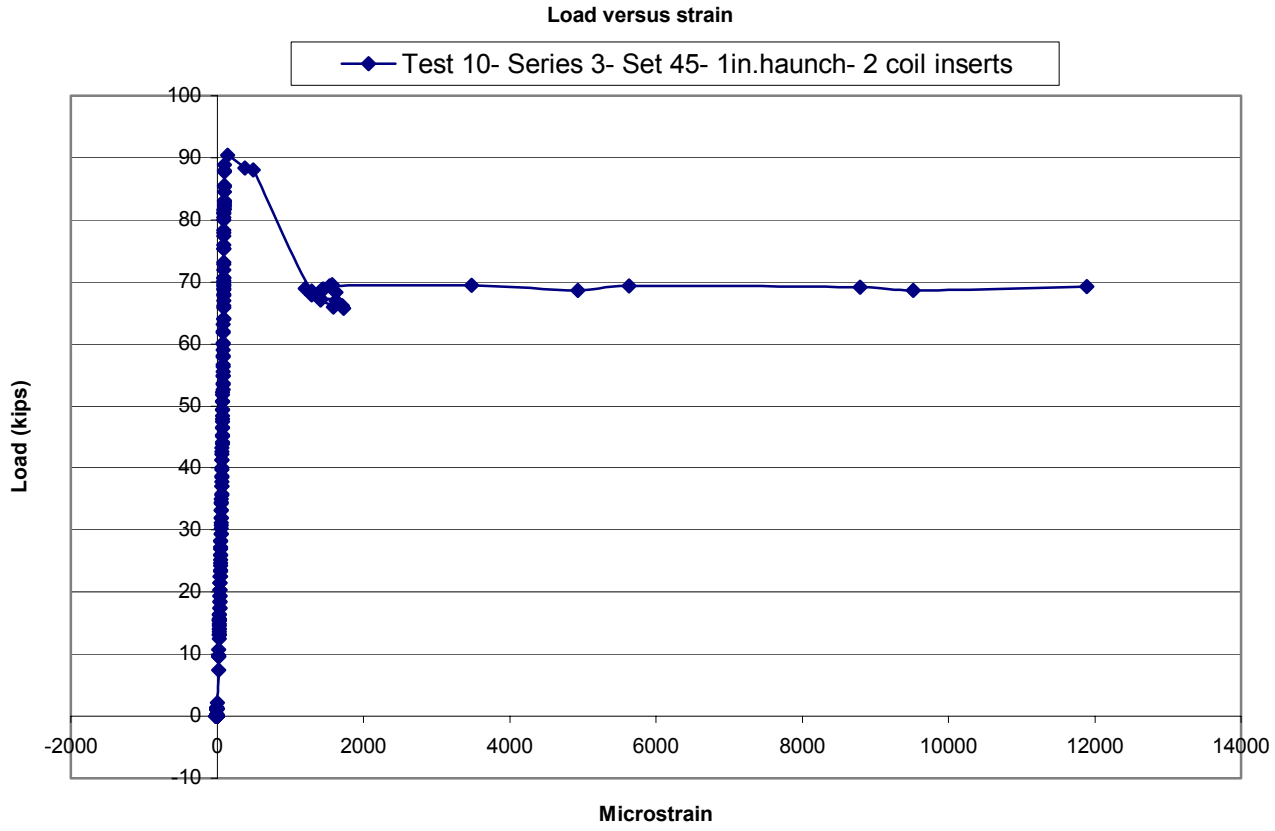
Load versus strain
Test 10- Series 3- Set 45- 1in.haunch- 2 coil inserts
Load (kips)
100
90
80
70
60
50
40
30
20
10
0
-10
-2000
0
2000
4000
6000
8000
10000
12000
14000
Microstrain

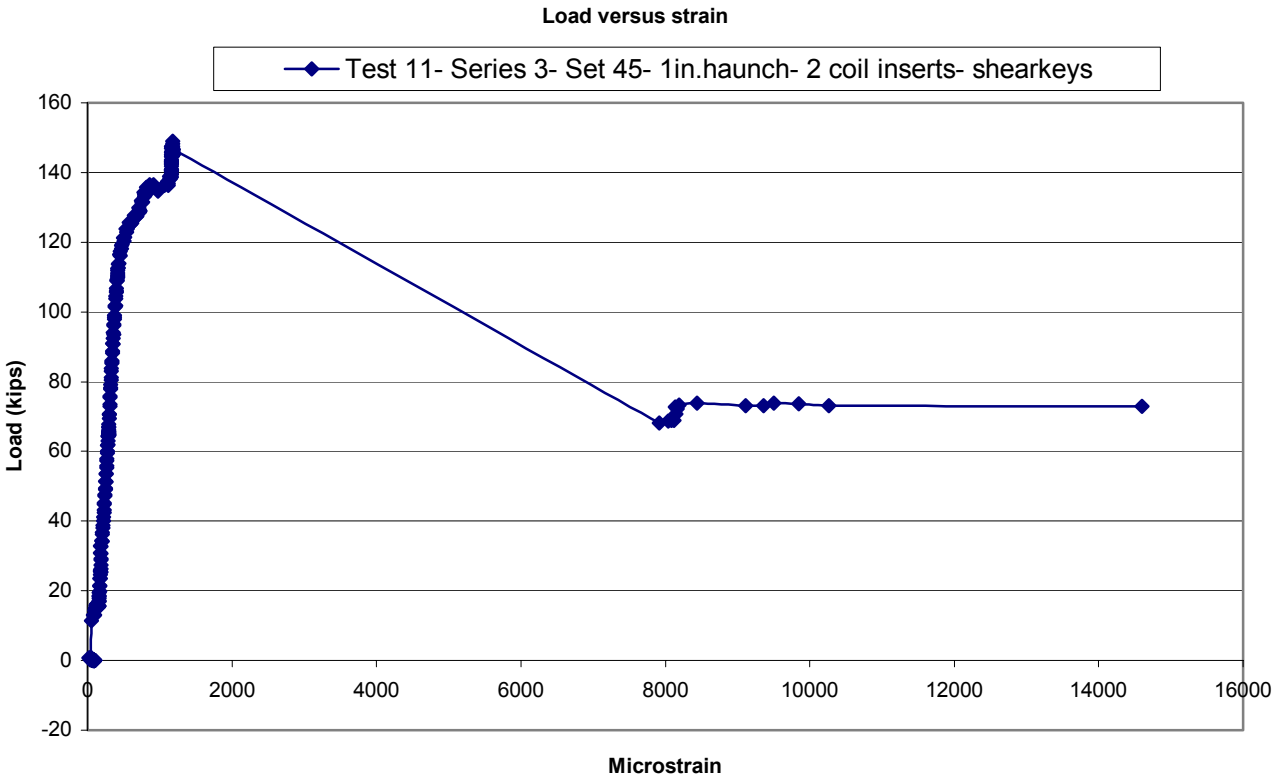
Load versus strain
Test 11- Series 3- Set 45- 1in.haunch- 2 coil inserts- shearkeys
Load (kips)
160
140
120
100
80
60
40
20
0
-20
0
2000
4000
6000
8000
10000
12000
14000
16000
Microstrain

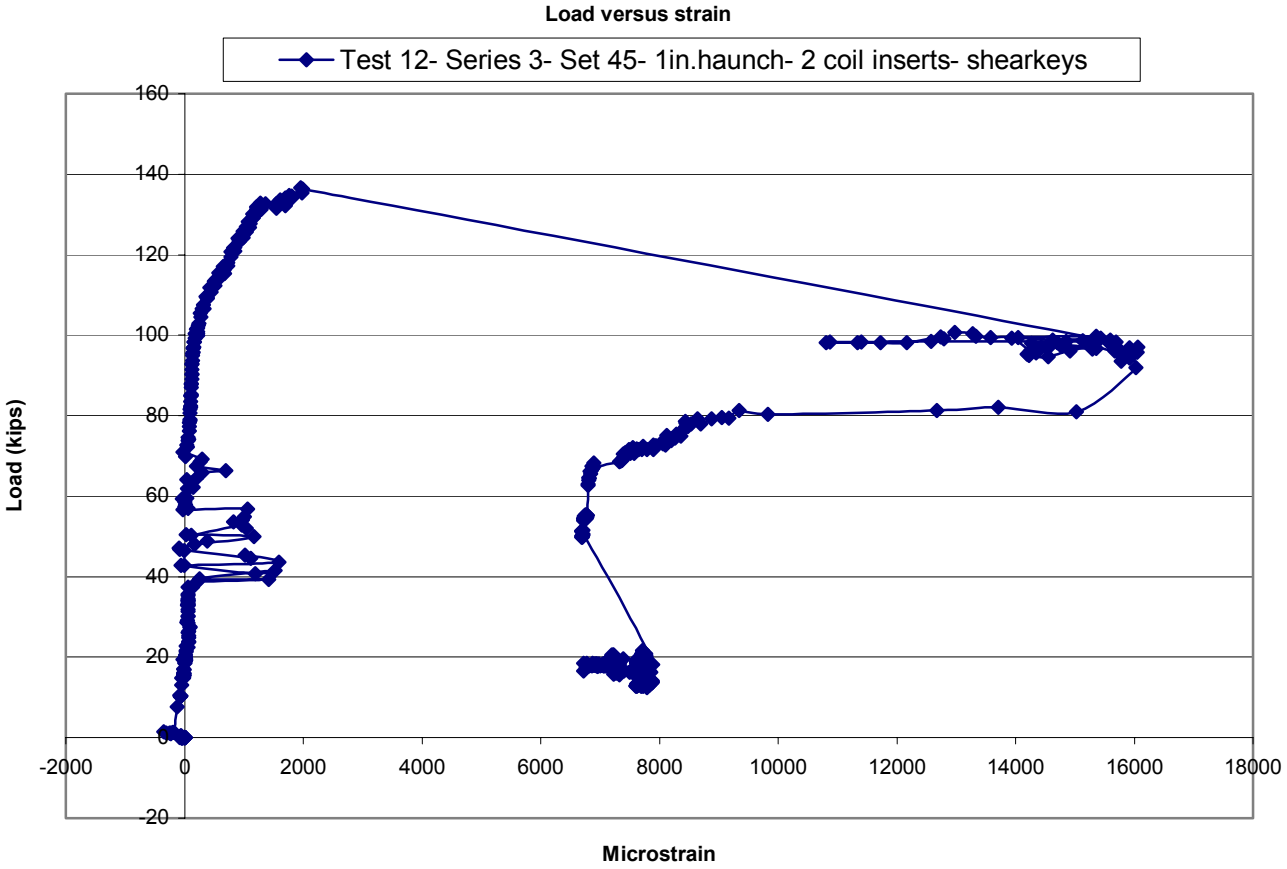
Load versus strain
Test 12- Series 3- Set 45- 1in.haunch- 2 coil inserts- shearkeys
Load (kips)
160
140
120
100
80
60
40
20
0
-20
-2000
0
2000
4000
6000
8000
10000
12000
14000
16000
18000
Microstrain

VITA

Fatmir Menkulasi was born on November 19, 1977 in Berat, Albania, the son of Gazmend and Kozeta Menkulasi. He grew up in the city of Berat and in 1992 he enrolled in Mehmet Akif High School in the city of Tirane, Albania. He graduated from high school in 1996.

Fatmir enrolled as an undergraduate at Middle East Technical University, Ankara, Turkey in the fall of 1996. In June 2000, he graduated with a Bachelor of Science degree in civil engineering. He began his graduate studies in structural engineering at Virginia Tech in the fall of 2000.

In August 2002, Fatmir will begin employment as an entry-level structural engineer with Stroud and Pence Associates, a structural engineering consulting firm located in Virginia Beach, VA.